Technical Letter Report on Evaluation of Head Loss by Products of Aluminum Alloy Corrosion

August 11, 2008

Prepared by
C. B. Bahn, K. E. Kasza, W. J. Shack, and K. Natesan
Argonne National Laboratory
Argonne, Illinois 60439

NRC Contract # JCN 3216
Program Manager: Emma Wong

Executive Summary

Previous ANL head loss tests[1,2] for $Al(OH)_3$* precipitates that can potentially form in sump solutions with high levels of dissolved aluminum (Al) have been performed with surrogates proposed by industry or by forming precipitates in situ with aluminum nitrate, $Al(NO_3)_3$ as the source of dissolved Al. In a post-loss of coolant accident (LOCA) environment, however, the precipitates would be formed in situ with the source of the Al being dissolution of Al by corrosion of Al metal and NO_3^- would not likely be present in amounts comparable to those encountered when $Al(NO_3)_3$ is the source of dissolved Al. The current head loss tests were performed with the source of Al being corrosion from Al alloy plates. The objective of these tests was to compare head loss associated with precipitate formation from aluminum coupon corrosion with those using WCAP-16530-NP precipitates or with precipitates formed in situ as a result of chemical injection.

The head loss tests were performed in the ANL vertical loop with 6061 Al alloy and "commercially pure" 1100 Al plates immersed in borated solution. The Al release rate from 6061 Al alloy in borated water at pH=9.35 (@room temperature) and 140°F with the flow rate of 0.1 ft/s was similar to predictions based on data from bench top tests and low-flow rate tests with 1100 and 3003 Al alloys. However, the Alloy 1100 corrosion rate is higher than predictions based on data from benchtop tests and appears to be flow dependent.

Alloy 6061 allowed to corrode in a flowing loop created a significant head loss at an Al concentration of 116 ppm with a pH of 9.35 and a temperature of 140°F. An additional increase in the head loss was observed when the temperature was lowered from 140 to 80°F. Post-test examination revealed that grayish black particles were trapped in the glass fiber bed. Stagnant bench top corrosion tests with Alloy 6061 also showed grayish black particles, which were released from the coupon surfaces rather than being generated as a precipitate from the solution. Based on microscopic analyses, it was concluded that the grayish black particles are intermetallic particles present in the alloy that are released by corrosion of the alloy matrix. The intermetallic particles are primarily (FeSiAl) ternary compounds ranging in size from a few tenths of a micrometer to 10 μm. ANL bench top tests and other loop tests show that the solubility limit for $Al(OH)_3$ at pH=9.35 (@room temp.) and 140°F is significantly greater than 116 ppm Al. This indicates that the head loss at 140°F was induced by the intermetallic particles present in the 6061 Al alloy. As the temperature of the loop was decreased additional head loss was experienced due to the formation of $Al(OH)_3$ from the decrease in temperature i.e. the dissolved aluminum exceeded its concentration limit at the lower temperature.

With an Al concentration of 118 ppm in the loop from corrosion of 1100 Al plates, no significant increase in head loss was observed at 140°F. Post-test examination for the glass fiber bed and bench top test results confirmed that Fe-Cu enriched intermetallic particles were present in the 1100 Al, which were released and captured in the bed during the loop test. The differences in head loss behavior associated with the intermetallic particles may be attributed to the fact that the sizes of the intermetallic particles in 6061 Al alloy are typically larger than those in 1100 Al alloy. At the Al concentration of ≈118 ppm no significant increase in head loss was observed in the 1100 Al test until the temperature was decreased to 100°F. This increase appears to be induced by Al hydroxide precipitation, not by intermetallic particles. Once the head loss began to increase, a rapid increase in head loss was observed even though the temperature was increased from 100 to 120°F.

*In this report, $Al(OH)_3$ is used a short–hand for a family of aluminum oxyhydroxides that could form in a variety of crystalline and amorphous forms.

The Al corrosion vertical head loss loop tests with 6061 and 1100 Al plates seem to suggest somewhat lower solubility than the chemical Al tests. It is conjectured that this may be due to heterogeneous nucleation of Al hydroxide on intermetallic particles and/or on the surfaces of preexisting Al hydroxide precipitates.

The test results suggest that the potential for corrosion of an Al alloy to result in increased head loss may depend on its microstructure, i.e., the size distribution and number density of intermetallic particles, as well as its Al release rate.

The increase in head loss due to in situ precipitation of $Al(OH)_3$ observed in these tests seems reasonably consistent with that expected from the addition of corresponding amounts of the WCAP surrogate. Per unit mass of Al removed from solution, the WCAP surrogate appears somewhat more effective in increasing head loss than the $Al(OH)_3$ precipitates formed in situ by corrosion or chemical addition of Al, and thus it gives conservative estimates of the head loss due to the precipitation of a given amount of Al from solution. However, in choosing the amount of surrogate that should be used, consideration must be given to the potential for additional head losses due to intermetallic particles and the apparent reduction in the effective solubility of $Al(OH)_3$ when intermetallic particles are present.

In-situ Al Corrosion Test with 6061 Al in Vertical Head Loss Loop

Experimental

A head loss test similar to earlier ANL tests was performed with 6061 class Al alloy plates immersed in the loop solution as the source of dissolved Al. The chemical composition of the 6061 plates given by the ASTM B209-06[3] specification as well as actual analysis results for the plates used in the test are shown in Table 1. The chemical composition was obtained by electron dispersive X-ray spectroscopy (EDS). The Mg concentration appears slightly higher than defined by the specification but the other alloying elements, Si, Fe, and Cr, are within the specification. The discrepancy in the Mg results may be the result of the size of the area being sampled. No significant Cu signal was observed in the EDS spectrum. Since EDS is not accurate for elements having less than 1–2 wt%, the EDS data should be used for qualitative comparison.

Eight Al plates (3"×4" ×1/8" thick) were machined and polished with a Scotch Brite pad and then ultrasonically cleaned in alcohol for 10 minutes. The Al plates were stacked onto threaded Al rods made of 6061 Al and separated by Teflon spacers (1/2" height). The Al plates were in contact with the threaded rods. The exposed area of the rods is at most 2% of the area of the Al plates.

Figure 1 shows the overall appearance of the Al bundle. The Al bundle is fixed to the top flange of the tee port in the loop so that the bundle can be easily installed or removed from the loop. Figure 2 shows the Al bundle being inserted into the tee port.

The test loop was filled with high purity water. The loop water temperature was raised to 120°F and 1687 g of boric acid (H_3BO_3, Fisher Scientific) was added into the loop, which gives a concentration of 2500 ppm B. Once the loop water pH became stable, the loop water temperature was decreased to 80°F. Sodium hydroxide (NaOH, Fisher Scientific) was added to obtain a target loop water pH of 9.0–9.4. The actual pH after NaOH addition was 9.35 at 80°F. After a stable pH value was achieved, the pH and conductivity were measured and recorded. NUKON insulation was shredded and processed following the procedures developed in prior

loop tests.[1] The processed NUKON fibers were added to the loop to build an approximately 13 mm thick NUKON bed on the horizontal perforated plate in the vertical test section. The flow in the loop was controlled to maintain a screen approach velocity of 0.1 ft/s during the development of the bed and throughout the test (or at least until head losses had increased to the point where the velocity had to be decreased to avoid the possibility of cavitation). Once the pressure drop became stable, the water chemistry was measured again, and a sample of the solution was taken. The Al bundle was then installed in the tee port. The loop water temperature was raised to 140°F to enhance Al dissolution. Inductively Coupled Plasma/Optical Emission Spectroscopy (ICP/OES) analyses of solution samples were performed daily. When the dissolved Al concentration reached a predetermined level, the Al bundle was taken out of the loop. The loop water temperature was decreased steps from 140 to ~70°F. At each step, the water temperature was held constant for about 30 minutes. If the pressure drop across the screen started to increase at a certain temperature level, the temperature was held longer at that level to determine whether the head loss would stabilize.

Table 1. Specification of the chemical composition for 6061 Al alloy compared with measured results by EDS (wt%).

	Al	Si	Fe	Cu	Mn	Mg	Cr	Zn	Ti	Others
ASTM B209-06	Bal.	0.40-0.8	0.7 max	0.15-0.40	0.15 max	0.80-1.2	0.04-0.35	0.25 max	0.15 max	0.15 max
Measured	96.54	0.38	0.44	NI[a]	NI	2.54	0.11	NI	NI	NI

[a] Element was not included in the EDS spectrum analysis because signal was negligible.

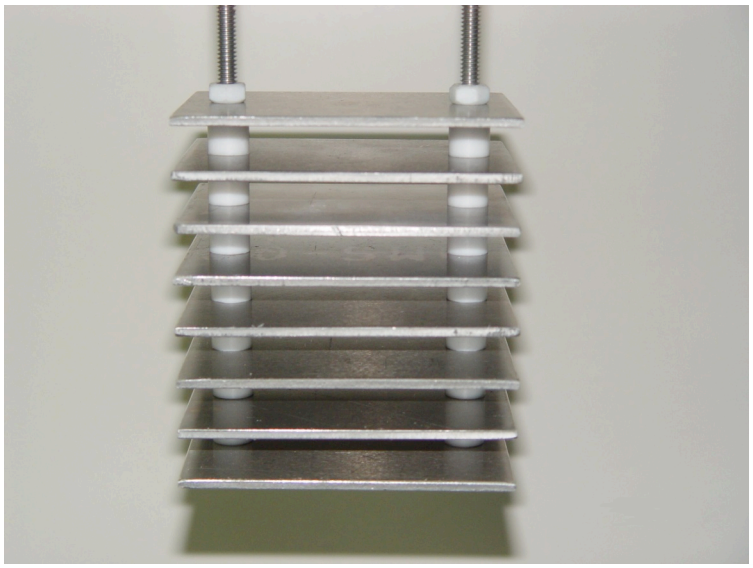

Figure 1.
Al bundle of eight Al plates with dimensions of 3" width, 4" length, and 1/8" thickness.

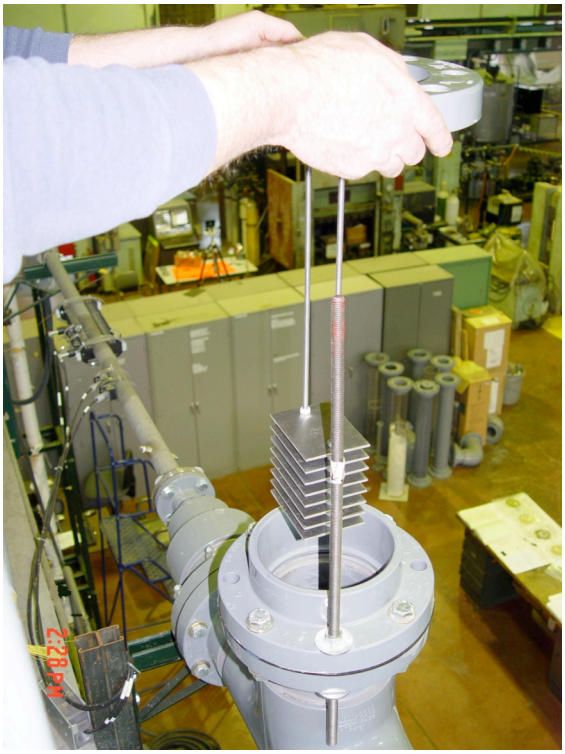

Figure 2.
Installation of the Al bundle into the tee port of the ANL vertical head loss test loop.

Head Loss Test Results

Figure 3 shows the variation of the dissolved Al concentration with exposure time in the loop, as determined by ICP analyses of the solution samples. As shown in Figure 3, the observed corrosion rate of the 6061 Al alloy is similar to that predicted by the Al release rate equation (6-1) proposed in Ref. 4;

$$RR=10^{[A + B(pHa) + C(1000/T) + D(pHa)^2 + E(pHa)(T)/1000]} \quad (1)$$

where:

RR= release rate in mg/(m^2min)

A= 13.455

B= 0.472

C= -4.615

D= 0.016

E= -1.327

pHa= initial pH corrected to 25°C

T= temperature in Kelvin (K).

As discussed in a previous ANL technical letter report,[5] the original values for the constants A through E in the WCAP-16530-NP Rev.0 are clearly incorrect. The values used here were determined by ANL based on a best fit to the WCAP[4] and ICET–1[6] test data. The WCAP tests[4] used 1100 Al, i.e., "commercially pure" Al; ICET-1[6] used 3003 Al alloy. Figure 3 shows the measured values of Al concentration, the predicted value according to Eq. (1), the

predicted value according to Eq. (6-2) in Ref. 4, and a best–fit power law for the measured data that gives a value of 0.81 for the exponent for time in the power law. The results suggest Eq. (6-1), as modified by ANL, slightly underestimates the Al release rate and that Eq. (6-2) significantly underestimates the Al release rate. The results also suggest that the Al release rate is not very dependent of the type of Al alloy. Table 2 shows the ICP analyses for loop solution samples. In Table 2, 't' and 't_{ex}' denote total test time from the beginning of the test and exposure time of the Al plates. The discrepancy between two times comes from the fact that the Al plates were taken out and reinstalled several times during the test.

After the concentration of Al in the loop water reached 100 ppm, the Al bundle was taken out and the loop was run for 2 days at 140°F at this concentration. Samples of loop water were taken daily and cooled for ICP analysis. A 250-mL loop water sample taken when Al concentration reached 100 ppm became very slightly cloudy when cooled down to room temperature. After 2 days, the temperature of the loop was reduced in steps down to ~70°F and the loop was run over night at 70°F to try to trigger Al precipitate formation. No indication of precipitation or increased head loss was observed over night. The loop water temperature was increased back up to 140°F, and the Al bundle inserted to allow corrosion to increase the Al concentration from 100 ppm to a new target value of 125 ppm. After running over night at 140°F with the Al bundle inserted, the pressure drop started rising. When the bed pressure drop reached 0.54 psi, water samples were taken for ICP analysis and the Al bundle was removed. This increase in pressure drop occurred while the loop temperature was being held at 140°F. ICP analysis showed that the Al concentration was 116 ppm (samples 05-07a and 05-07b) at this point, as shown in Table 2. The solution filtered at temperature using a 20 nm filter showed almost the same Al concentration (sample 05-07c). A 250-mL flask of water was also drawn from the loop and allowed to cool down to room temperature. The flask sample showed visible white flake-like precipitates on the bottom of the flask and the overall solution became slightly cloudy. The shapes of the flake–like precipitates, which were like thin plates with lengths less than 1 mm, did not resemble those produced in the ANL bench top tests[2] during the investigation of $Al(OH)_3$ surrogates used in industry tests, which were heavily flocculated and resembled cotton balls.

The test was continued over night without the Al bundle in place and with the temperature held at 140°F. The bed pressure drop increased to 1.71 psi overnight, but appeared to be starting to level off. To maximize the capability of the loop to deal with increasing head loss across the bed, the approach velocity was allowed to drift downward as the pressure drop increased. Figure 4 shows the pressure drop and screen approach velocity time history in this loop test, and the loop water temperature time history with the pressure drop is plotted in Figure 5. The decrease in flow velocity at about 180 h, shown in Figure 4, was caused solely by the temperature change because the head loss came back to the same value that was observed before the temperature was cycled.

As shown in Table 2, ICP analysis of a water sample taken at this time (sample 05-08a) gave an Al concentration of 113 ppm, which suggests that the overnight increase in pressure drop of 1.2 psi was associated with a decrease in Al concentration in the loop on the order of a few ppm (the uncertainty in the ICP values is about 1%). The loop temperature was then decreased to 120°F. With the decrease in temperature, the pressure drop across the bed started to rise again. Over a day of operation at 120°F, the pressure drop across the bed rose from 1.72 to 3.43 psi without any sign of leveling off. The loop water temperature was then decreased to 80°F; the decrease in temperature increased the rate of pressure drop increase. The pressure drop reached 4.4 psi and was still climbing but started to level off. The loop was shut down after taking water samples. Analysis of these samples (samples 05-09a and 05-09b)

showed the dissolved Al concentration at the end of the test was 109 ppm, as shown in Table 2. Thus, the increase in pressure drop of 2.7 psi as the temperature decreased was associated with a decrease of approximately 4 ppm in Al concentration. A solution sample taken at 80°F and filtered by a 20 nm filter gave an Al concentration of 31.7 ppm. As expected, Al hydroxide precipitation occurred at 80 F, and the precipitate size was bigger than 20 nm. Again, it should be noted that the approach velocity was not held constant, but allowed to drift downward to approximately 0.065 ft/s at the end of the test.

To investigate the possibility of contributions from calcium and silicon to head loss, two ICP sample results, 05-08a taken at 140°F and 05-09a taken after cooling to 80°F, were compared. The two samples were not filtered. Sample 05-09a shows a smaller Ca concentration which suggests a Ca precipitate, probably a Ca hydroxide, was trapped in the NUKON bed during cooling from 140 to 80°F. However, the Si concentrations in the two samples are almost the same, which suggests that if any Si precipitation did occur, the precipitates were too small to be trapped in the NUKON bed. The lower Si value in Sample 05-09c result suggests that Si precipitation has occurred, but although the precipitate size was too small to be trapped by the bed, it was greater than 20 nm and thus was removed from the filtered sample. Although Ca precipitates might contribute to the increase in head loss during cooling down, their contribution is small compared to that due to $Al(OH)_3$ precipitates.

The final loop water pH was 9.33 at 80°F, which was almost the same as the initial pH of 9.35 at 80°F before installing the Al bundle. The dissolution of Al at alkaline conditions tends to decrease the solution pH because Al cations react with OH^- ions to form $Al(OH)_4^-$. It appears, however, that the effect is small with only 100 ppm Al. The actual dissolved concentration may be even less, since some of the Al was probably tied up with intermetallic particles, which will be identified in a later section, rather than actually being dissolved.

After the loop was shut down, the NUKON bed was taken out for analysis. Figures 6a and 6b show top and side views of the NUKON glass fiber bed just after it was removed from the loop and was still wet. The color of the bed turned gray. The buildup of the dark materials was not limited to only the top surface but also occurred inside the bed, as shown in Figure 6b. This suggests full penetration of intermetallic particles into the NUKON bed.

Table 2. ICP analyses for loop solution samples of 6061 Al test.

Sample No.	Sample Description	Dissolved Ion Concentration (mg/L)							
		Al	B	Ca	Si	Na	Cr	Fe	Ni
05-01	Taken before Al bundle installation	<0.5	NA[a]	NA	NA	NA	NA	NA	NA
05-02	Taken at t = 26.0 h (t_{ex} =17.0 h), Unfiltered	29.6	NA	NA	NA	NA	NA	NA	NA
05-03	Taken at t = 33.0 (t_{ex} = 24.0 h)[b], Unfiltered	40.7	NA	NA	NA	NA	NA	NA	NA
05-04a	Taken at t = 49.5 h (t_{ex} = 40.5 hr), Unfiltered	61.2	NA	NA	NA	NA	NA	NA	NA
05-04b	Taken at t = 49.5 h (t_{ex} = 40.5 h), Unfiltered	61.9	NA	NA	NA	NA	NA	NA	NA
05-05a	Taken at t = 80.0 h (t_{ex} = 51.0 h), Unfiltered	74.5	NA	NA	NA	NA	NA	NA	NA
05-05b	Taken at t = 80.0 h (t_{ex} = 51.0 h), Unfiltered	76.2	NA	NA	NA	NA	NA	NA	NA
05-06a	Taken at t = 102 h (t_{ex} = 73.0 hr), Unfiltered	100	NA	NA	NA	NA	NA	NA	NA
05-06b	Taken at t = 102 h (t_{ex} = 73.0 hr), Unfiltered	99.5	NA	NA	NA	NA	NA	NA	NA
05-07a	Taken at t = 217 h (t_{ex} = 94.9 hr), Unfiltered	114	2180	0.76	2.06	2240	<0.5	<0.5	<0.5
05-07b	Taken at t = 217 h (t_{ex} = 94.9 hr), Unfiltered	118	2270	0.86	2.04	2330	<0.5	<0.5	<0.5
05-07c	Taken at t = 217 h (t_{ex} = 94.9 hr), 20 nm filtered	118	2230	<0.5	2.01	2270	<0.5	<0.5	<0.5
05-08a	Taken prior to cooling down from 140 to 120 F, t = 241 h Unfiltered	113	2220	1.81	2.24	2360	<0.5	<0.5	<0.5
05-08b	Taken prior to cooling down from 140 to 120 F, t = 241 h 20 nm filtered, filtered at 80 F	33.4	2130	<1	<1	2300	<1	<1	<1
05-09a	Taken at 80 F prior to shutting down, t = 272 h Unfiltered	108	2250	0.51	2.11	2330	<0.5	<0.5	<0.5
05-09b	Taken at 80 F prior to shutting down, t = 272 h Unfiltered	110	2250	<0.5	2.12	2340	<0.5	<0.5	<0.5
05-09c	Taken at 80 F prior to shutting down, t = 272 h 20 nm filtered	31.7	2200	<0.5	0.54	2320	<0.5	<0.5	<0.5

[a] NA indicates the element was not analyzed.

[b] t denotes total test time, t_{ex} denotes exposure time of the Al plates.

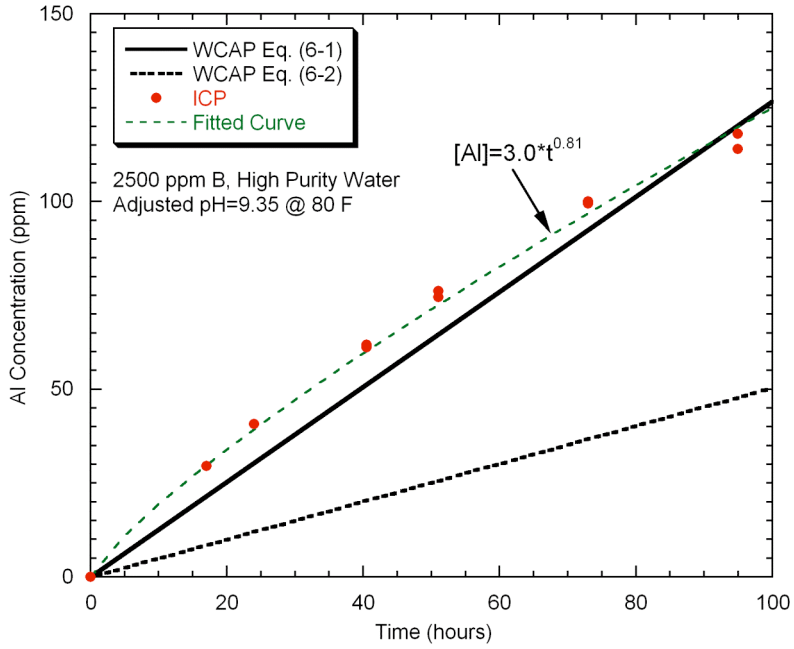

Figure 3.
Dissolved Al concentration in the loop by ICP analysis as a function of total exposure time compared with the predicted Al corrosion rates by Westinghouse. The curve labeled 6-1 uses the values for the coefficients determined by ANL rather than the values given in the WCAP

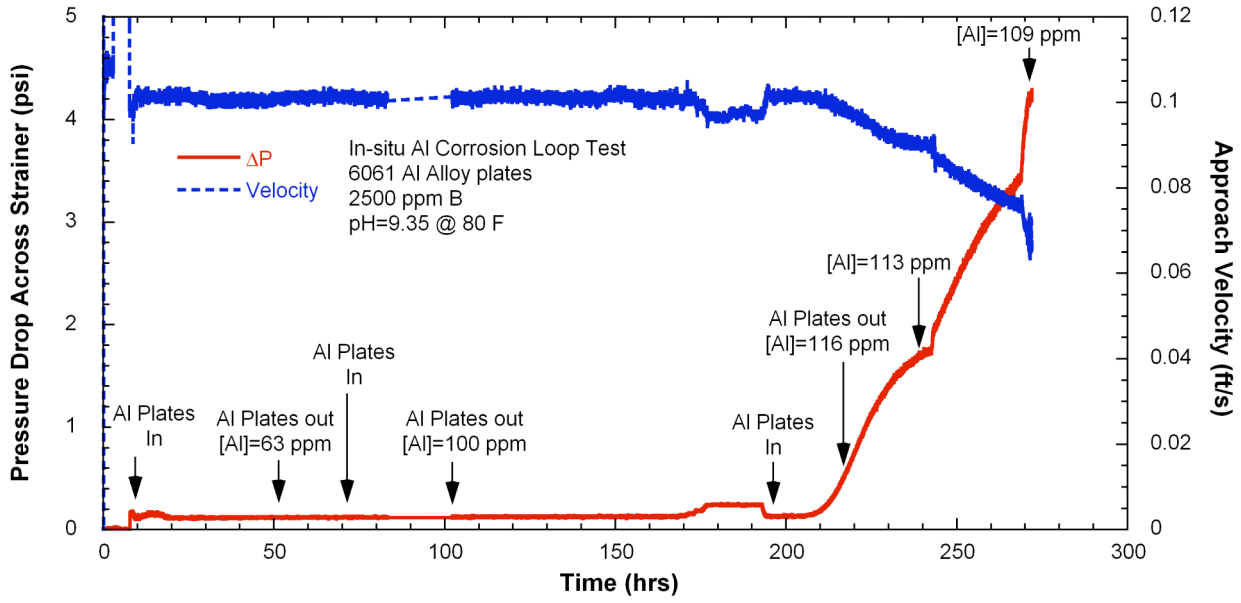

Figure 4. Pressure drop and screen approach velocity time history in a loop test using 6061 Al plates with 2500 ppm B and the initial pH=9.35 @ 80 F.

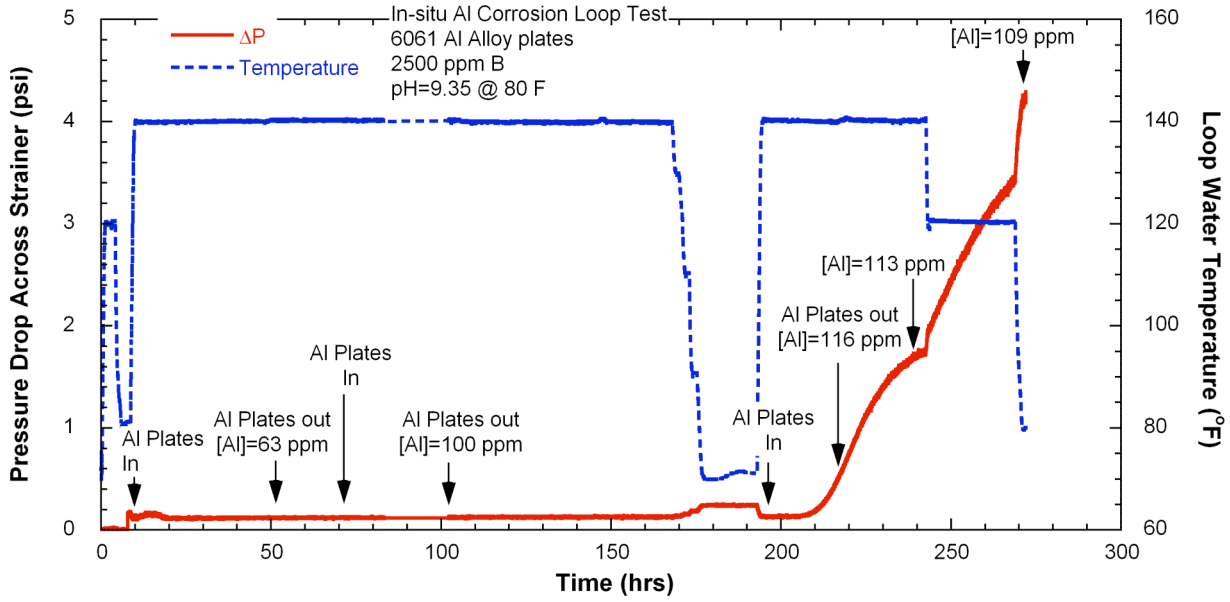

Figure 5. Pressure drop and loop water temperature time history in a loop test using 6061 Al plates with 2500 ppm B and the initial pH=9.35 @ 80 F.

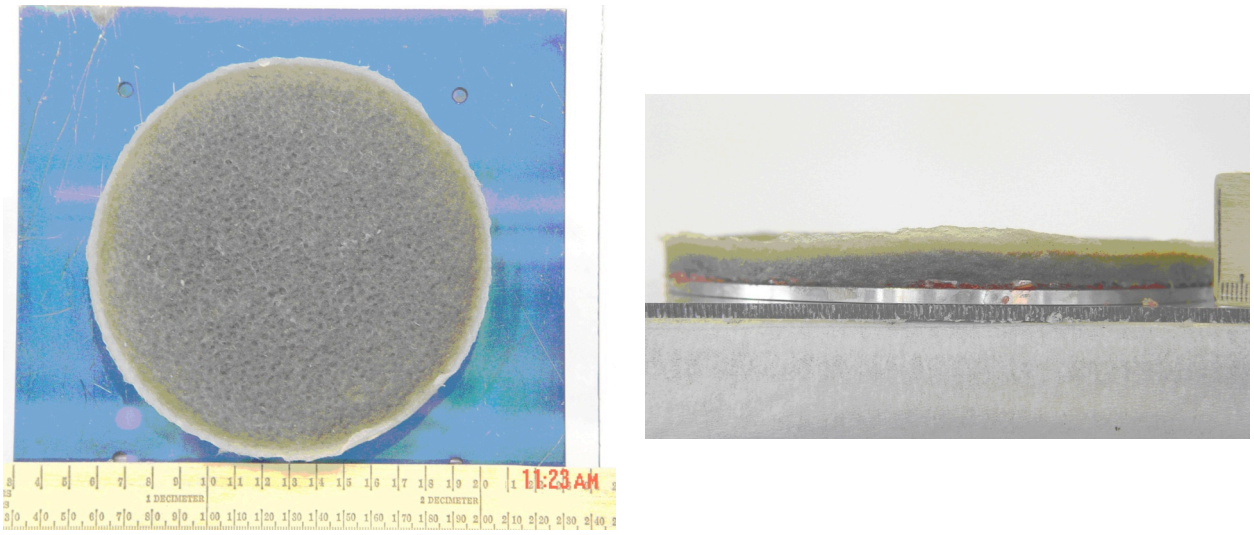

(a) top view (b) side view

Figure 6. NUKON glass fiber bed after the loop test with 6061 Al specimens showing (a) top view and (b) side view.

Post-Test SEM Analysis

After the test was finished and the loop shut down, the Al bundle was taken out. Figures 7a and 7b show the overall appearance of the test bundle and the 2nd Al plate from top, respectively. Figure 7a indicates some corrosion of the threaded Al rod, which contributes to the Al release rate. However, as noted previously, the exposed area of the rod is less than 2 % of the exposed area of the plates, so that the contribution from the rods is negligible. Figure 7b shows there are two distinct areas on Al surfaces: grayish black and metallic white areas. To characterize these two areas, a 5/8" by 1" section was taken from the 2nd Al plate specimen and placed in a scanning electron microscope (SEM). Figure 8a shows an SEM picture of the grayish black area on the Al specimen. Many particles with sizes ranging from 0.5 to 10 μm cover the whole surface. These particles are mainly composed of Al, Fe, Cu, Cr, Si, Mg, and Na according to EDS analysis. Compared with the original bulk Al alloy composition, Fe, Cu, Cr, and Si are enriched in the particles; the Na comes from the solution. The composition of the base material underneath the particles is very similar to that of a fresh coupon, which is shown in Table 1. In the metallic white area, as shown in Figure 8b, it is apparent even with the lower magnification used that the number density of the precipitates is much smaller than in the grayish black area. The chemical composition of the particles in the metallic white area is similar to that of the particles in the grayish black area. The particle-free region appears to be just Al metal surface, because the oxygen peak in the EDS analysis is negligible and the chemical composition is similar to that of the fresh Al coupons. Since the ICP analyses for loop water samples did not show any significant Fe or Cr concentration (less than 0.5 ppm), it appears that the Fe and Cr in the particles originated from the Al specimen itself. EDS spectra for the base material and the particles are summarized in Appendix A (see Figures A1 through A4).

During the loop test, the Al bundle was removed three times. Whenever the Al bundle was taken out, loosely–adhered, grayish–black particles were observed on the Al plates. Immediately after the Al specimen bundle was removed from the loop, the loosely adhered particles were collected with a tissue paper wipe. The precipitates were collected using adhesive carbon tape for SEM analysis. Figure 9 shows the SEM image for the particles on the carbon tape. The overall shape and size distribution are similar to those observed on the grayish black area shown in Figure 8a. The chemical composition of the particles in Figure 9 is similar to those in Figure 8a, but the EDS analyses show that the peaks for the non-Al elements, especially for Cu, Cr, and Si, are higher for the loose particles (cf. Figures A2 and A5). Also, the oxygen peak in the spectrum is higher, which suggests that the surfaces of these particles are more strongly oxidized. There was a particle-to-particle variation in terms of chemical composition; some particle showed higher enrichment of Cr and some particles showed higher enrichment of Cu or Si. The sodium concentrations in the particles are very low, only 2–7 at%, as shown in Figures A2 and A5. The ICP analyses in Table 2 show that boron concentration appears to be independent of temperature change. Therefore, although sodium borate crystallization might be possible, it does not appear that this compound is significant enough to consider. Further discussion of the characterization of the particles is presented in a later section.

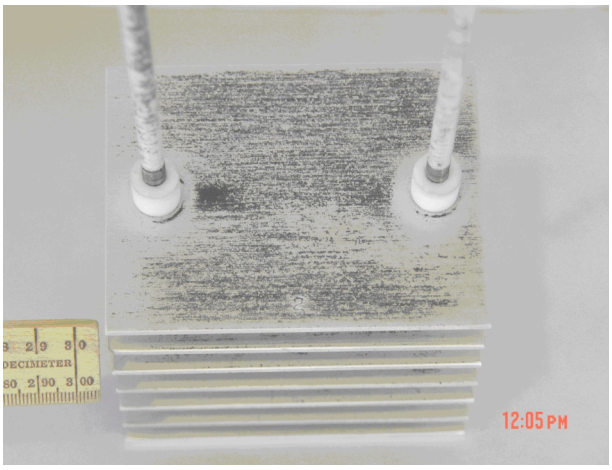

(a) test specimen bundle

(b) 2nd Al plate from top

Figure 7. Al specimens; appearance of (a) test specimen bundle and (b) 2nd Al plate from top after the loop test with 2500 ppm B and the pH=9.35 @ 80 F.

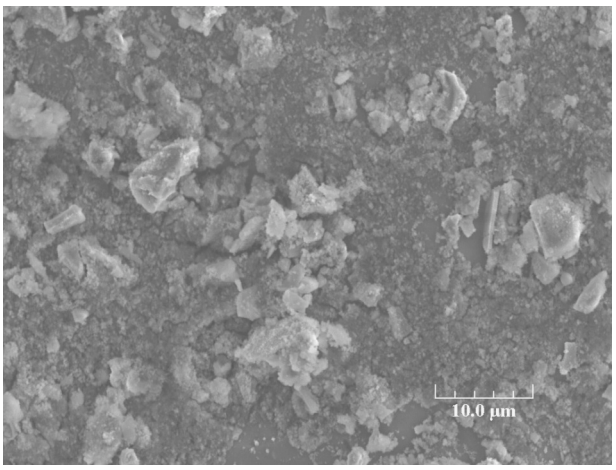

(a) Grayish black area

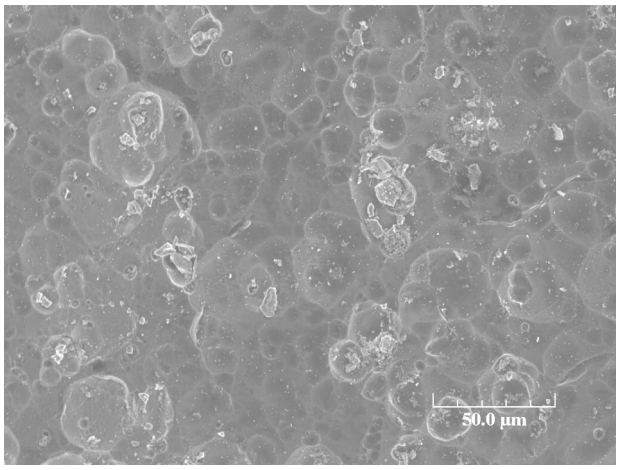

(b) Metallic white area

Figure 8. SEM images for two distinct surface areas formed on Al plates used in the loop test: (a) grayish black area and (b) metallic white area.

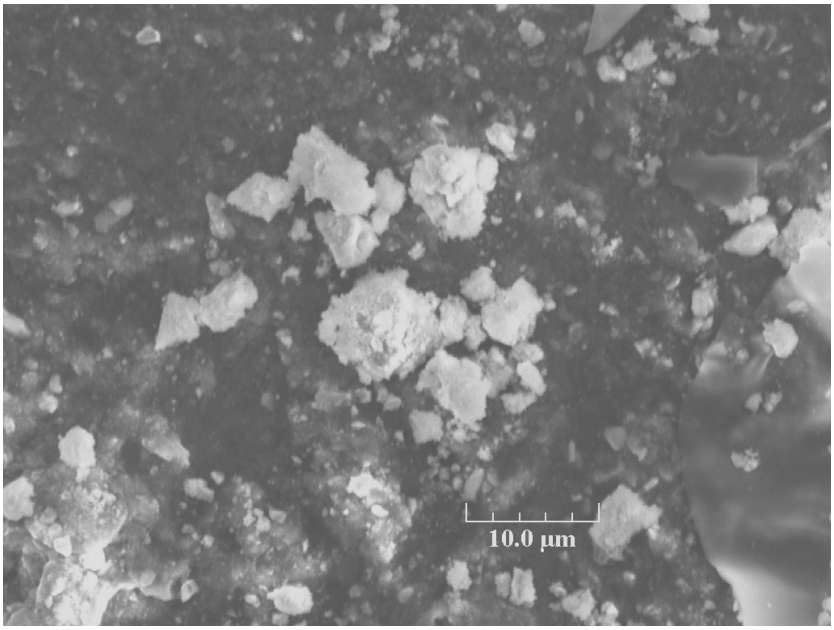

Figure 9.
SEM image for precipitates loosely adhered on the Al plate used in the loop test. Precipitates are attached to an adhesive carbon tape for analysis.

The particles trapped in the NUKON glass fiber bed were analyzed by SEM after completely drying the bed. The SEM/EDS analyses show that there are two kinds of particles attached to the fibers; one is composed of Al oxide with Na and Si and the other is similar to that found on the Al plate surfaces and mainly composed of Al, Si, Cr, Fe, Cu, Ca, and Na. The oxygen peak in this second type of particle is very weak compared with Al oxide particle. The Ca and Na peaks probably originate from the glass fiber and the test solution, respectively. Figure 10 shows SEM images of the particles attached to the NUKON fibers at two different locations. Particles appear to form on the Al surface, detach and transfer to the NUKON bed, and attach to the glass fibers. Detailed EDS spectra and chemical composition analyses for the precipitates are presented in Appendix A (see Figures A6 and A7).

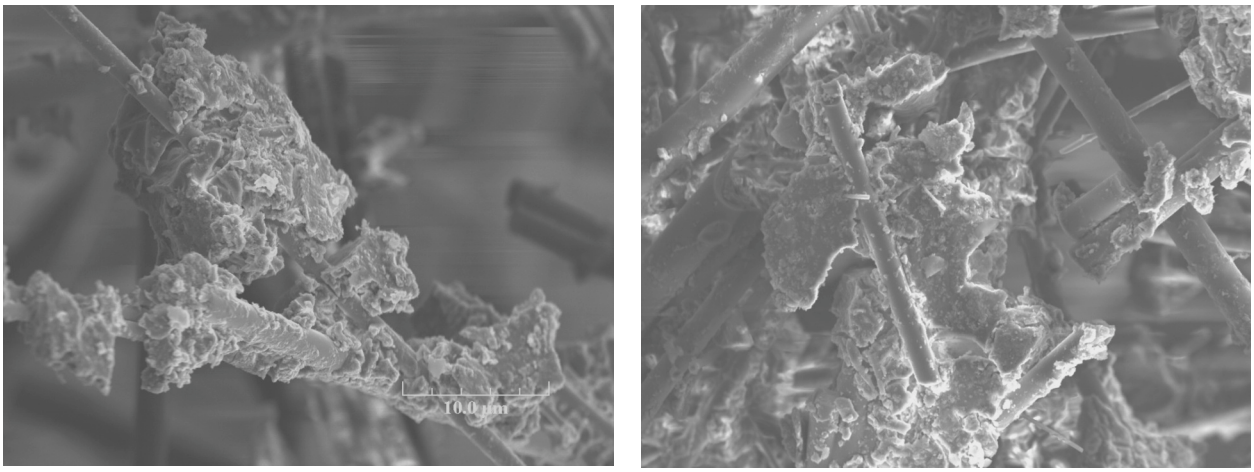

(a) (b)

Figure 10. SEM images for precipitates attached on the NUKON glass fiber bed at different locations.

The increase in head loss in this loop test can be attributed to both the grayish black particles and Al hydroxide precipitates. Numerous other tests performed in this work indicate that the solubility limit for amorphous $Al(OH)_3$ at pH 9.4 and 140°F is significantly greater than 116 ppm. Thus, the head loss observed at 140°F is probably attributable to the grayish–black AlSiFeCr particles generated from the Al coupon surfaces. These particles transport to the NUKON bed and accumulate there. The onset of the increase in pressure drop was fairly abrupt. The accumulated exposure time of the Al bundle had reached about 75 hours, and the loop had then been operated for an additional ≈ 75 hours at 140°F. The loop was then cooled down and the bundle re–inserted. The first indication of a pressure drop increase appeared at 140°F about 10 hours after the bundle was re-inserted. The Al bundle was kept immersed in the loop for another 10 hours and then removed. The pressure drop continued to steadily increase for about 15 hours and then started to level off and approach saturation about 30 hours after the bundle was removed. Based on the ICP analyses, there was a decrease of 3-ppm in Al concentration in the loop as the pressure drop increased after the removal of the bundle. This would seem to suggest that the bed is slowly removing Al–rich particles from the fluid. However, filtered and unfiltered solution samples did not show any significant difference, which would require that the particles should be very small. At this temperature, pH and Al concentration condition, precipitation of Al hydroxide within the bed seems unlikely, unless the presence of the process is somehow enhanced by the grayish particles trapped in the bed. Lowering the water temperature from 140 to 120°F caused a continuous increase of head loss without any sign of saturation. This suggests that the increase of the head loss was caused by precipitation, although even at 120°F, the concentrations seem low for precipitation of Al hydroxide. The head loss increase due solely to the change in viscosity as the water temperature changes from 140 to 120°F would be about 0.1 psi or less. Lowering the loop water temperature from 120 to 80°F caused additional increase of the head loss at an increased rate. This increase is consistent with expected behavior based on solubility limits under these conditions. ICP analyses for solution samples also showed that Al concentration decreased from 113 to 109 ppm after lowering the loop temperature. Since the estimated uncertainty in the ICP measurements is ≈1%, this corresponds to a decrease in the Al concentration of 4±2 ppm. As mentioned earlier, the solution sample drawn from the loop became cloudy after cooling to ambient temperature and on the bottom of the solution sample white precipitates were found.

The grayish particles are unlike any precipitation product we have seen from $Al(NO_3)_3$ or sodium aluminate solutions. The particles do seem to be able to produce increases in head loss under conditions in which Al hydroxide precipitates will not form.

In-situ Al Corrosion Test with 1100 Al in Vertical Head Loss Loop

Experimental

A head loss test similar to the test with 6061 Al alloy was performed with “commercially pure” Al plates (1100 Al, McMaster-Carr, Part# 88685K13) immersed in the loop solution as the source of dissolved Al. The chemical composition for 1100 Al is given in Table 3. The concentrations of impurity elements are much smaller than the corresponding values for the 6061 Al alloy. Major impurities are Fe, Si, and Cu.

Sample preparation procedures are the same as those of the previous test with 6061 Al. Figure 11 shows the photographs of the 1100 Al plates bundle and NUKON patches. Eight plates of 1100 Al (3” by 4”, 1/8” thick) were assembled using two 6061 Al rods, which were

fixed at a flange. In this test, six NUKON patches were exposed in the loop water to determine if any chemical compound like sodium aluminum silicate is formed on the surface of NUKON fibers during the test or Al hydroxide precipitates preferentially on the fibers, as shown in Figure 11 (b). Each patch was removed at different exposure time. Each NUKON patch was secure in a 304 SS wire mesh bag. The wire mesh bags had sufficient volume to ensure that the NUKON patches were not compressed. The 6061 Al rod was covered by Teflon so that the corrosion of the rod was minimized.

The procedures for preparing the test solution and the NUKON bed were the same as those used for the loop test with 6061 Al described in the previous section. The final pH of the solution before making the NUKON bed was 9.31 at 80°F. The flow in the loop was controlled to maintain a screen approach velocity of 0.1 ft/s during the development of the bed and throughout the test as in the previous test with 6061 Al. Once the pressure drop across the NUKON bed became stable, the Al bundle was installed in the tee port. The loop water temperature was then raised to 140°F to enhance Al dissolution. When the dissolved Al concentration reached a predetermined level, the Al bundle was taken out of the loop. Then, the loop ran overnight to determine if any significant head loss would occur at 140°F. The water temperature was decreased from 140 to 120°F and decreased again from 120 to 100°F. When the pressure drop across the screen started to increase at a given temperature level, the temperature was raised to determine whether the head loss would decrease by dissolution of precipitates or not.

Table 3. Specification of the chemical composition for 1100 commercially pure Al compared with measured results by EDS (wt%).

	Al	Si	Fe	Cu	Mn	Mg	Cr	Zn	Ti	Others
ASTM B209-06	99.00 min	0.95 Si+Fe max		0.05-0.20	0.05 max	-	-	0.10 max	-	0.15 max
Measured	99.75	0.07	0.14	NI[a]	NI	NI	0.05	NI	NI	

[a] Element was not included in the EDS spectrum analysis because signal was negligible.

Test Results

Figure 12 shows the total Al concentration in the loop water samples as a function of exposure time. The loop water samples were not filtered, and at each time, duplicate samples were analyzed by ICP/OES. The Al release rate of the 1100 Al is significantly higher than the release rate observed in the 6061 Al test, and the Al release of the 1100 Al appears linear with time over the test period. The differences in release rate appear comparable to similar results reported in the literature. Griess and Bacarella[7] reported that 6061 and 1100 Al corrosion rates were similar in a spray of 3000 ppm B and pH=9.4-9.5 solution at 55°C, but when immersed in the same solution the 6061 Al corrosion rate was about 75% of that of 1100 Al, which appears to be consistent with our Al corrosion loop tests. The release rate of 1100 Al in the loop is significantly higher than the predictions of Eq. (1), which is based on bench top corrosion tests of 1100 Al. This discrepancy suggests that flow rate affects the Al release rate. However, in most cases, the actual flow rate in the sump will be much less than 0.1 ft/sec used in the loop tests. The analyses for loop water samples are summarized in Table 4.

Figure 13 shows the pressure drop across the bed and the approach velocity as a function of time. Figure 14 shows the loop water temperature and the pressure drop as a function of time. During the period of the test between 40 and 48 hours, a linear increase of head loss was observed. About 3-in thick gas layer had developed underneath the NUKON bed during the period (an over night portion of the test). The sudden decrease of head loss at the test time of 48 hour was associated with opening a valve and bleeding the gas out.

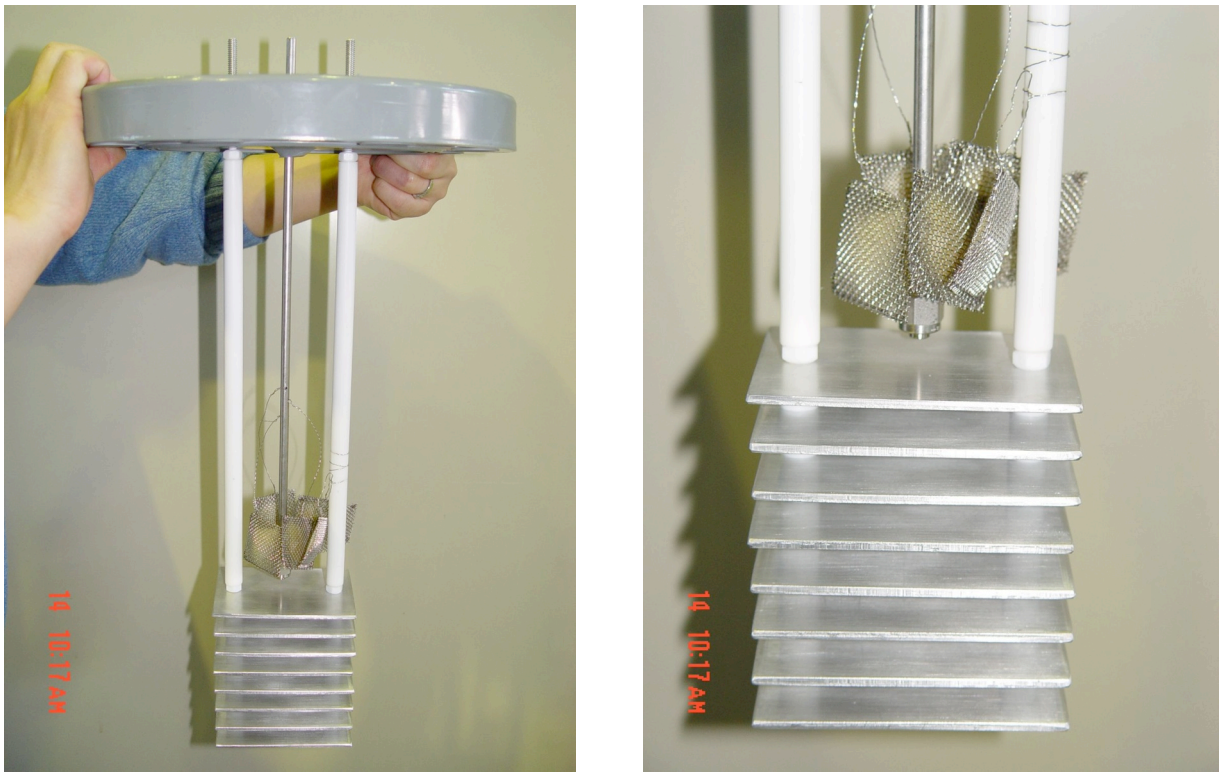

(a) Overall view (b) NUKON patches

Figure 11. Photographs for (a) 1100 Al plates bundle and (b) six NUKON patches (in wire mesh bags).

Even after the gas layer was removed, the pressure drop did not immediately return to the initial value. However, after removing the Al plates from the loop, the pressure drop gradually decreased overnight and came back to the initial value. These observations seem to suggest that the source of the gas is corrosion of the Al plates. Eq. (2) shows the anodic and cathodic reactions for Al dissolution. One mole of Al dissolves into the loop water and generates three mole of electron (anodic reaction); three mole of water molecule reacts with the electrons generated by Al dissolution and generates 1.5 moles of hydrogen gas (cathodic reaction). Since the loop water is alkaline, the Al ion would become $Al(OH)_4^-$.

$$\begin{aligned} &Al \Leftrightarrow Al^{3+} + 3e \quad \text{(anodic)} \\ &3H_2O + 3e \Leftrightarrow \frac{3}{2}H_2 + 3OH^- \quad \text{(cathodic)} \end{aligned} \tag{2}$$

The total Al concentration in the loop water when the Al plates were taken out was 118 ppm (4.37 mmol/kg). The total volume of the loop water is 118 kg and assuming that Al dissolution

occurs at ambient pressure and 140°F, the total volume of hydrogen gas generated by Al dissolution of 118 ppm can be estimated by using the equation of state of ideal gas:

$$V = \frac{nRT}{p}. \tag{3}$$

In Eq. (3), V is the gas volume, n is the total mole of hydrogen gas, R denotes the universal gas constant, T is the absolute temperature, and p is the pressure. The estimated hydrogen gas volume equivalent to the 118 ppm of Al dissolution is about 20 L, which is a large volume compared to the volume of the 3-in thick gas layer, which is about 1 L. Therefore, the volume of hydrogen gas created by the Al dissolution is more than sufficient to account for the gas layer underneath the bed. The decrease of the pressure drop after taking out Al plates can be attributed to the removal of hydrogen source and the escape of trapped hydrogen bubbles in the bed. Since in an actual nuclear power plant the free containment volume is very large compared to the free volume in the ANL loop, the hydrogen gas would easily escape from the sump water so that no significant head loss due to hydrogen gas bubbles would be expected.

After removing the Al plates, the loop was run at 140°F for additional 24 hours to determine if any head loss would occur at 140°F as in the 6061 Al test. No significant increase of head loss was observed. The water temperature was then decreased to 120°F. The head loss remained constant for a hold of approximately 24 hours. The temperature was then reduced to 100°F. As shown in Table 4, the samples taken immediately before decreasing the temperature from 120 to 100°F indicated an Al level of 115 ppm. Unfiltered and filtered samples using 20-nm size filters gave almost identical results. The measured concentration at 140°F was 118 ppm. Considering the uncertainties associated with the ICP measurements, this suggests that 2–4 ppm of Al was removed from the loop water at this point. Since an addition of WCAP surrogate corresponding to a decrease of 1.5 ppm Al was sufficient to plug the bed, this suggests that the Al was trapped by the bed in a different manner, perhaps as very fine Al hydroxide or alumino-silicate deposits on the NUKON fibers. About 30 hours after the temperature was decreased to 100°F, the pressure drop started to gradually increase. The rate of increase accelerated until the water temperature was increased up to 120°F. The samples of the loop solution taken immediately before increasing the temperature to 120°F indicated a total of 110 ppm of Al unfiltered and 80 ppm filtered. This suggests that Al hydroxide precipitates larger than 20 nm were formed and circulating in the loop. The 5 ppm reduction in total Al compared to Al in the solution immediately before the temperature was decreased from 120 to 100°F was associated with an increase in head loss of 1.2 psi. The temperature was increased from 100 to 120°F to try to control the increase in head loss. A decrease of head loss was expected because of dissolution of Al hydroxide precipitates trapped in the NUKON bed at the higher temperature. During the first 1.5 hours after the temperature was increased, the pressure drop did decrease, but then began to increase rapidly and within 3 hours exceeded the loop capacity. The rapid increase of pressure drop occurred overnight, and the loop was shut down the next morning. A sample taken before shutdown indicated 79 ppm of Al, which suggests Al hydroxide precipitates equivalent to 31 ppm of Al were filtered by the NUKON bed after increasing the loop temperature. This apparent continued formation of Al hydroxide precipitation after increasing the water temperature is inconsistent with our bench top test results on solubility as a function of temperature and pH. This issue is further explored in the Discussion section. The reported Al concentration in the filtered sample taken just before shut-down (06-10c) is higher than the reported Al concentrations in the unfiltered samples (06-10a and 06-10b). This is an artifact, probably due to contamination during sampling or analyzing.

Figure 15 shows the top and side views of the NUKON bed after the loop test. On the top of the bed Al hydroxide gel was formed, which was confirmed by SEM/EDS analysis. A grayish black area is observed under the Al hydroxide gel, which suggests that the grayish black particles were trapped in the NUKON bed, as was the case in the 6061 Al test.

Table 4. ICP analyses for loop solution samples of the 1100 Al test.

Sample No.	Sample Description	Dissolved Ion Concentration (mg/L)				
		Al	B	Ca	Si	Na
06-02	Taken before Al bundle installation	<0.5	NA[a]	NA	NA	NA
06-03a	Taken at t = 25.3 h (t_{ex} =16.3 h), Unfiltered	51.3	NA	NA	NA	NA
06-03b	Duplicate sample of 06-03a	52.0	NA	NA	NA	NA
06-04a	Taken at t = 33.0 h (t_{ex} =24.0 hr), Unfiltered	75.4	NA	NA	NA	NA
06-04b	Duplicate sample of 06-04a	75.0	NA	NA	NA	NA
06-05a	Taken at t = 49.2 h (t_{ex} = 40.2 h), Unfiltered	117	NA	NA	NA	NA
06-05b	Duplicate sample of 06-05a	119	NA	NA	NA	NA
06-08a	Taken prior to cooling down from 120 to 100 F, t = 97.8 h, Unfiltered	115	2250	1.02	1.08	2650
06-08b	Duplicate sample of 06-08a	115	2250	1.25	1.16	2630
06-08c	Taken prior to cooling down from 120 to 100 F, t = 97.8 h, 20 nm filtered	116	2240	<0.5	1.14	2590
06-09a	Taken prior to heating up from 100 to 120 F, t = 176.7 h, Unfiltered	110	2230	0.50	1.08	2610
06-09b	Duplicate sample of 06-09a	109	2220	1.20	1.06	2570
06-09c	Taken prior to heating up from 100 to 120 F, t = 176.7 h, 20 nm filtered	79.5	2210	<0.5	0.65	2590
06-10a	Taken prior to shutting down, t = 193.2 h Unfiltered	79.8	2230	0.54	0.76	2610
06-10b	Duplicate sample of 06-10a	78.8	2200	<0.5	0.77	2560
06-10c	Taken prior to shutting down, t = 193.2 h 20 nm filtered	90.0	2230	<0.5	0.81	2590

[a] NA indicates the element was not analyzed.

[b] t denotes total test time, t_{ex} denotes exposure time of the Al plates.

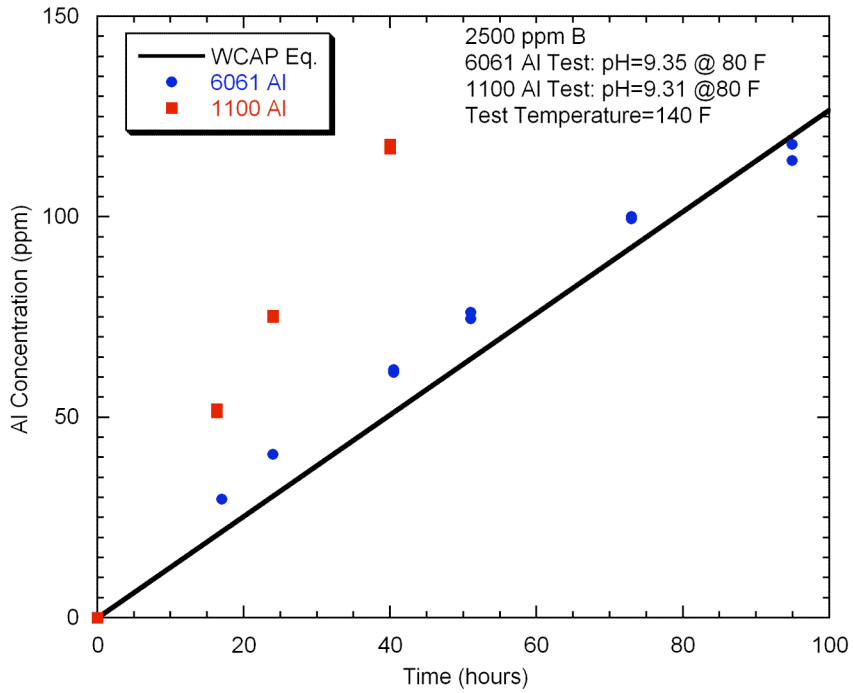

Figure 12.
Total Al concentration in the loop water of the 1100 Al test analyzed by ICP/OES as a function of exposure time compared to the results of the 6061 Al test and the predicted results using WCAP-16530, Eq. (1), with the coefficients modified by ANL.

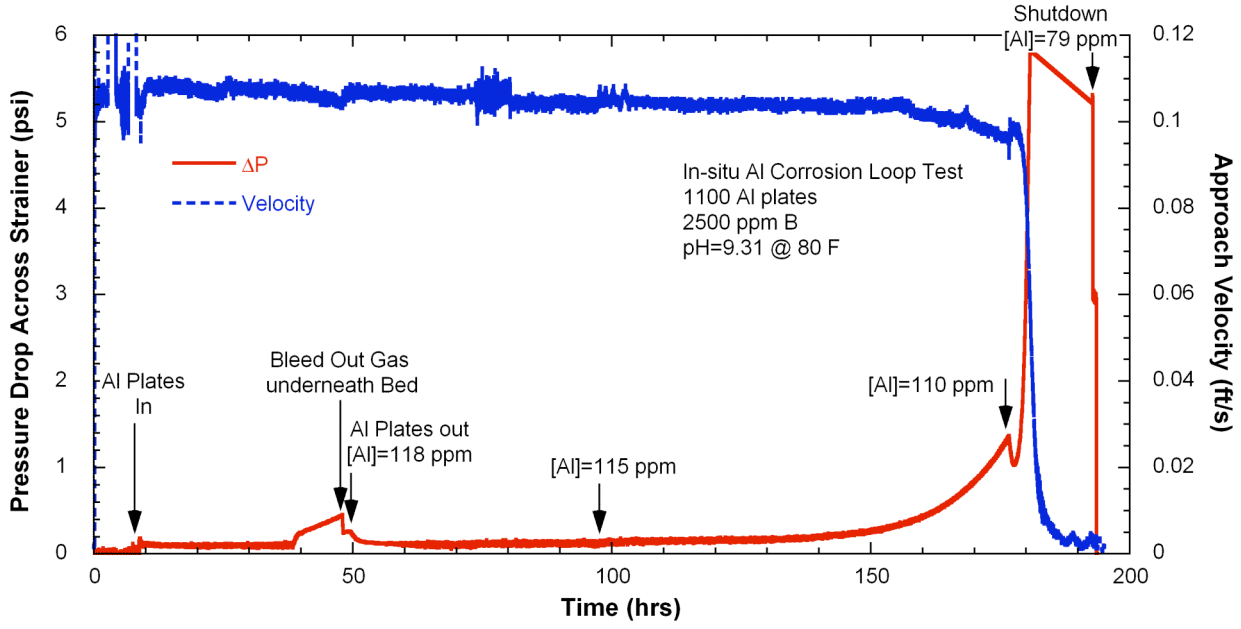

Figure 13. Pressure drop across a strainer and approach velocity time history in the 1100 Al loop test.

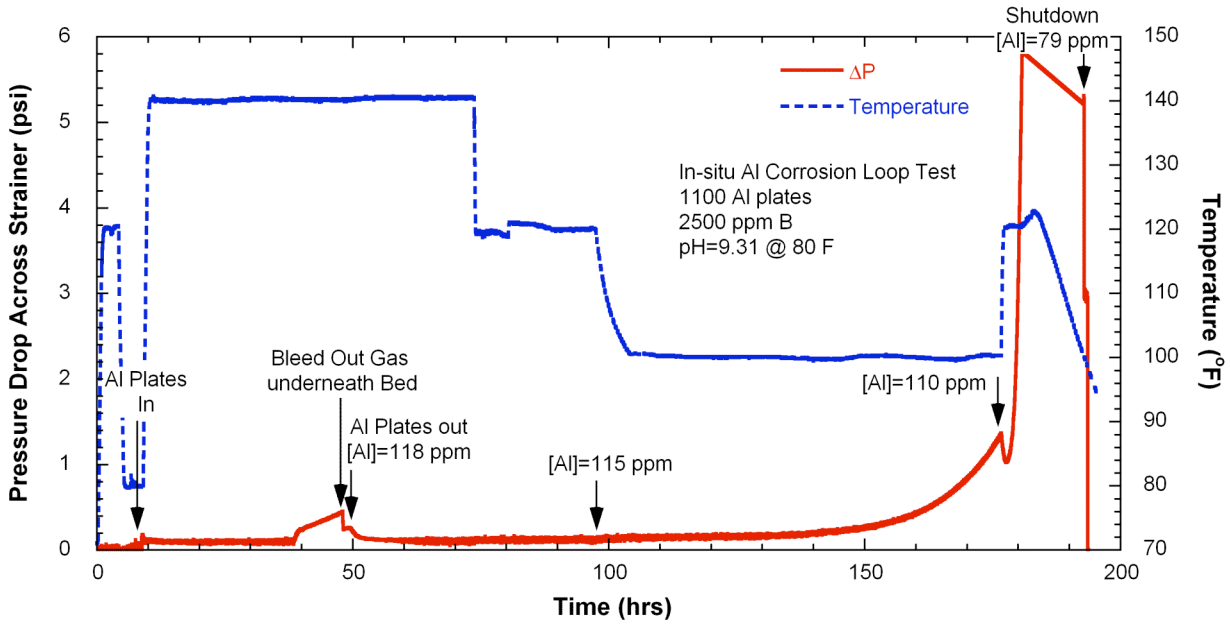

Figure 14. Pressure drop across the strainer and temperature time history in the 1100 Al loop test.

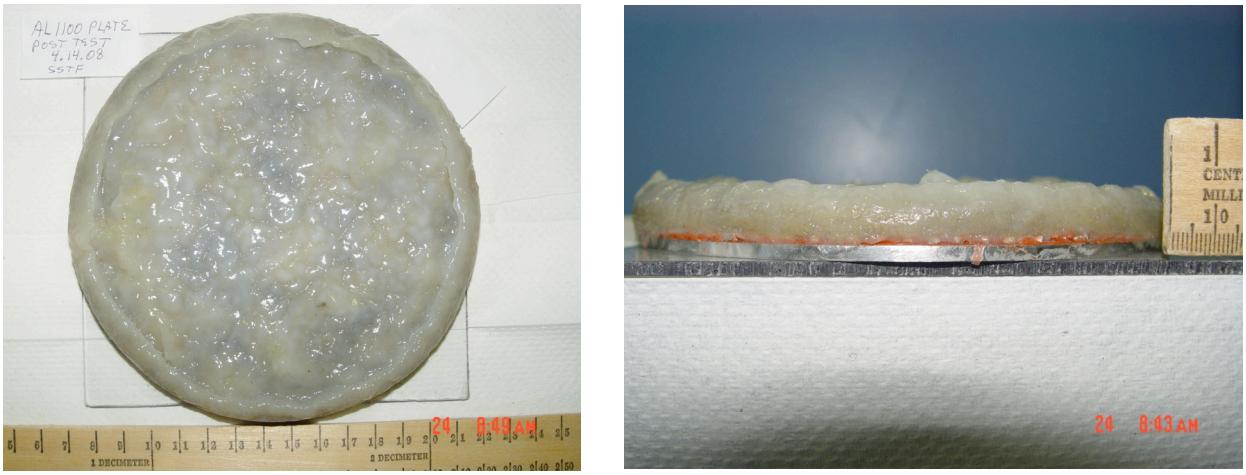

(a) top view (b) side view

Figure 15. NUKON glass fiber bed after the loop test with 6061 Al specimens showing (a) top view and (b) side view.

Post-Test SEM Analysis

Figure 16 shows the surface of one of the Al plates after the loop test. Its appearance is quite different from that of the 6061 Al plates (Figure 7). There is no significant amount of grayish area and most of the surface appears to be covered by oxide. To analyze surface morphology and chemistry, a plate was sectioned and examined using SEM. Figure 17 shows

SEM micrographs of the Al plate surface. A thick Al oxide was formed, as also observed for the 6061 Al plate. The back-scattered electron image (Figure 17 (b)) shows the presence of particles including Fe and Cu in the Al hydroxide precipitates and on the oxide surface. The region where heavier elements are present is brighter in the image. The size of particles ranges from sub-micron to 3 micron, smaller than in the case of the 6061 Al. EDS analyses of the spots designated as 1, 2, and 3 in Figure 17 (a) are presented in Appendix A (see Figures A8-A10).

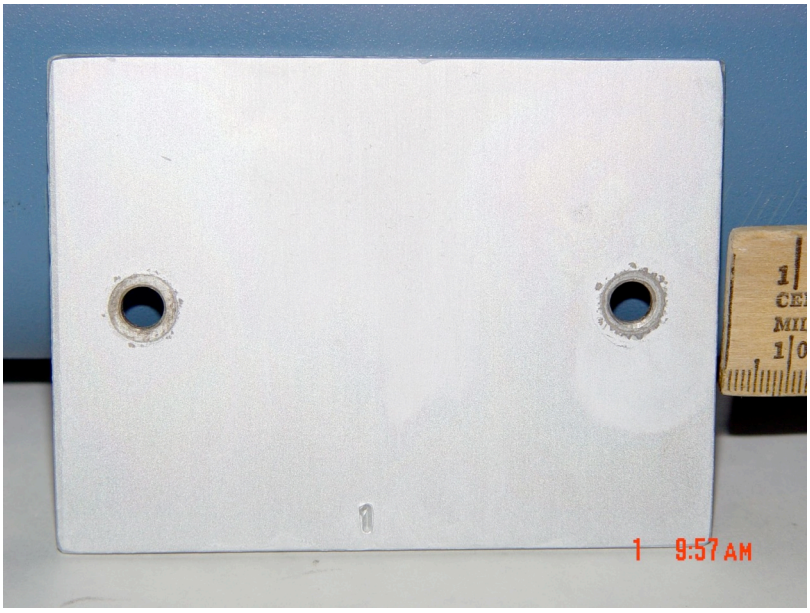

Figure 16. Photograph of the Al plate used in the 1100 Al corrosion loop test.

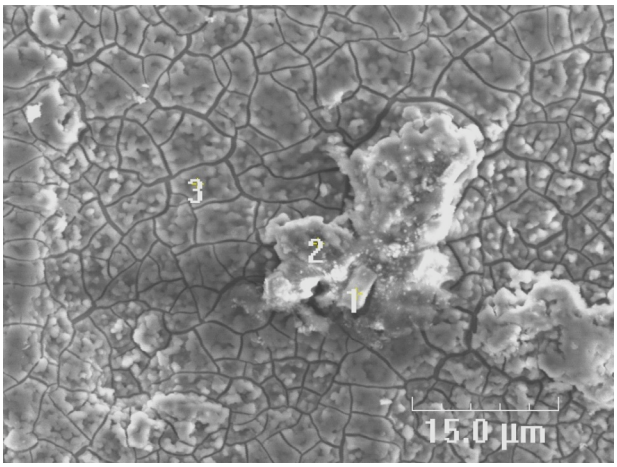

(a) Secondary electron image

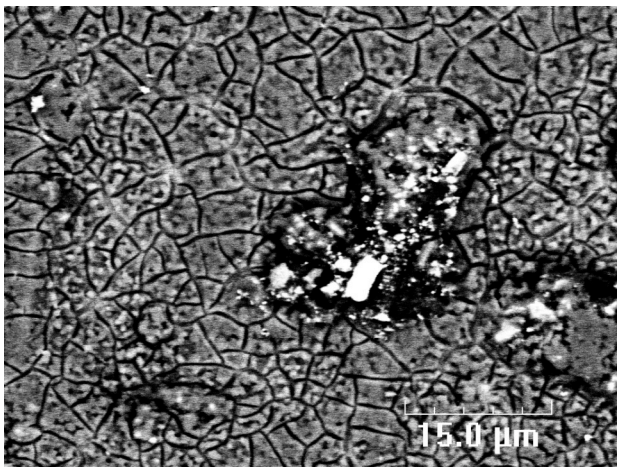

(b) Back-scattered electron image

Figure 17. SEM micrographs for 1100 Al plate used in the loop corrosion test with (a) secondary electron and (b) back-scattered electron.

The NUKON bed was also examined using SEM after drying the bed. Figure 18 shows SEM micrographs of the top side of the NUKON bed. The thick scales were mainly composed of Al hydroxide. Some sodium was detected probably because of NaOH precipitation while drying the NUKON bed. The analyses confirmed that the thick gel layer formed on the top of the bed was Al hydroxide. Figures 19 and 20 show SEM micrographs of the middle region of the NUKON bed. Al hydroxides are formed on the fibers but not as much as the top region of the bed. As shown in Figure 20(b), back-scattered electron image reveals the presence of Fe-Cu enriched particles. Figures 21 and 22 show the SEM micrographs from the bottom side of the NUKON bed. Compared to the middle region, the volume of Al hydroxide precipitation is larger. At the bottom side of the bed, Fe-Cu enriched particles are also observed, as shown in Figure 22(b). The size distribution of the particles looks similar to that on the Al plate surface. The SEM examination strongly suggests that Fe-Cu enriched particles were released from the 1100 Al plates and trapped in the NUKON bed before the formation of Al hydroxide gel on the top of the bed. However, since the particle sizes are relatively small, they have been trapped only after Al hydroxide precipitation had decreased the effective pore size of the NUKON bed.

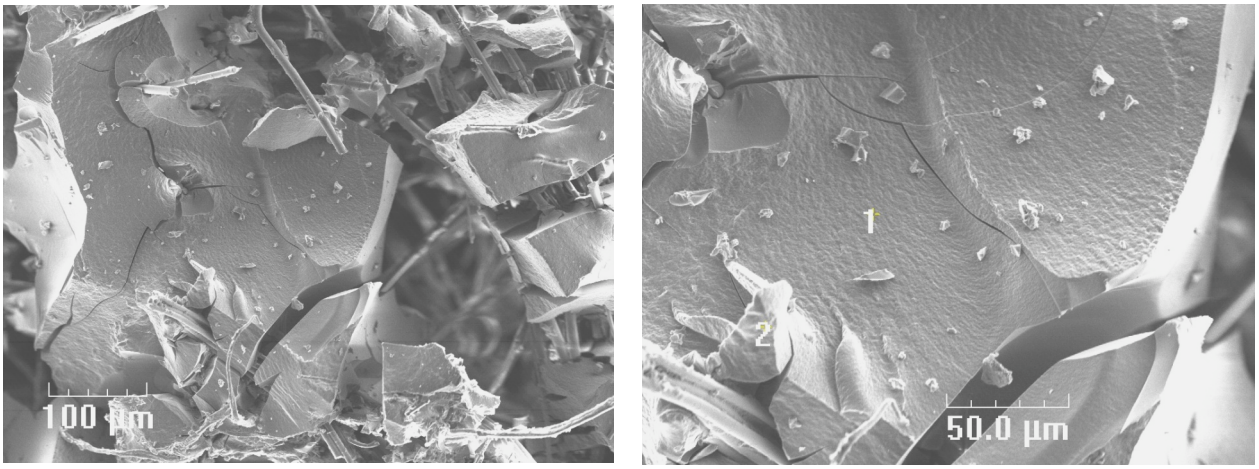

(a) 200X (b) 500X

Figure 18. SEM micrographs for the top side of the NUKON bed after the 1100 Al corrosion loop test with (a) 200X and (b) 500X magnifications. EDS analyses of spots 1 and 2 are presented in Figures A11-A12.

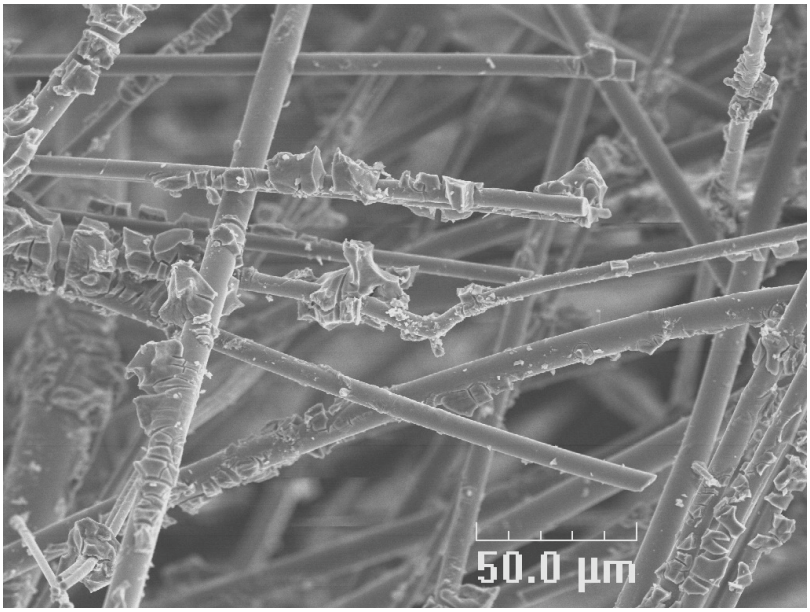

Figure 19.
SEM micrograph for the middle region of the NUKON bed after the 1100 Al corrosion loop test (500X magnification).

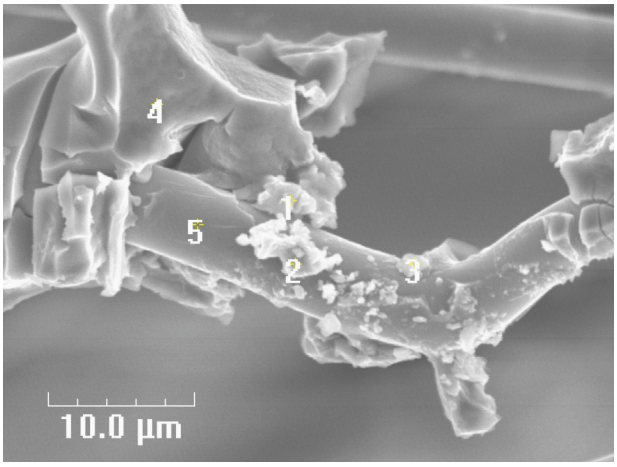

(a) Secondary electron image

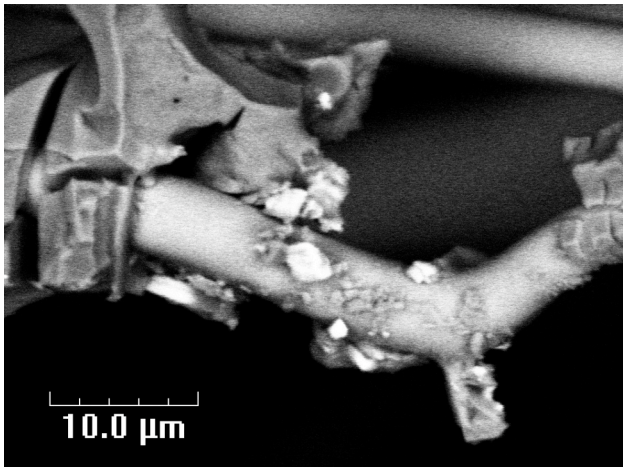

(b) Back-scattered electron image

Figure 20. SEM micrographs for the middle region of the NUKON bed after the 1100 Al corrosion loop test at a higher magnification than Figure 19 with (a) secondary electrons and (b) back-scattered electrons. The EDS spot analyses are presented in Figures A13-A17.

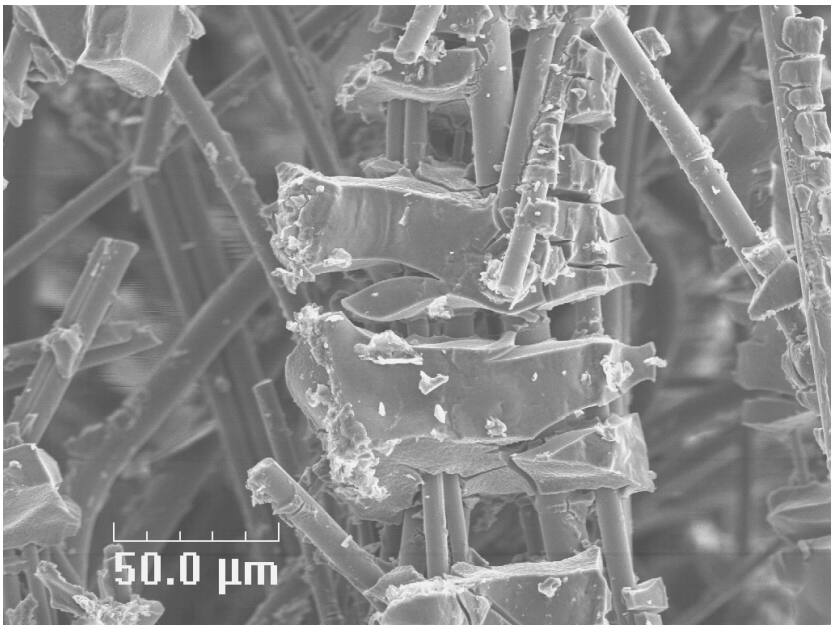

Figure 21.
SEM micrograph for the bottom side of the NUKON bed after the 1100 Al corrosion loop test (500X magnification).

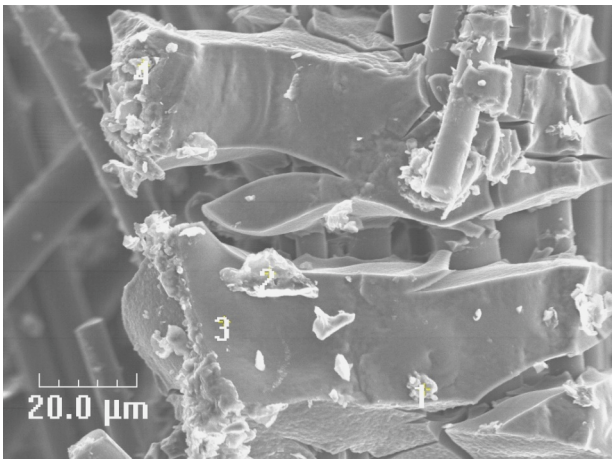

(a) Secondary electron image

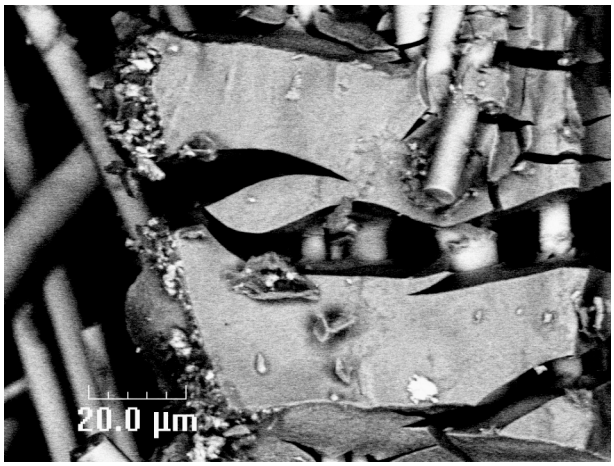

(b) Back-scattered electron image

Figure 22. SEM micrographs for the bottom side of the NUKON bed after the 1100 Al corrosion loop test at a higher magnification than Figure 21 with (a) secondary electrons and (b) back-scattered electrons. The EDS spot analyses are presented in Figures A18-A21.

NUKON Patch Analysis

Six NUKON patches were placed in the loop. Five of the patches were taken out before the loop was shut down. Figure 23 shows SEM micrographs of unexposed NUKON fibers and the five NUKON patches from the loop test. All micrographs have the same magnification of 500X. NUKON patch #1 was taken out 24 hours after the startup ([Al]=75 ppm); #2 was taken out when the Al plates bundle was taken out ([Al]=118 ppm; t = 49 h); #3 was taken out 24 hours after the removal of the Al plates (t = 73 h); #4 was taken out at the end of the 100°F portion of

the test (t =177 h); and #5 was taken out at 120°F just before the loop shut down t ≈ 185 h). Since a carbon coating was applied to all NUKON samples, some carbon particles were observed on fibers. On unexposed NUKON fibers, Ca and Mg enriched oxides were observed, which were also observed in the NUKON bed. Ca-Mg enriched oxide particles seem to be transferred and trapped in the NUKON bed, but it does not appear that these particles caused any significant head loss because the particle size is relatively small (~5 micron) and the number density is very low. In all of the NUKON patches, NaOH precipitates were detected on the fibers. In NUKON patches #2 through #5, Al enriched oxide precipitates were observed. It is not clear whether the Al-enriched precipitates are sodium aluminum silicates or Al hydroxides covered by Na hydroxides on fiber, except for patch #5. In the case of #5, as shown in Figure 23(f), SEM/EDS analysis confirmed that Al hydroxide precipitates covered the NUKON fiber. These Al hydroxide precipitates do not appear to be formed during drying the NUKON patch at ambient condition because #2, #3, and #4 did not show significant Al precipitates on fibers even though they were taken out at higher Al concentration in the loop test solution. This suggests that Al hydroxide precipitation occurred after increasing the loop water temperature from 100 to 120°F not only in the NUKON bed but also in the NUKON patch. In Figure 23, some precipitates are observed on the fiber but most of them are NaOH precipitates formed during the drying process at ambient condition. Al-enriched precipitates were difficult to find except for patch #5. SEM micrographs with higher magnification and EDS spot analyses for the NUKON patches are presented in Appendix A (see Figures A24-A27).

Surfaces of fibers from all NUKON patches, not visually covered by other precipitates, were examined by SEM/EDS to determine if a thin layer sodium aluminum silicate was formed on the fiber surface as has been hypothesized to explain the low rate of dissolution of NUKON fibers in solutions containing dissolved Al. Unexposed NUKON fibers were also analyzed as a reference. Figure 24 shows the atomic ratio between Na, Si, and Al on the fibers of NUKON patches as a function of acceleration voltage. NUKON contains Ca (~5 at%) and Mg (~5 at%) but they are not included in this analysis. As the acceleration voltage is lowered, the penetration depth of the electron beam becomes shallower. Therefore, elemental concentration data at lower acceleration voltages tend to give elemental information closer to surface. For the unexposed NUKON, Al concentration is independent of the acceleration voltage but Na is enriched inside the NUKON fiber. Since the NUKON contains Si, Na, Al, Mg, and Ca, this is called soda-lime alumino-silicate glass and its general formula can be described as $x\mathrm{CaO}\cdot y\mathrm{MgO}\cdot(1-x-y)\mathrm{Na_2O}\cdot z\mathrm{Al_2O_3}\cdot(3-z)\mathrm{SiO_2}$.[8] The molar ratio between the alkali metal oxides and the sum of aluminum and silicone oxides is 1:3. The EDS data for the unexposed NUKON using 10 kV, give values of the ratio very close to 1:3. On the surface of the NUKON fiber silicon oxide may be more dominant, which caused the offset from the predicted ratio of 1:3.

Figure 24(a) suggests that Al becomes enriched in the fiber surface during the loop test compared to unexposed NUKON, especially in the case of NUKON patch #5. For patches #3, #4, and #5, like the Al concentration, the Na concentration gradually increases, but the atomic ratio of Na is less than that of the unexposed NUKON fiber. This appears to suggest that on the fiber surface Na was dissolved out at early stage, and then a Na and Al mixture compound was formed at later stage. However, it is difficult to determine whether a thin sodium aluminum silicate layer is formed or whether there is a Al hydroxide layer on the surface covered by NaOH precipitation. As shown in Figure 24 (b), the Na concentration inside the NUKON fibers is always less than that of the unexposed NUKON, and Al concentration appears to be constant. As observed in the Figure 24 (b), Na in the NUKON fiber appears to be dissolved into alkaline water at high temperature. The chemical composition data used to develop Figure 24 is summarized in Table A1.

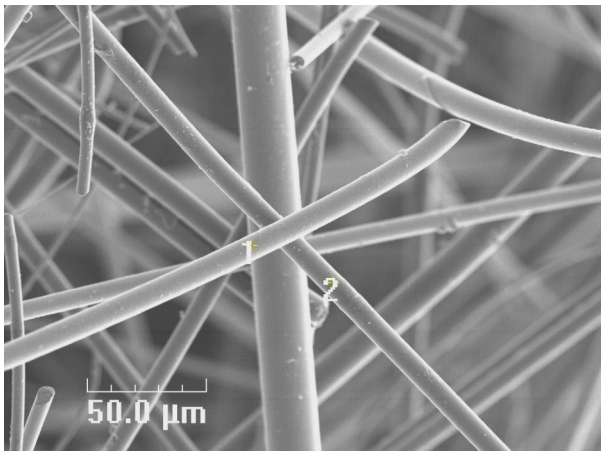

(a) Unexposed NUKON fiber

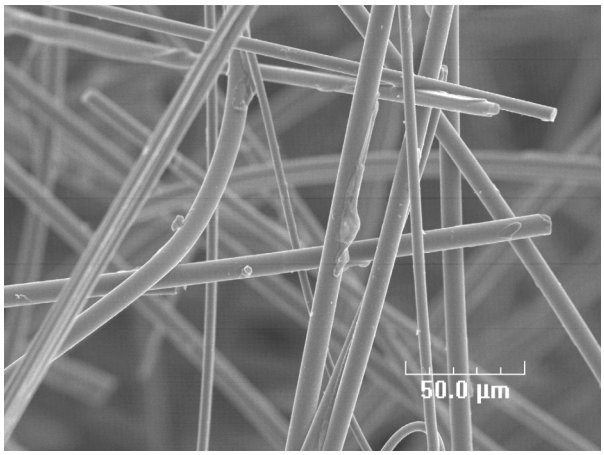

(b) #1 NUKON patch

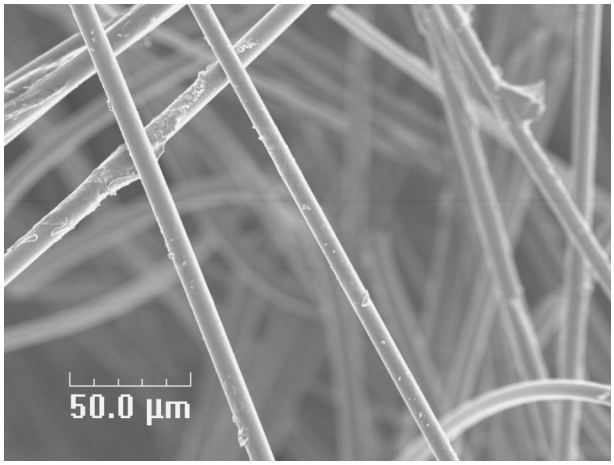

(c) #2 NUKON patch

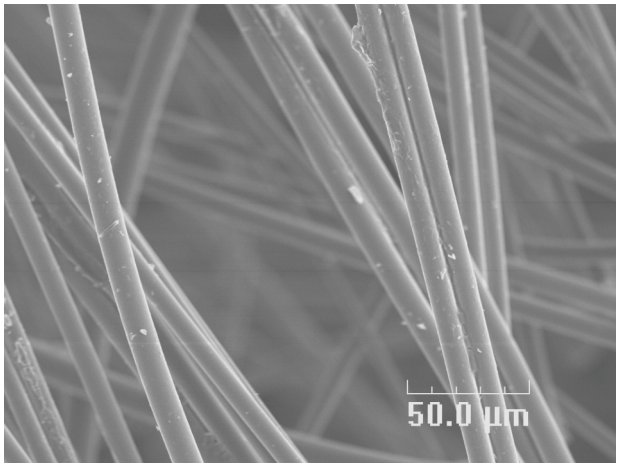

(d) #3 NUKON patch

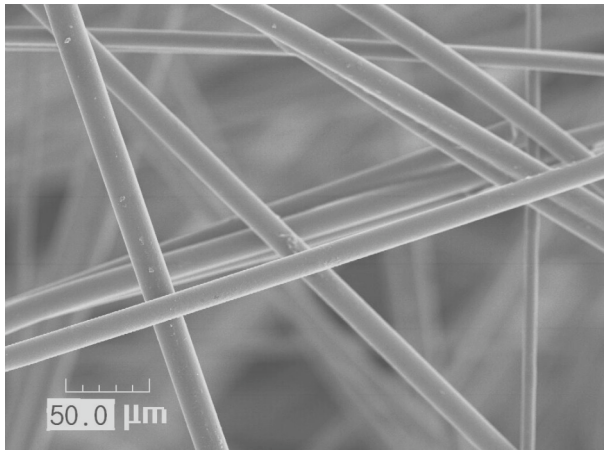

(e) #4 NUKON patch

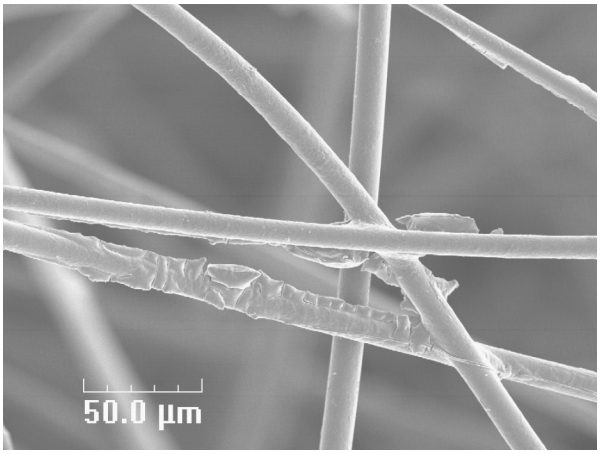

(f) #5 NUKON patch

Figure 23. SEM micrographs for NUKON patches (500 X magnification); (a) unexposed NUKON, (b) #1 NUKON, (c) #2 NUKON, (d) #3 NUKON, (e) #4 NUKON, and (f) #5 NUKON. The EDS spot analyses for the unexposed NUKON fiber are presented in Figures A22-A23.

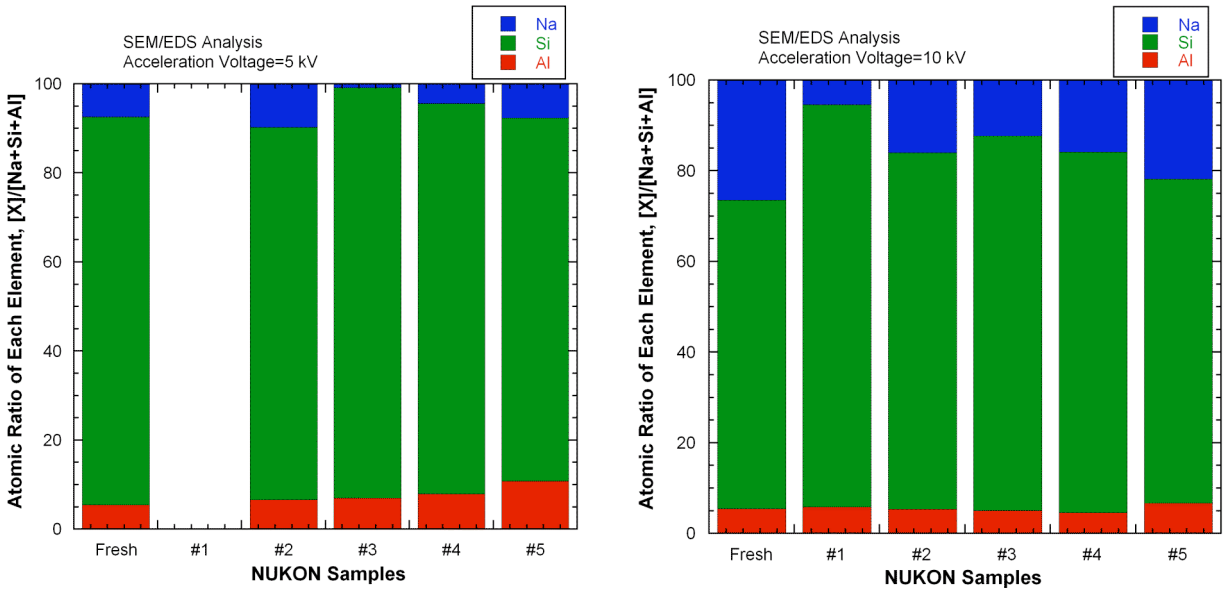

(a) Acceleration voltage=5 kV (b) Acceleration voltage=10 kV

Figure 24. Atomic ratio between Na, Si, and Al on the fibers of NUKON patches as a function of acceleration voltage analyzed by SEM/EDS: (a) 5 kV and (b) 10 kV.

To further examine whether or not sodium aluminosilicate (albite, $NaAlSi_3O_8$) was formed on the fibers, the patches were investigated by X-ray diffraction (XRD). The XRD patterns were developed using a Phillips XPERT-PRO diffractometer operated at 40 kV and 40 mA using CuKα radiation. Figure 25 shows the XRD patterns for unexposed NUKON and NUKON patch #5, removed just before shutdown. Figure 25(b) shows XRD patterns in a narrower region around the major peak. NUKON #5 shows an amorphous background and clear peaks at 2θ=22, 24, and 40 degrees. Based on literature data[9] and ANL's XRD data[10], bayerite ($Al(OH)_3$) has major peaks at 2θ=18, 20, 28, 41 degrees. Other literature data shows that albite[11] has major peaks at 2θ=22, 24, 28, and 36 degrees, aluminum silicate[12] (kaolinite, $Al_2Si_2O_5(OH)_4$) has major peaks at 2θ=12.5, 18, 25, and 30 degrees, and aluminum borate[13] ($Al_4B_2O_9/Al_{18}B_4O_{33}$) has major peaks at 2θ=17, 20, 26, and 33 degrees. Aluminum borate precipitates were obtained at 80°C by mixing chemical solutions but the precipitates were amorphous at that temperature.[12] Since the measured peaks do not exactly match any of the possible precipitates, it is difficult to determine whether observed peaks are from sodium aluminosilicate or something else. It is likely, however, that those peaks are bayerite, because we know that in NUKON patch #5 Al-enriched oxides were formed. Thin amorphous albite, aluminum silicate, or aluminum borate film might be possible but it is impossible to detect amorphous phase by XRD. The unexposed NUKON shows peaks similar to those for NUKON #5, although signal intensity is very weak. It is not clear whether it is reasonable to assume that unexposed NUKON has Al hydroxide phase or not. These uncertainties make it difficult to determine whether sodium aluminosilicate phase is present on the NUKON fiber exposed in alkaline high temperature water, and further examination would be needed to get more conclusive results.

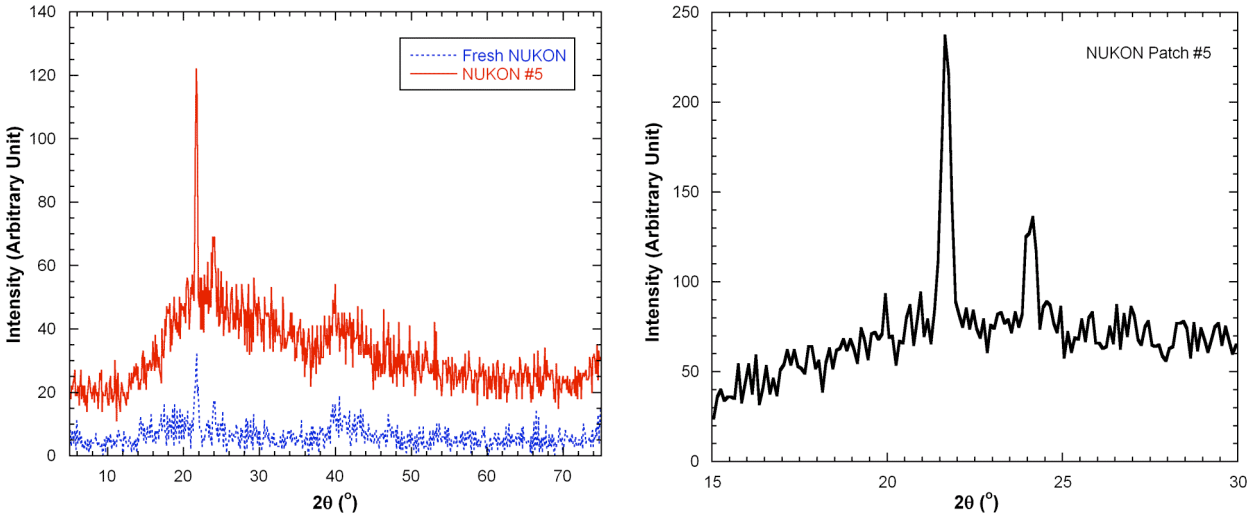

(a) 2 θ = 5-75 degrees

(b) 2 θ = 15-30 degrees

Figure 25. XRD patterns of unexposed NUKON and NUKON patch #5 showing spectrum within (a) wide and (b) narrow angles.

Test Results: Bench Top Al Corrosion Tests

Experimental

To support the results obtained from the loop tests, especially to understand better the origin of the grayish black particles, bench top tests were performed with Al alloy coupons. Figure 26 shows the bench top test setups. Each test set consists of a 250-mL flask, 2000-mL beaker, condenser, thermocouple, and electric heater. Table 5 shows the test matrix for the bench top tests. The effect of solution pH was also studied; it was expected that lowering pH would decrease the Al release rate, but might increase the release rate of other elements. Two different Al alloys were tested: 6061 Al alloy and 1100 "commercially pure" aluminum. The same Al alloy materials as used in the loop tests were used for these tests. The Al coupons are 5/8"-wide, 1"-long, and 1/8" thick.

In the ANL head loss test loop, 304 stainless steel (SS) pipes used in a heating section are exposed to the test solution. Since this could potentially provide a source of dissolved Fe and Cr, some tests are performed with a SS coupon having 2.5 times larger surface area than an Al coupon to roughly mimic the area ratio in the loop. Some tests were with a carbon steel coupon having around half of the surface area of the Al coupon to mimic the expected ratios of the materials in containment as determined from the ICET test plan.[14] All coupons were polished using a Scotch Brite pad and then cleaned using alcohol and high purity water.

The 2500 ppm boron test solution was prepared by adding 3.572 g boric acid [H_3BO_3, Fisher Scientific] to about 200 mL of deionized water. The solution pH was then adjusted using sodium hydroxide [NaOH, Fisher Scientific] to a target pH of 9.4 or 8.0 at room temperature, and the final solution volume is adjusted to 250 mL. The 250-mL pH-adjusted borated solution was transferred to a designated Pyrex flask. Twenty-four mg of NUKON glass fiber was added to maintain the same mass ratio between NUKON and total test solution as in the ANL

test loop. A condenser to minimize the water loss by evaporation at high temperature and a thermocouple were mounted on the flask. The flask was submerged in a 2000-mL Pyrex beaker filled with deionized water placed on an electric heater. The open top of the 2000-mL beaker is covered with plastic transparent film and aluminum thin foil to minimize evaporative loss of water from the beaker.

In the tests, the solution temperature was raised to 140°F. Once the solution temperature reached 140°F and stabilized, the solution pH was measured at temperature. An aluminum alloy coupon was then inserted into the flask, along with a SS or CS coupon, if needed. The coupons rested on the bottom of the flask but they were not in contact to each other. Since round-bottom flasks were used, solution was present in the space between the coupons and the bottoms of the flasks. The tests were continued for one week at a constant temperature of 140°F. After finishing a test, the Al coupon was analyzed by SEM/EDS to characterize the surface and determine if any particles were left on the surface. The test solution was filtered using a coarse paper filter to trap any particles generated during the test. The particles were then analyzed by SEM/EDS.

Table 5. Test matrix of the bench top tests for Al alloy corrosion in borated water (Circle means test data is available and cross means test was not conducted).

		Al Only	Al & SS	Al & CS
6061 Al Alloy	pH=9.4	O	O	O
	pH=8.0	O	X	O
1100 Al	pH=9.4	O	O	O

Figure 26.
Bench top test setup for Al coupon corrosion tests at 140 F and with 2500 ppm B and the pH=9.4 or 8.0.

Results: 6061 Al Alloy

As soon as the Al coupon was immersed in the test solution, bubbles were generated from the surface, especially at the edge. The bubbles are hydrogen gas generated by the water reduction reaction that balances the Al dissolution reaction. Discoloration of the surface became apparent about one day after the initiation of the test, and small grayish–black particles also started to appear on the surface at that time. As the exposure time increased, the color of the Al coupon turned more grayish and some particles settled on the bottom of the flask. The hydrogen bubble generation rate continuously decreased with time and no bubbles were being generated after 3 or 4 days of exposure. When the test solutions were cooled down to room temperature, the solution became cloudy and higher pH solutions (pH=9.4) was cloudier than lower pH solutions (pH=8.0), because at long enough times the higher Al release rate at pH=9.4 dominates over the reduced solubility at pH=8.0. The solution did not become flocculated at any case. Figure 27 shows various test coupons used in the bench top tests. All the aluminum coupons discolored, but for those at the lower pH, the surface looks more reddish especially for the case with a CS coupon present. The SS coupons were still shiny indicating minimal corrosion. Figure 28 shows the filter paper and the filtered particles for the test solutions. More of the grayish black particles were generated at the higher pH, but based on the amount of filtered particles, the presence of SS or CS has little effect on the amount of particle generation.

Figure 29 shows the SEM images of the Al coupon surfaces. Some areas are covered by particles while other areas are not. According to the SEM/EDS analyses, the particle-free areas are mainly Al oxide with small amount of Mg, Si, Fe, and Cr. The amounts of the trace elements are unaffected by the presence of other metal coupons. “Mud cracking” is observed on the Al coupon surfaces. This is typically observed when the oxide formed on the surface is very thick. Earlier LANL[6] observed similar surface appearance on Al coupons in their test at pH=9.3-9.5 (ICET-1), and Birbilis et al.[15] also observed such “mud cracking” in an Al alloy at tested at pH=12.5. The Al specimen used in the loop test did not show either Al oxide or “mud cracking” on the surface. This difference between the loop and bench top test is probably due to the water flow. The water flow enhances mass transfer from the surface, which could reduce the tendency for Al hydroxide formation on the surface. The absence of the thick oxide layer also suggests that under the flowing conditions Al release may not saturate or at least it may take a much longer time for a thick enough Al oxide layer to be formed on the surface which reduces the release rate.

The particles on the surfaces of the Al coupons are mainly composed of Al, Si, and Fe, which is similar to the composition of the particles observed in the loop test, although for those particles there typically was a stronger Cu peak. The chemical composition of the particles does not depend significantly on the presence of other metal coupons, but the SEM micrographs, as shown in Figure 29, seem to suggest that the number density of particles on the Al surface is dependent on that the presence of the other coupons. However, on a more macro scale the amount particles filtered from the solution did not show a significant dependence on the presence of other metal coupons. All EDS spectra for the 6061 Al coupons and particles are summarized in Appendix A (see Figures A28-A33).

The effect of solution pH on the formation of the particles was also examined. Figure 30 shows SEM images for the 6061 Al coupon surfaces tested at pH=8.0 and 140°F for one week. The surface shows “mud cracking” similar to those tested at pH=9.4, but the number density of particles on surface is drastically decreased. Some particles were observed on the Al coupon

tested with CS coupon, as shown in Figure 30b, but the numbers are much smaller than at the higher pH. Again, an Al oxide layer was formed on the Al metal surface. This layer may be more stable at pH=8.0 than at pH=9.4, corresponding to a large decrease in release rate, so that the particle formation is inhibited. The chemical composition of the particles showed the enrichment of Fe and Si similar to that of the particles observed in the pH=9.4 tests. EDS spectra for the Al oxide and precipitates on the 1100 Al coupons are presented in Appendix A (see Figures A34-A37).

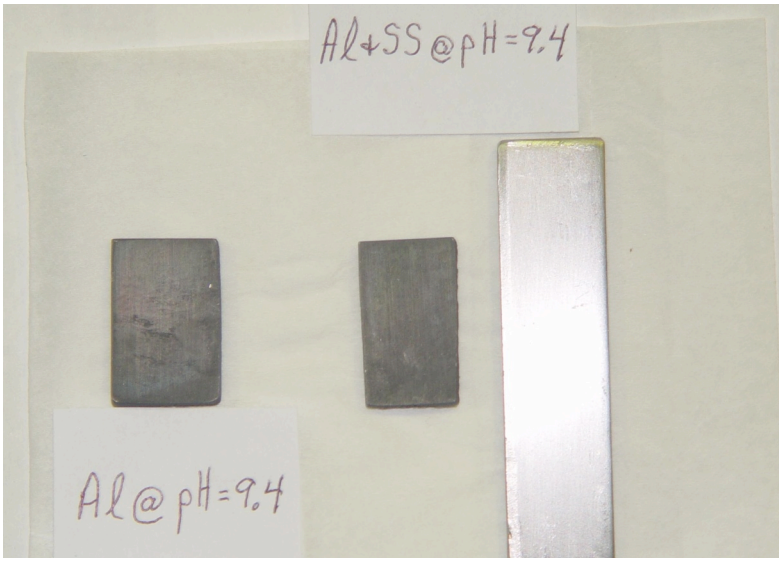

(a) Left: Al @ pH=9.4 and Right: Al & SS @ pH=9.4

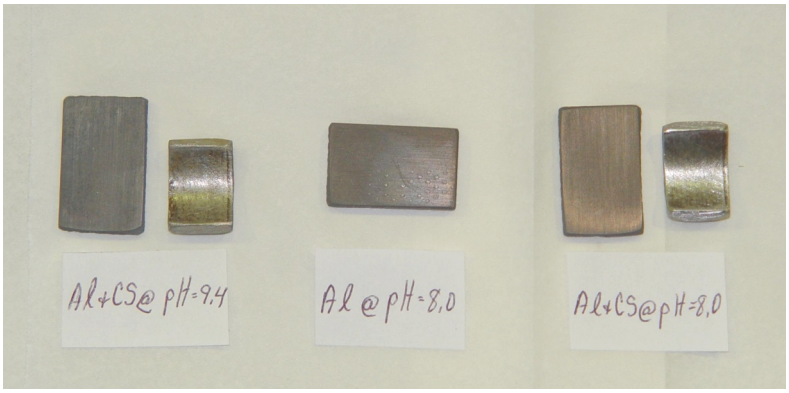

(b) Left: Al & CS @ pH=9.4, Middle: Al @ pH=8.0, and Right: Al & CS @ pH=8.0

Figure 27. Photographs showing test coupons used in the 6061 Al tests of (a) Al with and without SS at pH=9.4 and (b) Al with CS at pH=9.4 and Al with and without CS at pH=8.0.

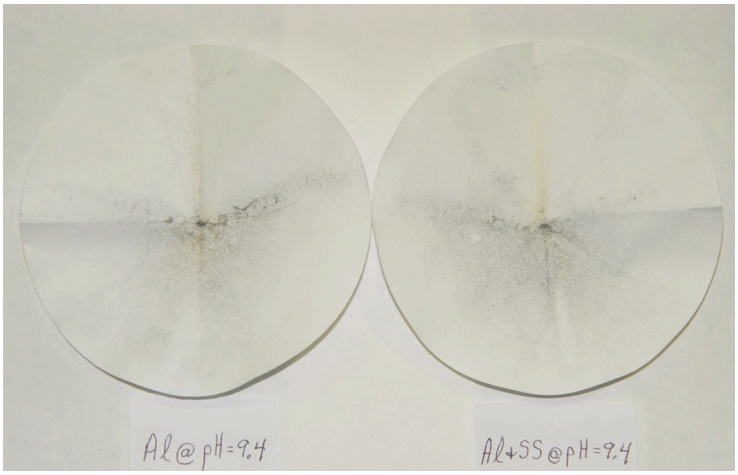

(a) Left: Al @ pH=9.4 and Right: Al & SS @ pH=9.4

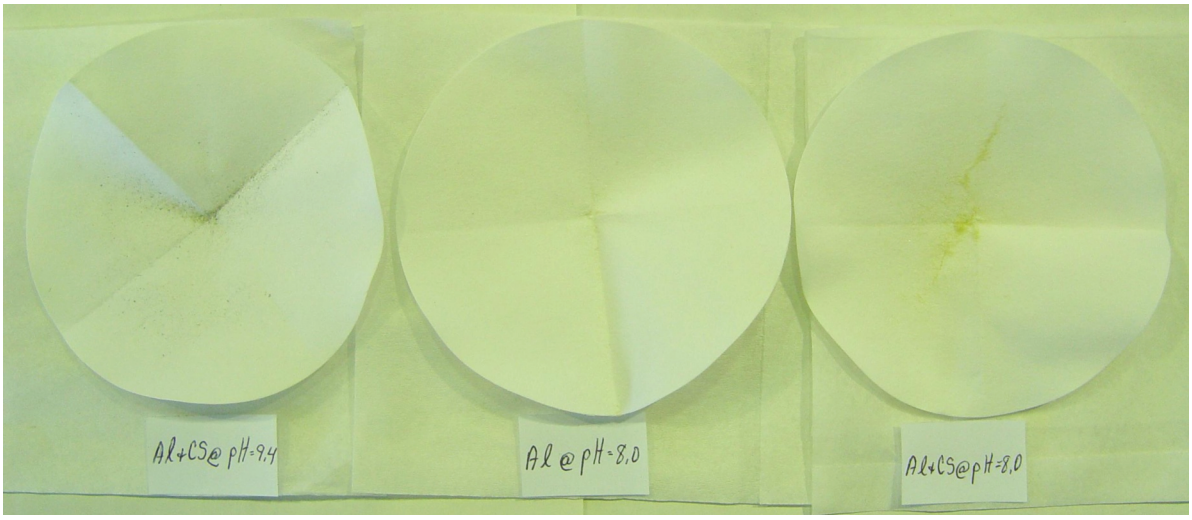

(b) Left: Al & CS @ pH=9.4, Middle: Al @ pH=8.0, and Right: Al & CS @ pH=8.0

Figure 28. Photographs showing filter papers and filtered particles of test solutions for (a) Al @ pH=9.4 and Al & SS @ pH=9.4 and (b) Al & CS @ pH=9.4, Al @ pH=8.0, and Al & CS @ pH=8.0. Note that yellow particles on filter papers are NUKON fiber glass.

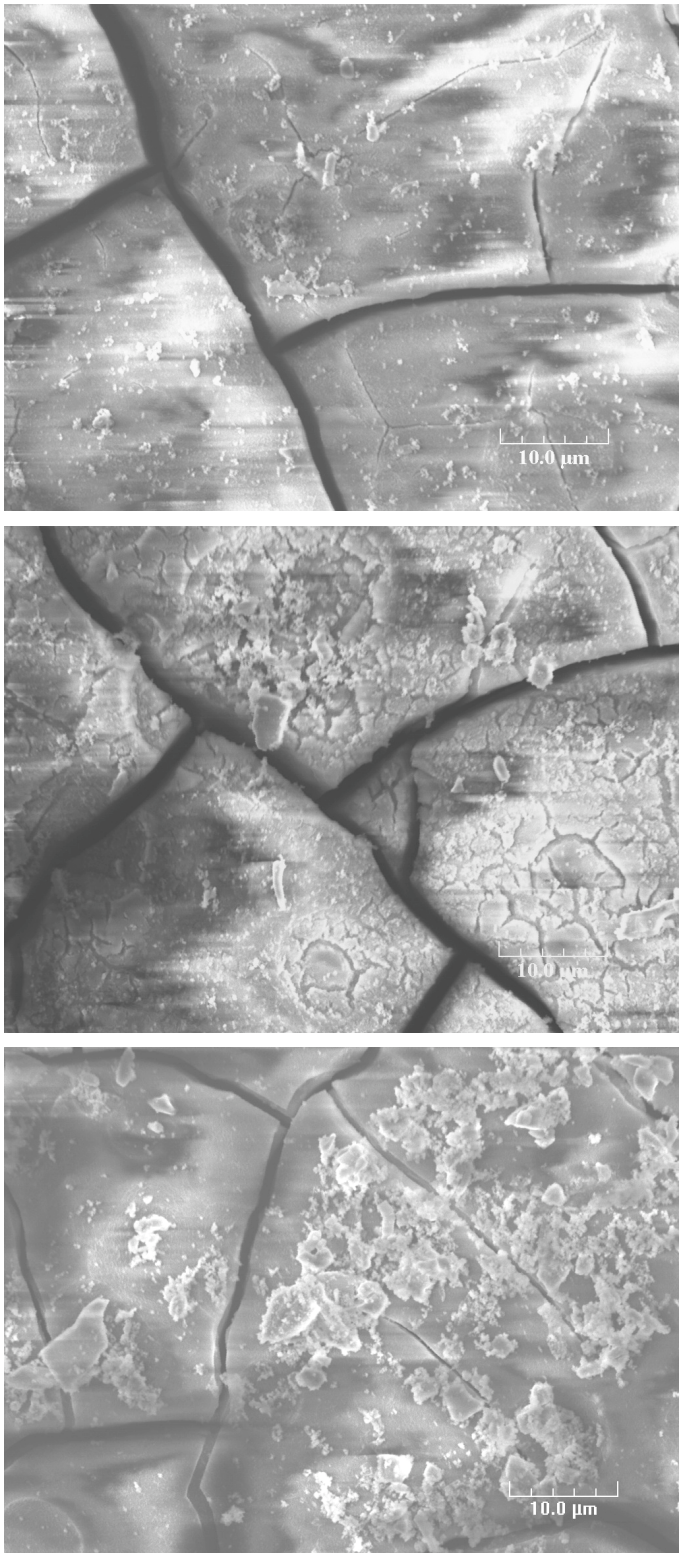

(a) Al only

(b) Al with SS coupon

(c) Al with CS coupon

Figure 29. SEM images for the 6061 Al coupon surface exposed in a static test solution at pH=9.4 and 140°F for one week (a) without any other metal coupon or with (b) SS or (c) CS coupon.

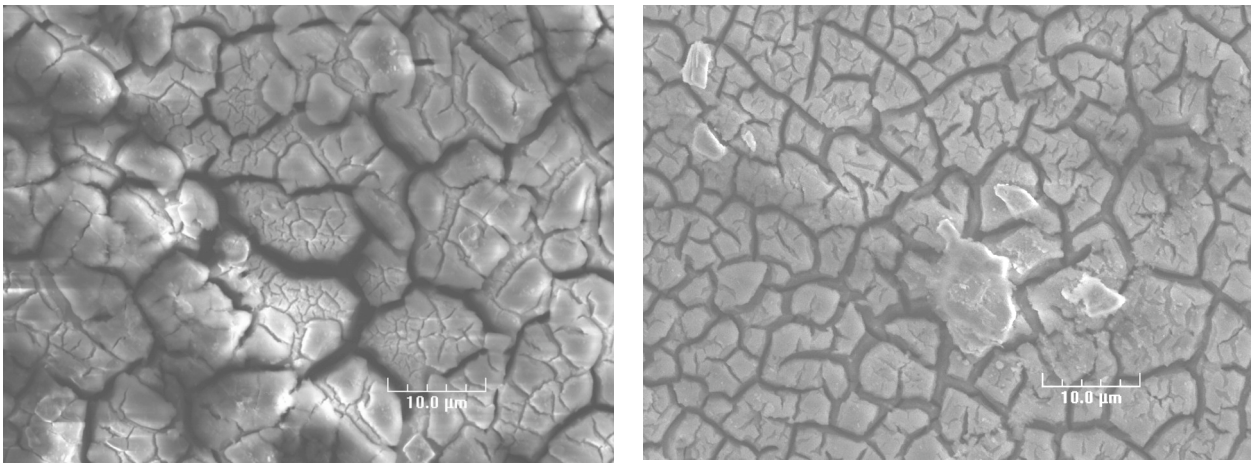

(a) Al only (b) Al & CS coupon

Figure 30. SEM images for the 6061 Al coupon surface exposed in a static test solution at pH=8.0 and 140°F for one week (a) without and (b) with CS coupon.

Results: 1100 "Commercially Pure" Al

Bench top tests with 1100 Al coupons were performed at 140°F and pH=9.4 (room temperature). As in the case of the 6061 Al coupons, hydrogen bubbles were generated from the 1100 Al coupon surface when immersed in the test solution. About a day after the initiation of the test, grayish black particles started to appear on the surface. This happened about the same time in the test with only an Al coupon and in the tests with other metal coupons. Discoloration also started to appear about 2 to 3 days after the start of the test. The hydrogen bubble generation rate appeared to be higher in 1100 Al tests than in the 6061 Al tests. The test solution pH change after the one week exposure was very small ranging from 0.02 to 0.04 for 1100 Al tests.

About a week after the start of the test, white, flocculated precipitates were formed on inner surface of the flask, the coupon surface, and the NUKON fiber surface at 140°F, as shown in Figure 31. Similar Al hydroxide flocculation was seen in the previous ANL bench top solubility tests with aluminum nitrate and sodium aluminates as the source of Al.[16] The 6061 Al tests became cloudy when cooled to room temperature, but flocculation was not observed. Previous ANL bench top tests[16] showed that even for a given pH the Al hydroxide flocculation tendency was dependent on total Al concentration. Therefore, the flocculation observed in the tests with 1100 Al coupons suggests that the Al release rate of 1100 Al is higher than that of 6061 Al. Westinghouse performed corrosion tests with various Al alloys at pH=8.0 and 200°F for 24 hours.[17] They reported that the corrosion rate of 6061 Al is about 90% of 1100 Al's corrosion rate. This result does not seem consistent with our bench top results, but relatively lower pH tests (pH=8.0) might result in the formation of a more stable Al hydroxide layer and minimize the difference between various Al alloys. The Westinghouse tests were also short–term, 24 hour exposures. As stated in the 1100 Al loop test, the 1100 Al showed a higher Al release rate in the loop test than the 6061 Al, which is consistent with the results of the bench top tests. As noted previously, the corrosion rates observed in the loop test with 6061 Al were

slightly higher than those exposed based on static tests with 1100 Al[4] and a low flow rate test with 3003 Al (ICET-1).[6]

Figure 32 shows the Al coupon surfaces after the bench top tests. There is no significant difference between the three Al coupons. Compared to 6061 Al coupons tested at pH=9.4, as shown in Figure 27, the surface color has a more reddish tone. The 1100 Al plate in the loop test did not show as much discoloration as the 1100 Al coupon in the bench top test. Figure 33 shows material filtered from the test solution with only an 1100 Al coupon. Because of drying, the Al hydroxide gel shows "mud cracking." Al hydroxide gel is typically milky white when generated from a chemical source of Al, but here is slightly gray, presumably because fine grayish particles are mixed with the Al hydroxide gel. As compared with 6061 Al coupon tests, the amount of particles appears similar or slightly less.

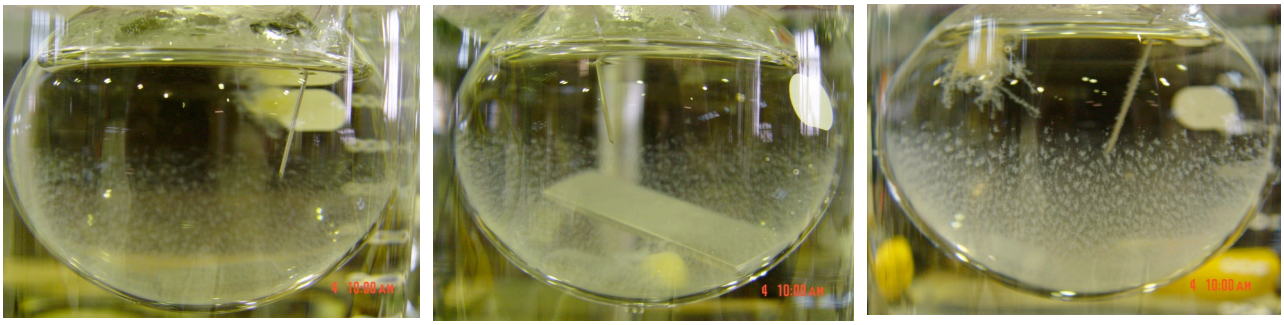

(a) Al only (b) Al & SS (c) Al & CS

Figure 31. Test solutions of 1100 Al coupon bench top tests showing white and flocculated precipitates at 140 F for (a) Al only, (b) Al & SS, and (c) Al & CS tests.

(a) (b) (c)

Figure 32. Appearance of 1100 Al coupons tested at 140 F and pH=9.4 for one week (a) without other metal coupon, (b) with a SS coupon, and (c) with a CS coupon.

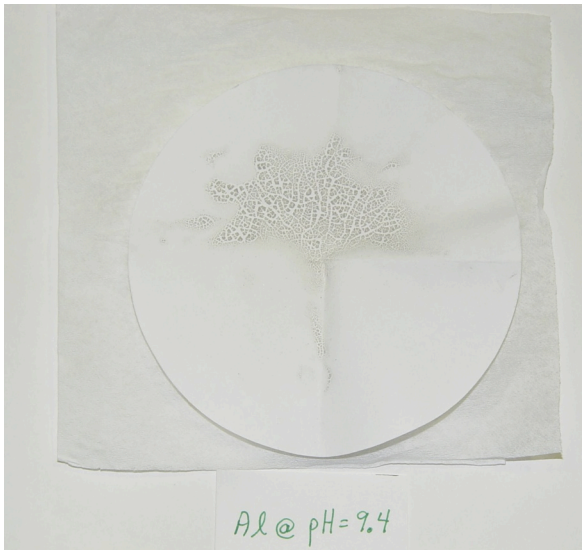

Figure 33.
Filtered particles of the test solution with 1100 Al coupon without other metal at pH=9.4 and 140 F showing that Al hydroxide gel discolored due to the grayish black particles.

After completion of the bench top tests, the 1100 Al coupons were analyzed using SEM. Figure 34 shows the back-scattered electron images for three different 1100 Al coupons tested at pH=9.4 and 140°F for one week. Bright areas indicate the presence of heavy elements; in this case the bright regions represent Fe and Cu containing particles. The size distribution and number density of particles for three different cases look similar, which suggests other metal dissolution, especially Fe ions, does not affect significantly formation of the particles. As in the case of 6061 Al, "mud cracking" was observed on all 1100 Al coupon surfaces, indicating the presence of a thick Al oxide. EDS analysis for the particle-free region confirmed that the particle-free area is Al oxide with some Na. The chemical composition of particles on the surface was analyzed by EDS analyses. EDS analyses showed that there are three different kinds of particles: Al oxide, Al-Fe-Si (or Cu) particle, and Fe-enriched particle. Al oxide appears to be formed when the solution exceeded the Al solubility limit and flocculation occurred. Al-Fe-Si or Al-Fe-Cu particles appear to be originated from the Al metal matrix itself. This issue will be discussed more in a later section. Fe-enriched particles have a high oxygen peak so that it may be Al-Fe oxide or Al-Fe-Cu particle covered by Al oxide. The chemical composition of those particles is very similar to that of particles observed in the 1100 Al loop test. As compared with the particles observed on 6061 Al surfaces, particles on 1100 Al do not have Cr or Mg but Cu appears to be enriched in the particles. This is consistent to the discrepancy in the chemical compositions of 6061 and 1100 Al coupons. Full EDS spectra for all 1100 Al coupons and particles observed on the surfaces are presented in Appendix A (see Figures A38-A44).

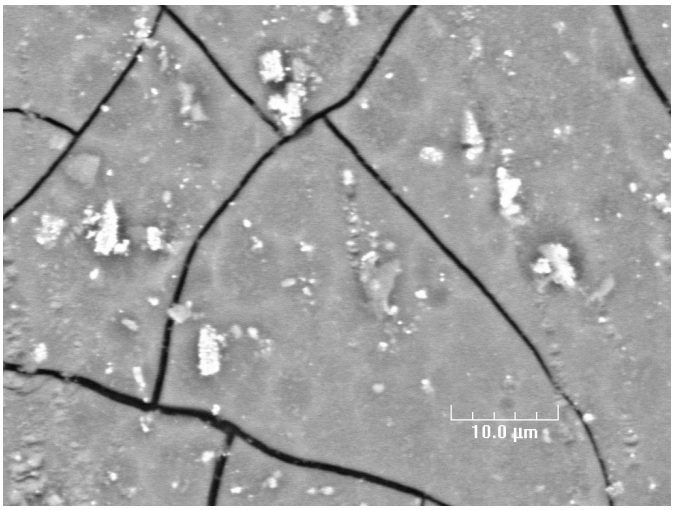

(a) 1100 Al only

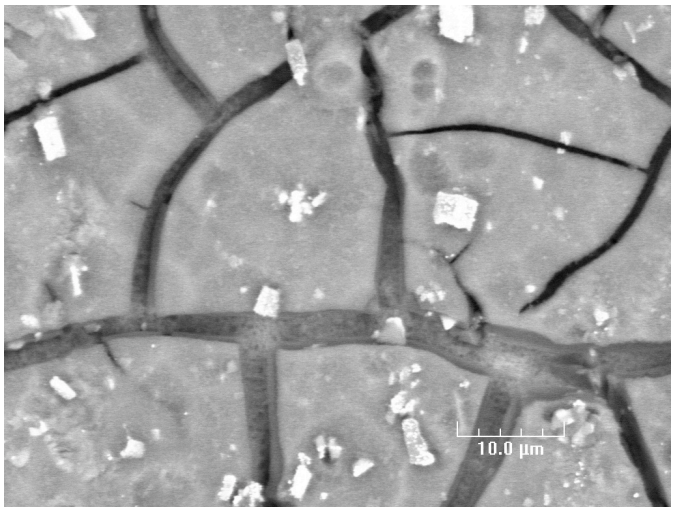

(b) 1100 Al with SS coupon

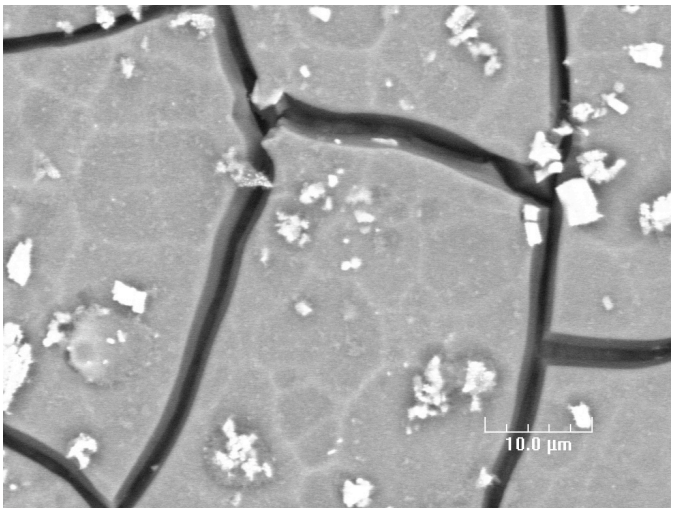

(c) 1100 Al with CS coupon

Figure 34. Back-scattered electron images for (a) 1100 Al only, (b) 1100 Al with SS, and (c) 1100 Al with CS tested at pH=9.4 and 140 F for one week.

Discussion

Identification of the Grayish Particles as Intermetallic Particles

The major alloying elements of 6061 Al alloy are Mg, Si, Cu, and Cr; Fe is present as impurity. Since 6061 Al alloy is mechanically strengthened by precipitation formation, various kinds of intermetallic particles are present. Possible intermetallic particles include Mg_2Si, Al_7Cu_2Fe, Al_2Cu, Al_2CuMg, Al_3Fe, $Al_{12}Mg_2Cr$, Mg_2Al, Mg(AlCu), etc.[18] Also, it has been reported that the microstructure of the 6061 base metal contains two types of precipitates, Mg_2Si phases and iron compounds, typically of the FeAlSi form.[19] The intermetallic particles range in size from Angstroms to 10 μm, depending on the type of particles.[18] The FeAlSi intermetallics has been reported to range from 2 to 20 μm in diameter.[19] SEM/EDS analyses of the grayish particles formed in the loop and bench top tests showed that they ranged in size from a few tenths of a micrometer to about 10 μm and were enriched in Fe and Si (and for some particles, Cu, Cr, and Mg), but were without significant oxygen peaks. These observations strongly suggest that the particles observed in the loop and bench top tests are intermetallic compounds. To support this conclusion, additional SEM/EDS analyses were performed. Figure 35 shows a back-scattered electron image for the fresh 6061 Al alloy surface. In this figure, brighter region means heavier elements are present at that region. Table 6 shows the chemical composition by EDS analysis of the bright regions in Figure 35. Based on this analysis, it appears that intermetallic particles in 6061 Al alloy are mainly (FeSiAl) compounds with a small fraction of the particles containing Cr, Mg, and Cu. Chemical composition of the intermetallics is not limited to that in Table 6, but the ratio between each element was very similar. Based on earlier literature and our analysis results, it is concluded that the grayish black particles observed in the loop and bench top tests are mainly Al-Fe-Si ternary intermetallic particles.

This conclusion is also supported by the results of the tests with carbon steel coupons present. If the particles were forming by a precipitation from dissolved Fe, Al, and Si, the presence of additional Fe would be expected to lead to increased precipitate formation. However, this was not observed.

The major impurity elements of 1100 Al are Fe and Si, and Al-Fe-Si ternary intermetallic compounds, such as $FeAl_3$, Fe_3SiAl_{12}, $Fe_3Si_2Al_9$, $Fe_2Si_2Al_9$, etc. can be present.[20] Figure 36 shows a back-scattered electron image for the fresh 1100 Al surface. Compared with 6061 Al alloy, the particle sizes appear to be smaller ranging from a few tenths of a micrometer to 4-5 μm, but the particle number density looks similar to that of 6061 Al alloy. It was difficult to tell in the bench top tests whether there were significant differences in the number of grayish particles formed in the 1100 and 6061 tests. As shown in Table 6, the chemical composition of the intermetallic compounds in 1100 Al is similar to those in 6061 except that those in 1100 Al have higher Cu content and negligible Mg or Cr content as compared with those in 6061 Al. The major intermetallic compound in 1100 Al observed in these bench top tests is a (FeSiAl) intermetallic compound containing Cu, which is consistent to not only literature data[20] but also observation results in the 1100 Al loop test.

Based on literature data[15], intermetallic particles can behave as anodes or cathodes with respect to the base Al matrix. Either way these intermetallic particles induce pitting corrosion in neutral or acidic solutions. Under alkaline environments, general corrosion of Al base

matrix becomes dominant. The damage is best described as a large-scale matrix dissolution in a general sense.[15] The Al base matrix dissolves into the solution or forms Al hydroxide on the surface, and the intermetallic particles can be disjoined from the base matrix and loosely adhered on the surface or swept away by flow. The SEM analyses for the surfaces of 6061 Al and 1100 Al specimen used in the loop tests did not show any sign of pitting corrosion, as expected.

Table 6. Chemical composition by SEM/EDS analysis for the intermetallic particles observed in fresh 6061 and 1100 Al coupons (wt%).

	Al	Si	Fe	Cu	Mn	Mg	Cr	Zn	Ti	Others
6061 Al	66.00	6.78	21.36	1.56	NI[a]	1.95	2.35	NI	NI	NI
1100 Al	65.33	5.70	23.35	5.56	NI	NI	0.06	NI	NI	NI

[a] Element was not included in the EDS spectrum analysis because its signal was negligible.

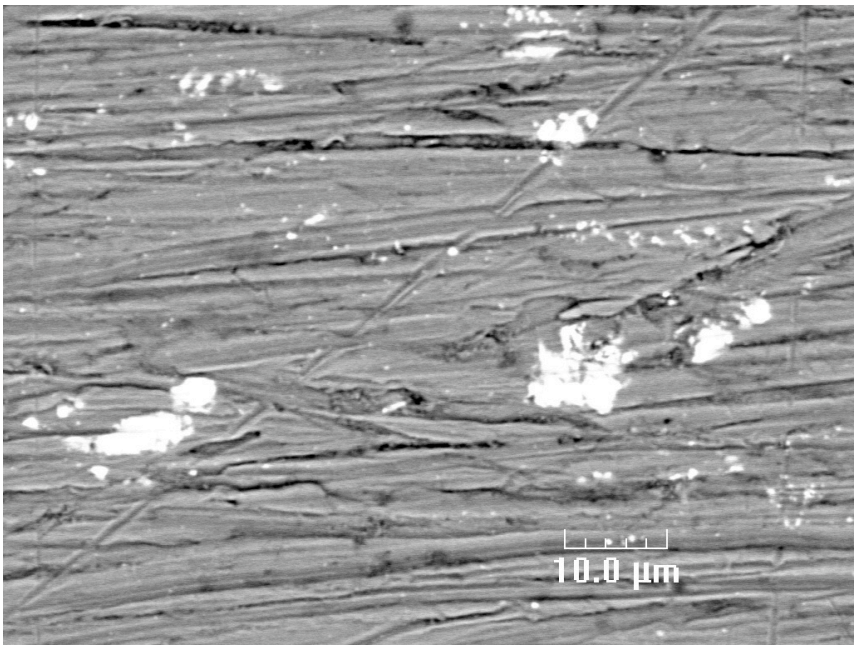

Figure 35.
Back-scattered electron image for the fresh 6061 Al alloy surface; brighter region means heavier elements are present at that region.

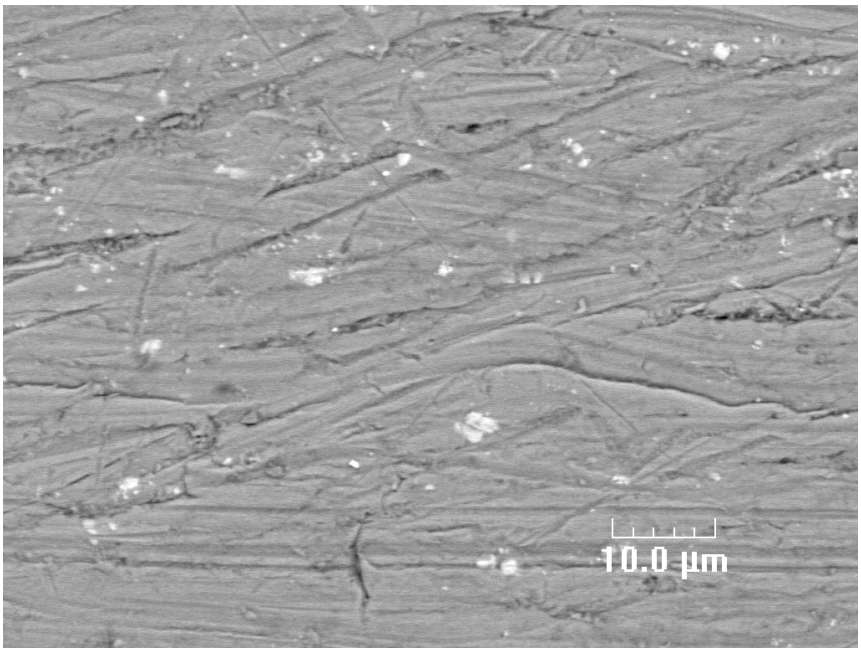

Figure 36.
Back-scattered electron image for the fresh 1100 Al alloy surface; brighter region means heavier elements are present at that region.

Implications for Head Loss and Al Solubility

Two unexpected features of the head loss test with the 6061 Al plates were the occurrence of a significant increase in head loss at a temperature of 140°F and the continued increase in head loss at a temperature of 120°F after the aluminum plates were removed. These occurred at pH and Al concentrations at which previous tests had suggested that formation of $Al(OH)_3$ precipitates would not occur. The increased head loss at 140°F appears due to the release of intermetallic particles from the alloy, which are captured in the fiber bed. The particles may also be involved in the increase in head loss at 120°F. By providing seeds, they may induce precipitation more readily than would be expected.

The presence of intermetallic particles is not unique to the 6061 alloy. Intermetallic particles were observed in 1100 Al and are probably present in the 3003 alloy. However, the intermetallic particles in the 6061 Al alloy are somewhat larger than those in the 1100 Al, and this may be the reason why no significant head loss was observed at 140°F in the 1100 Al loop test. However, an unexpected feature of the head loss test with the 1100 Al was the continued rapid increase in head loss after increasing the loop water temperature from 100 to 120°F once head loss had begun to increase at 100°F. It is conjectured that this phenomenon is again due to the presence of intermetallic particles as seeds to more readily induce precipitation.

The Al corrosion loop tests with 6061 and 1100 Al plates seem to suggest somewhat lower Al solubility than the chemical Al tests. Figure 37 shows an Al solubility map in the '$pH+p[Al]_T$' vs. temperature domain. '$p[Al]_T$' is the negative logarithmic value of total molar Al concentration in solution. In the figure, a filled symbol indicates Al hydroxide precipitation was observed at that condition and an open symbol indicates Al hydroxide precipitation was not observed. The circle symbols represent the ANL's long-term Al solubility bench top test data[16] including some room temperature data points from the previous ANL report.[1] In cases where the precipitates were flocculated, a red symbol was used. The stable Al concentrations observed in ICET-1 and 5[6] are plotted, the solubility test data[17] by Westinghouse at 140 and 200°F, and the ANL bench top test data in sodium tetraborate solution[10] are also included. The

previous ANL head loss test data associated with Al hydroxide precipitates[1,2] including the two Al plate tests described in this report are designated as diamond symbols. This map is intended to only describe the behavior of borated, alkaline solutions. The boundary between precipitation and non-precipitation area appears to be well represented by a straight line that depends on solution temperature up to 160°F. Above 160°F the dependence of the boundary between precipitation and non-precipitation on the solution temperature is weaker. The data from the loop tests appear to be more conservative than bench top data. The loop tests using chemical sources are relative close to the proposed solubility limit. Two data points obtained from the Al corrosion loop tests at 120°F are located above the boundary line. This result appears to suggest that intermetallic particles observed only in the loop tests with Al plates behaves as a seed by providing surface area for Al hydroxide precipitation.

The free energy for formation of stable nuclei (ΔG) depends on the degree of supersaturation (S), the temperature (T), the net solution-particle interfacial energy (σ), and the particle surface area (A):[21]

$$\Delta G = -RT \ln S + \sigma A \tag{4}$$

where R is the ideal gas constant. Similar expressions apply to heterogeneous nucleation and film formation at an interface, except that the surface free energy is described by three terms:[21]

$$\Delta G = -RT \ln S + \sigma_{cl} A_{cl} + \left(\sigma_{cs} - \sigma_{sl}\right) A_{cs} \tag{5}$$

where c, s, and l subscripts refer to interfaces involving the crystalline particle, the substrate, and the liquid phases, respectively. If interactions between the growing nucleus and a substrate surface represent a lower net interfacial energy than the particle-solution interfacial energy, heterogeneous nucleation is favored over homogeneous nucleation.[21] Figure 38 shows the schematic solubility diagram for species in water. Above the saturation limit line the solution becomes supersaturated. However, the degree of supersaturation is not enough to cause homogeneous nucleation. Instead, heterogeneous nucleation on any given surface is preferred. When the degree of supersaturation is very high, homogeneous nucleation can occur. Two exceptional data points observed in the Al plates loop tests in Figure 37 may be able to be explained by considering the possibility of heterogeneous nucleation. Intermetallic particles may provide extra large surface area so that heterogeneous nucleation of Al hydroxide occurs on the intermetallic particle surface at the condition where homogeneous nucleation cannot occur because of low supersaturation. In the case of the 1100 Al loop test, the Al hydroxide precipitates formed at 100°F, as well as intermetallic particles, might behave as a seed at 120°F and cause rapid increase of head loss by Al hydroxide precipitation.

The bounding line precipitation and no precipitation below 160°F in Figure 37 for tests with chemical addition of Al gives

$$\log[Al(OH)_4^-] = pH - 14.1 + 0.0243\ T, \tag{6}$$

where $\log[Al(OH)_4^-]$ is the log to the base 10 of the molar concentration of $Al(OH)_4^-$ and T is the temperature in degrees Fahrenheit. To bound all the data including the Al corrosion loop tests, it is necessary to shift the bounding curve upward. This yields

$$\log[Al(OH)_4^-] = pH - 14.4 + 0.0243\ T. \tag{7}$$

The Al solubility predicted by Eq. (7) is about a factor of 2.2 lower than that predicted by Eq. (6). The predicted solubility limits for Al at 70 and 140°F are shown as a function of pH in Figure 39.

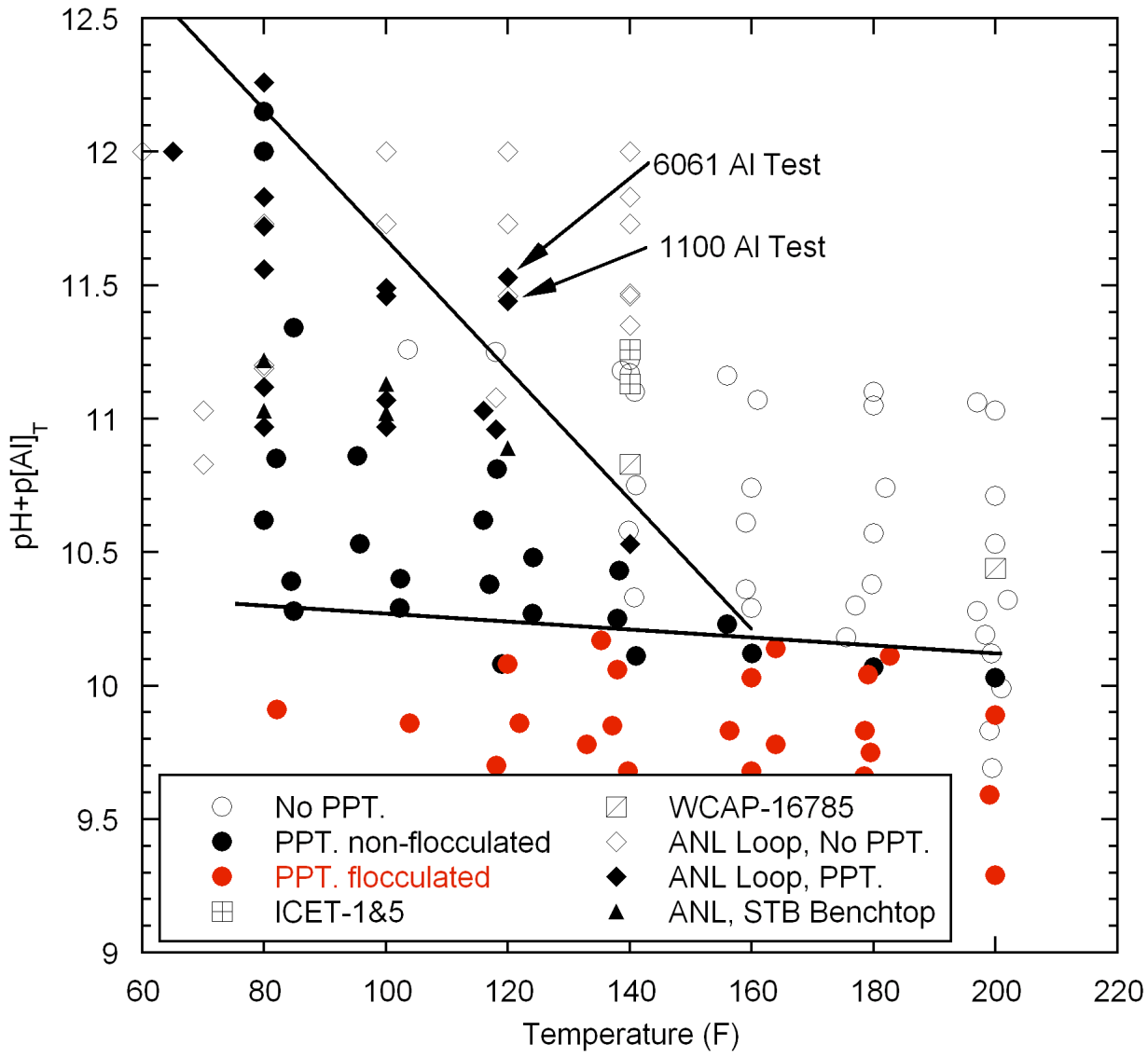

Figure 37. Al solubility map in the 'pH+p[Al]$_T$' vs. temperature domain; Filled and open symbols mean the occurrence of Al hydroxide precipitation and no precipitation, respectively.

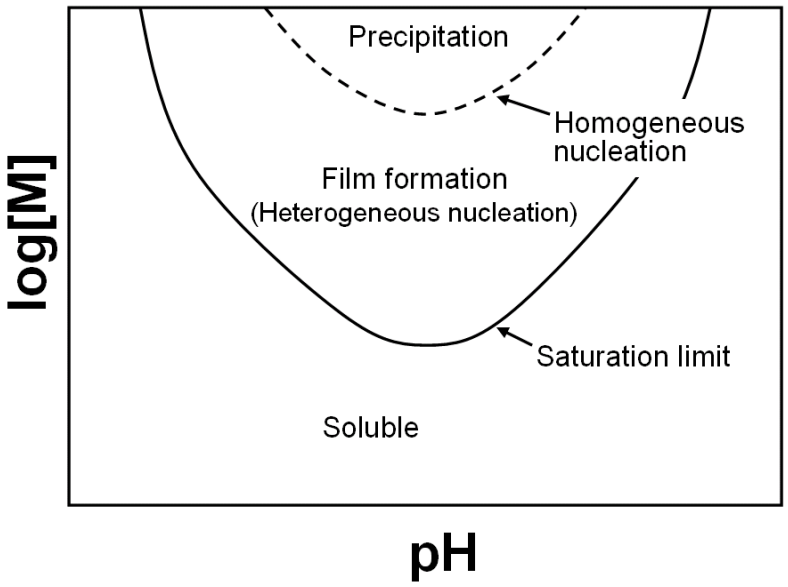

Figure 38. Schematic solubility diagram for film-forming species dissolved in water (modified from Figure 1 in Ref. [21]).

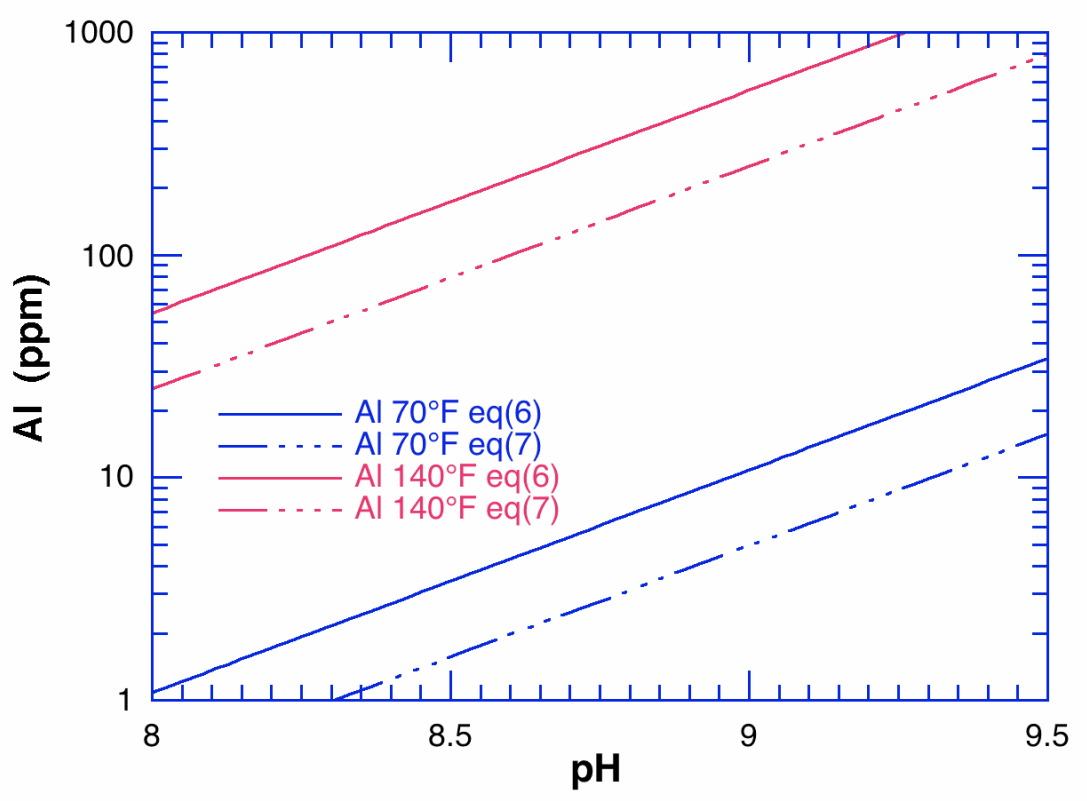

Figure 39. Predicted Al solubility in borated solutions at 70 and 140°F as a function of pH.

Comparison with Head Loss Tests using WCAP–16530 $Al(OH)_3$ surrogate

Previous head loss tests with WCAP–16530 $Al(OH)_3$ surrogates showed that in the ANL vertical head loss loop with a 13 mm NUKON bed, a surrogate addition equivalent to removal of 1.5 ppm Al from the loop was sufficient to exceed the loop capacity.[2] In the case of the current tests with in situ formation of precipitate, Fig. 5 shows that a decrease in the nominal concentration from 116 to 113 ppm Al resulted in an increase in head loss of ≈ 1 psi; Fig. 14 shows that a decrease in the nominal concentration from 115 to 110 ppm Al resulted in an increase in head loss of ≈ 1 psi. Due to the uncertainty in the ICP measurements, this suggests that decreases of 3±2 ppm and 5±2ppm will result in a head loss increase of ≈ 1 psi in the ANL vertical loop. The increase in head loss due to in situ precipitation of $Al(OH)_3$ thus seems reasonably consistent with that expected from the addition of corresponding amounts of the WCAP surrogate. Per unit mass of Al removed from solution, the WCAP surrogate appears somewhat more effective in increasing head loss than the $Al(OH)_3$ precipitates formed in situ by corrosion or chemical addition of Al, and thus it gives conservative estimates of the head loss due to the precipitation of a given amount of Al from solution. The increased effectiveness of the surrogate in producing head loss is probably due to the size of the surrogate, which is fairly close to the available pore size in the glass-fiber bed, whereas the $Al(OH)_3$ precipitates formed in-situ by corrosion or chemical addition must grow to this size from sub-micron scale.[2] However, in choosing the amount of surrogate that should be used, consideration must be given to the potential for additional head losses due to intermetallic particles and the apparent reduction in the effective solubility of $Al(OH)_3$ when intermetallic particles are present.

Major Findings and Summary

- The Al release rate of 6061 Al alloy in borated water at pH=9.35 (room temp.) and 140°F with the flow rate of 0.1 ft/s is predicted well by a release rate equation based on previous test data with 1100 and 3003 Al alloys in quasistatic solutions. However, the 1100 Al showed a much higher Al release rate in the loop test than either of the prediction results and the 6061 Al. This is consistent with other data showing that 6061 has a lower release rate than 1100 Al. It also indicates that estimates of Al release need to consider the flow velocity.
- Based on static bench top tests at pH=8.0 and 140°F, 6061 Al alloy releases fewer intermetallic particles than at pH=9.4 in borated solution presumably because at lower pH Al solubility and Al release rate become less, which leads to stable Al hydroxide formation on the metal surface.
- With a total Al concentration of 116 ppm Al in the loop produced by corrosion of 6061 Al specimen a significant increase in head loss across a glass fiber bed was observed at 140°F. At the temperature, Al concentration, and pH of this test, formation of $Al(OH)_3$ precipitates is not expected.
- The increase in head loss at 140°F appears to be due to the release of intermetallic particles present in the 6061 Al alloy. The presence of these intermetallic particles may also induce precipitation of $Al(OH)_3$ more readily than would be expected based on solubility tests using chemical addition of Al.
- With a total Al concentration of 118 ppm Al in the loop produced by corrosion of 1100 Al plates no significant increase in head loss was observed at 140°F. This is

attributed to the fact that the size of the intermetallic particles in 1100 Al is smaller than that of the 6061 Al.

- In the 1100 Al corrosion vertical head loss loop test, once head loss had begun to increase at 100°F, a rapid increase in head loss continued even as the loop water temperature was increased from 100 to 120°F. It is conjectured that this may be interpreted as a heterogeneous nucleation of Al hydroxide on intermetallic particles and/or preexisting Al hydroxide precipitates surface.
- To investigate whether sodium aluminosilicate precipitate was formed on the fiber surface, one glass fiber patch exposed in the loop water of the 1100 Al head loss test was analyzed using XRD and compared with unexposed glass fiber. Exposed and unexposed glass fiber samples showed same peaks, but it is inconclusive whether these peaks are from aluminum hydroxide (bayerite) or sodium aluminosilicate (albite).
- To determine the potential of Al alloys to cause head loss, their microstructure, especially the size distribution and number density of intermetallic particles should be considered along with their Al release rate.
- The increase in head loss due to in situ precipitation of $Al(OH)_3$ seems reasonably consistent with that expected from the addition of corresponding amounts of the WCAP surrogate. Per unit mass of Al removed from solution, the WCAP surrogate appears somewhat more effective in increasing head loss than the $Al(OH)_3$ precipitates formed in situ by corrosion or chemical addition of Al, and thus it gives conservative estimates of the head loss due to the precipitation of a given amount of Al from solution. However, in choosing the amount of surrogate that should be used, consideration must be given to the potential for additional head losses due to intermetallic particles and the apparent reduction in the effective solubility of $Al(OH)_3$ when intermetallic particles are present.

References

1. J.H. Park, K. Kasza, B. Fisher, J. Oras, K. Natesan, and W.J. Shack, *Chemical Effects Head-Loss Research in Support of Generic Safety Issue 191,* NUREG/CR–6913, U.S. Nuclear Regulatory Commission, Washington, D.C., 2006.
2. C. B. Bahn, K. E. Kasza, W. J. Shack, and K. Natesan, *Technical Letter Report on Evaluation of Chemical Effects: Studies on Precipitates Used in Strainer Head Loss Testing,* ADAMS Accession No. ML080600180, U.S. Nuclear Regulatory Commission, Washington D.C., January 2008.
3. ASTM Standard B 209-06, "Standard Specification for Aluminum and Aluminum-Alloy Sheet and Plate," Annual Book of ASTM Standards, Volume 02.02, ASTM International: PA, USA, 2007.
4. A. E. Lane, T. S. Andreychek, W. A. Byers, R. J. Jacko, E. J. Lahoda, and R. D. Reid, *Evaluation of Post-Accident Chemical Effects in Containment Sump Fluids to Support GSI-191*, WCAP-16530-NP, Revision 0, Westinghouse Electric Company LLC, February 2006 (ADAMS Accession No. ML060890509).

5. W. J. Shack, *Technical Letter Report on WCAP-16530-NP, Evaluation of Post-Accident Chemical Effects in Containment Sump Fluids to Support GSI-191*, U.S. Nuclear Regulatory Commission, Washington, D.C., February 2007.

6. J. Dallman, B. Letellier, J. Garcia, J. Madrid, W. Roesch, D. Chen, K. Howe, L. Archuleta, and F. Sciacca, *Integrated Chemical Effects Test Project: Consolidated Data Report, Vol. 1*, NUREG/CR-6914 Vol.1, U.S. Nuclear Regulatory Commission, Washington D.C., 2006.

7. J. C. Griess and A. L. Bacarella, "The Corrosion of Materials in Reactor Containment Spray Solutions," *Nucl. Tech.* **10** (1971) 546-553.

8. C. Leonelli, et al., "Influence of Small Additions of Al2O3 on the Properties of the Na2O-3SiO2 Glass," *J. Phys. Chem. B* **105** (2001) 919-927.

9. Xavier Carrier, Eric Marceau, Jean-Francois Lambert, and Michel Che, "Transformations of –alumina in aqueous suspensions: 1. Alumina chemical weathering studied as a function of pH," *J. Colloid Interface Sci.* **308** (2007) 429-437.

10. C. B. Bahn, K. E. Kasza, and W. J. Shack, *Technical Letter Report on Follow-on Studies in Chemical Effects Head-Loss Research; Studies on WCAP Surrogates and Sodium Tetraborate Solutions,* ADAMS Accession No. ML070580086, U.S. Nuclear Regulatory Commission, Washington D.C., February 2008.

11. Chunling Liu, Sridhar Komarneni, and Rustum Roy, "Crystallization of Anorthite-Seeded Albite Glass by Solid-State Epitaxy," *J. Am. Ceram. Soc.* **75** (1992) 2665-2670.

12. Mahir Alkan, Ozkan Demirbas, and Mehmet Dogan, "Electrokinetic properties of kaolinite in mono- and multivalent electrolyte solutions," *Microporous and Mesoporous Materials* **83** (2005) 51-59.

13. Jian Wang, Guiling Ning, Xuefeng Yang, Zhihong Gan, Hongyu Liu, and Yuan Lin, "Large-scale synthesis of Al4B2O9/Al18B4O33 whiskers via a novel method," *Materials Letters* **62** (2008) 1208-1211.

14. T. S. Andreychek, *Test Plan: Characterization of Chemical and Corrosion Effects Potentially Occurring Inside a PWR Containment Following a LOCA,* Westinghouse Electric Company LLC, July 2005. (ADAMS Accession No. ML052100426)

15. N. Birbilis and R. G. Buchheit, "Investigation and Discussion of Characteristics for Intermetallic Phases Common to Aluminum Alloys as a Function of Solution pH," *J. Electrochem. Soc.* **155** (2008) C117-C126.

16. C. B. Bahn, K. E. Kasza, W. J. Shack, and K. Natesan, *Technical Letter Report on Evaluation of Long-term Aluminum Solubility in Borated Water Following a LOCA,* ADAMS Accession No. ML081550043, U.S. Nuclear Regulatory Commission, Washington D.C., February 2008.

17. Richard D. Reid, Kurtis R. Crytzer, and Ann E. Lane, *Evaluation of Additional Inputs to the WCAP-16530-NP Chemical Model,* WCAP-16785-NP, Revision 0, Westinghouse Electric Company LLC, May 2007 (ADAMS Accession No. ML072010381).

18. N. Birbilis and R. G. Buchheit, "Electrochemical Characteristics of Intermetallic Phases in Aluminum Alloys: An Experimental Survey and Discussion," *J. Electrochem. Soc.* **152** (2005) B140-B151.

19. A.B.M. Mujibur Rahman, S. Kumar, and A.R. Gerson, "Galvanic corrosion of laser weldments of AA6061 aluminum alloy," *Corrosion Science* **49** (2007) 4339-4351.

20. O. Seri and K. Furumata, "Effect of Al-Fe-Si intermetallic compound phases on initiation and propagation of pitting attacks for aluminum 1100," *Materials and Corrosion* **53** (2002) 111-120.

21. B. C. Bunker, et al., "Ceramic Thin-Film Formation on Functionalized Interfaces Through Biomimetic Processing," *Science* **264** (1994) 48-55.

Appendix A: EDS Analysis Results for Al Specimens, Coupons, and Particles.

Table A1. Summary of chemical composition data for the precipitate-free fiber regions used in Figure 24 analyzed by SEM/EDS.

Sample Description		Acceleration Voltage (kV)	Chemical composition (at%)				
			Na	Si	Ca	Al	Mg
Unexposed NUKON	Spot1	5	7.2	81.5	0.0	5.7	5.9
		10	25.0	60.0	4.9	4.6	5.6
	Spot2	5	6.5	79.2	5.1	4.3	5.1
		10	22.6	62.8	4.7	5.1	4.9
NUKON Patch #1	Spot 1	10	5.0	79.1	6.1	5.3	4.6
	Spot 2	10	4.7	80.0	6.2	5.1	4.0
NUKON Patch #2	Spot 1	5	9.0	77.4	0.5	6.1	7.0
		10	14.4	70.7	5.6	4.8	4.6
NUKON Patch #3	Spot 1	5	1.5	88.3	0.4	6.4	3.4
		10	9.5	74.6	6.8	4.7	4.4
	Spot 2	5	0.0	91.5	0.0	4.4	4.0
		10	7.5	77.5	7.6	4.0	3.5
	Spot 3	5	1.0	84.4	0.9	9.1	4.7
		10	15.8	68.9	6.4	4.7	4.2
NUKON Patch #4	Spot 1	5	3.1	82.1	3.7	6.9	4.2
		10	14.7	72.1	5.3	4.3	3.6
	Spot 2	5	4.9	78.5	4.6	7.5	4.6
		10	14.0	72.0	5.8	4.1	4.1
NUKON Patch #5	Spot 1	5	7.2	76.4	1.9	10.1	4.5
		10	19.9	65.4	5.0	6.1	3.7

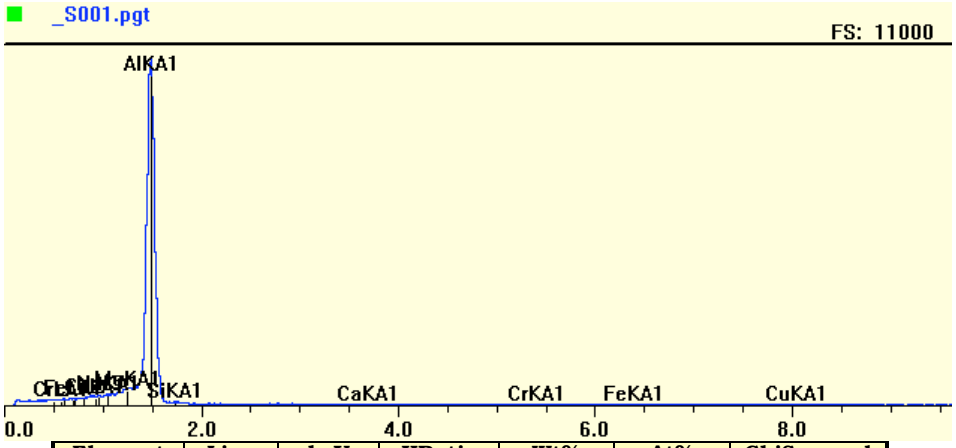

Element	Line	keV	KRatio	Wt%	At%	ChiSquared
Na	KA1	1.041	0.0000	0.00	0.00	0.00
Al	KA1	1.487	0.9404	96.74	96.55	56.47
Si	KA1	1.740	0.0000	0.00	0.00	0.00
Ca	KA1	3.691	0.0002	0.03	0.02	1.22
Cr	KA1	5.414	0.0003	0.03	0.02	1.11
Fe	KA1	6.403	0.0016	0.20	0.10	1.10
Mg	KA1	1.254	0.0328	3.00	3.32	56.47
Cu	LA1	0.930	0.0000	0.00	0.00	0.00
Total				**100.00**	**100.00**	**52.16**

Figure A1. EDS spectrum for the base matrix underneath particles in the grayish black area of the Al specimen used in the loop test and its chemical composition.

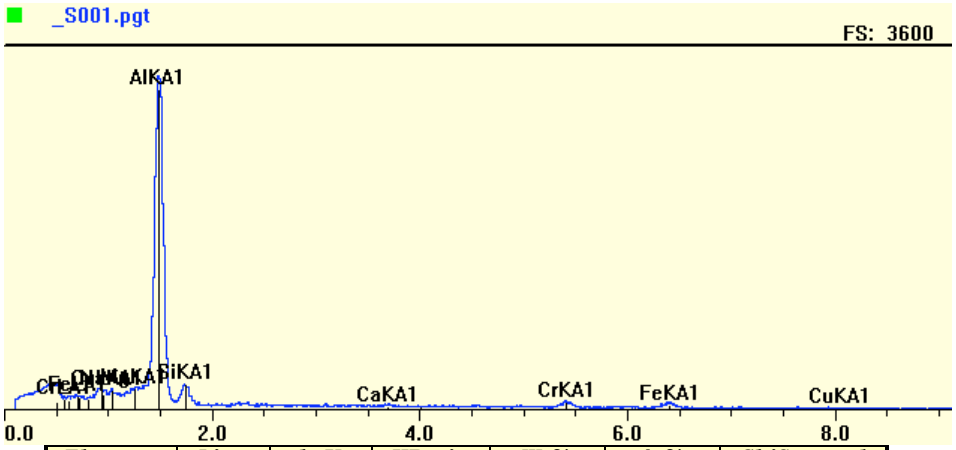

Element	Line	keV	KRatio	Wt%	At%	ChiSquared
Na	KA1	1.041	0.0148	2.11	2.93	26.26
Al	KA1	1.487	0.5135	60.31	71.60	26.26
Si	KA1	1.740	0.0291	4.16	4.74	26.26
Ca	KA1	3.691	0.0037	0.39	0.31	1.13
Cr	KA1	5.414	0.0500	5.58	3.44	1.35
Fe	KA1	6.403	0.1075	12.45	7.14	1.31
Mg	KA1	1.254	0.0232	2.81	3.70	26.26
Cu	LA1	0.930	0.0815	12.20	6.15	26.26
Total				**100.00**	**100.00**	**22.35**

Figure A2. EDS spectrum for the particles formed on the grayish black area of the Al specimen used in the loop test and their chemical composition.

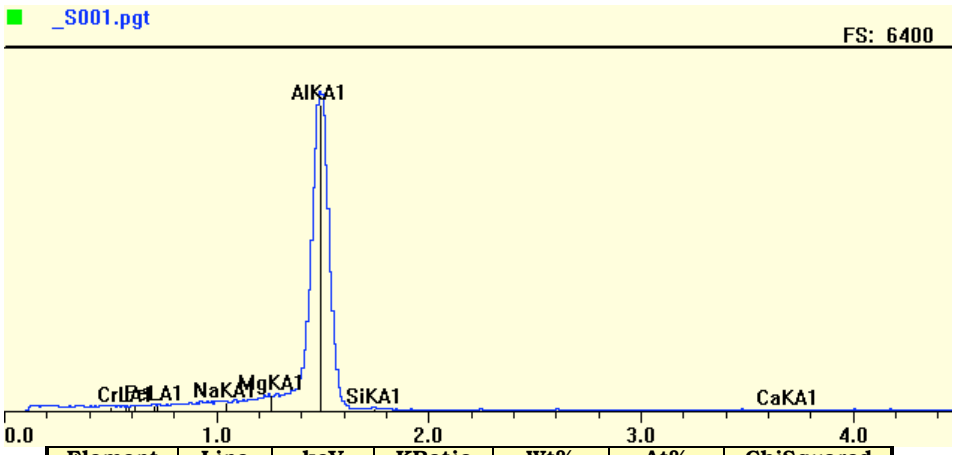

Element	Line	keV	KRatio	Wt%	At%	ChiSquared
Na	KA1	1.041	0.0000	0.00	0.00	0.00
Al	KA1	1.487	0.9368	96.18	96.43	35.03
Si	KA1	1.740	0.0000	0.00	0.00	0.00
Ca	KA1	3.691	0.0011	0.12	0.08	1.11
Cr	KA1	5.414	0.0023	0.28	0.14	0.92
Fe	KA1	6.403	0.0061	0.74	0.36	0.92
Mg	KA1	1.254	0.0291	2.68	2.98	35.03
Total				**100.00**	**100.00**	**29.49**

Figure A3. EDS spectrum for the metallic white area of the Al specimen used in the loop test and its chemical composition.

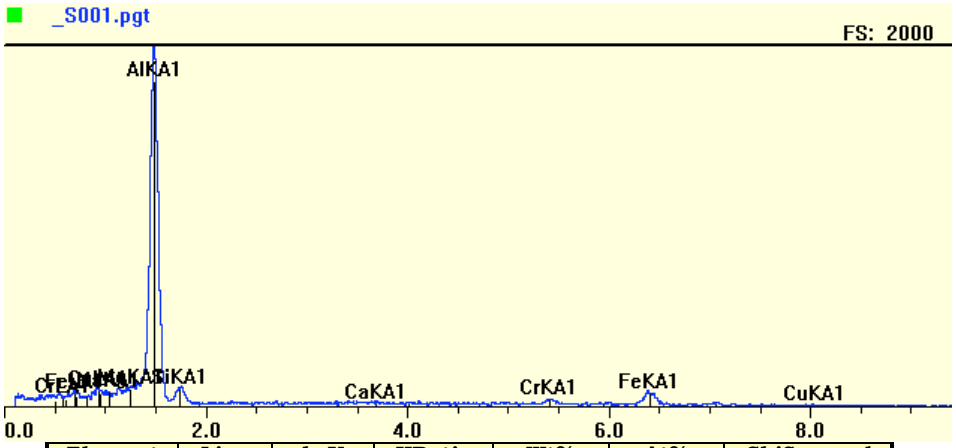

Element	Line	keV	KRatio	Wt%	At%	ChiSquared
Na	KA1	1.041	0.0056	0.85	1.25	11.43
Al	KA1	1.487	0.4642	55.47	69.44	11.43
Si	KA1	1.740	0.0187	2.62	3.15	11.43
Ca	KA1	3.691	0.0037	0.38	0.32	0.80
Cr	KA1	5.414	0.0331	3.52	2.29	1.20
Fe	KA1	6.403	0.2177	24.78	14.98	1.26
Mg	KA1	1.254	0.0185	2.33	3.23	11.43
Cu	LA1	0.930	0.0588	10.06	5.35	11.43
Total				**100.00**	**100.00**	**9.39**

Figure A4. EDS spectrum for the particle formed on the metallic white area of the Al specimen used in the loop test and its chemical composition.

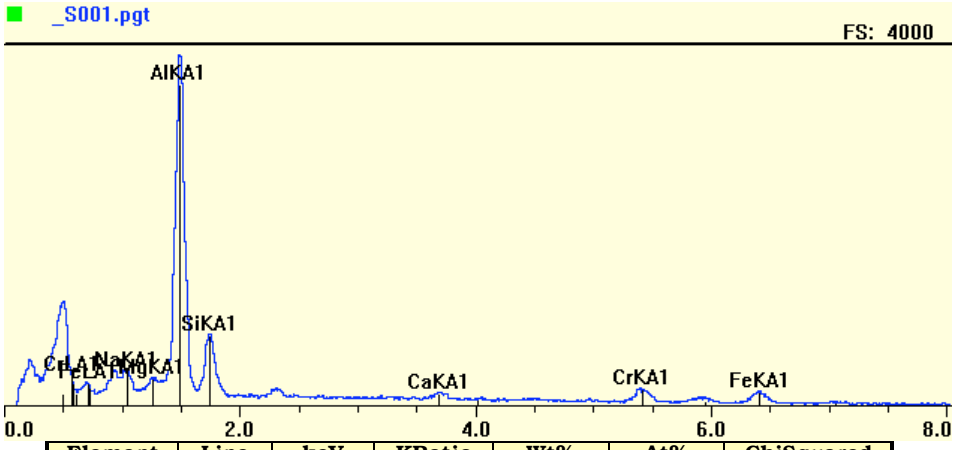

Element	Line	keV	KRatio	Wt%	At%	ChiSquared
Na	KA1	1.041	0.0314	4.63	6.58	28.81
Al	KA1	1.487	0.3908	46.47	56.39	28.81
Si	KA1	1.740	0.0743	9.97	11.62	28.81
Ca	KA1	3.691	0.0180	1.85	1.51	1.13
Cr	KA1	5.414	0.1043	11.39	7.17	3.87
Fe	KA1	6.403	0.2034	23.47	13.75	1.32
Mg	KA1	1.254	0.0177	2.21	2.98	28.81
Total				**100.00**	**100.00**	**100.46**

Figure A5. EDS spectrum for the particles loosely adhered on the Al specimen used in the loop test and their chemical composition (Cu peak is significant but it is not included in the chemical composition table).

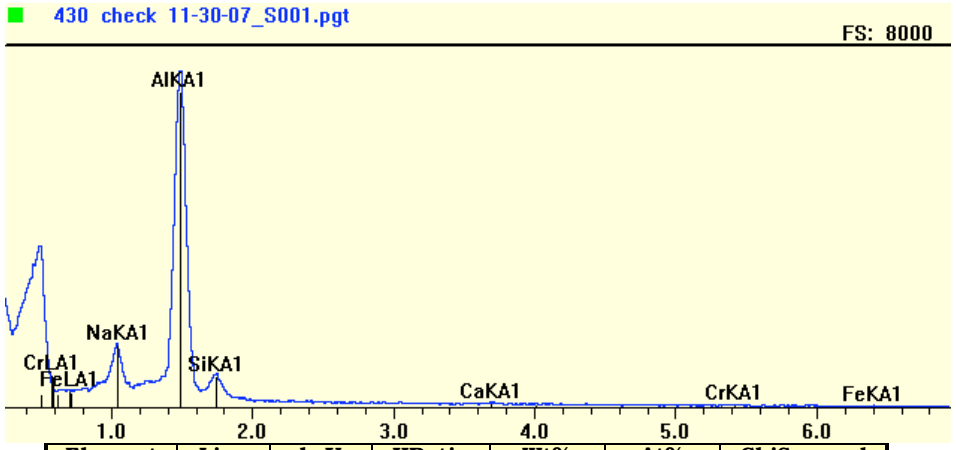

Element	Line	keV	KRatio	Wt%	At%	ChiSquared
Na	KA1	1.041	0.1383	14.78	17.11	23.16
Al	KA1	1.487	0.6829	75.31	74.35	49.01
Si	KA1	1.740	0.0522	7.84	7.43	49.01
Cr	KA1	5.414	0.0040	0.48	0.24	1.43
Fe	KA1	6.403	0.0083	1.02	0.49	0.78
Ca	KA1	3.691	0.0053	0.58	0.39	1.22
Total				**100.00**	**100.00**	**718.65**

Figure A6. EDS spectrum for the precipitate attached on a glass fiber of the NUKON bed used in the loop test suggesting mainly Al oxides.

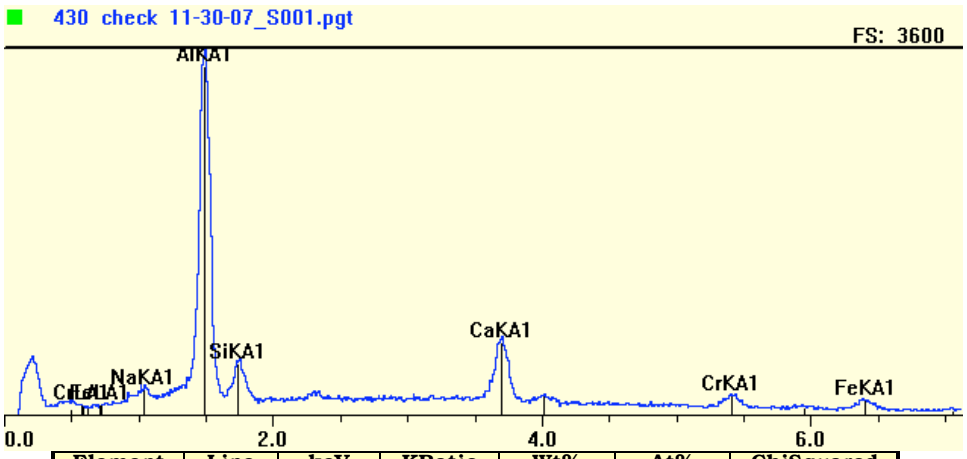

Element	Line	keV	KRatio	Wt%	At%	ChiSquared
Na	KA1	1.041	0.0134	2.00	2.94	2.99
Al	KA1	1.487	0.3880	45.11	56.67	23.52
Si	KA1	1.740	0.0449	5.89	7.10	23.52
Ca	KA1	3.691	0.1758	18.01	15.23	6.06
Cr	KA1	5.414	0.0912	10.17	6.63	1.30
Fe	KA1	6.403	0.1630	18.83	11.42	1.01
Total				**100.00**	**100.00**	**30.33**

Figure A7. EDS spectrum for the precipitate attached on a glass fiber of the NUKON bed used in the loop test suggesting Al, Si, Cr, Fe, and Cu mixture particle (Cu peak is located at the left side of the Na peak, but it is not included in the composition table).

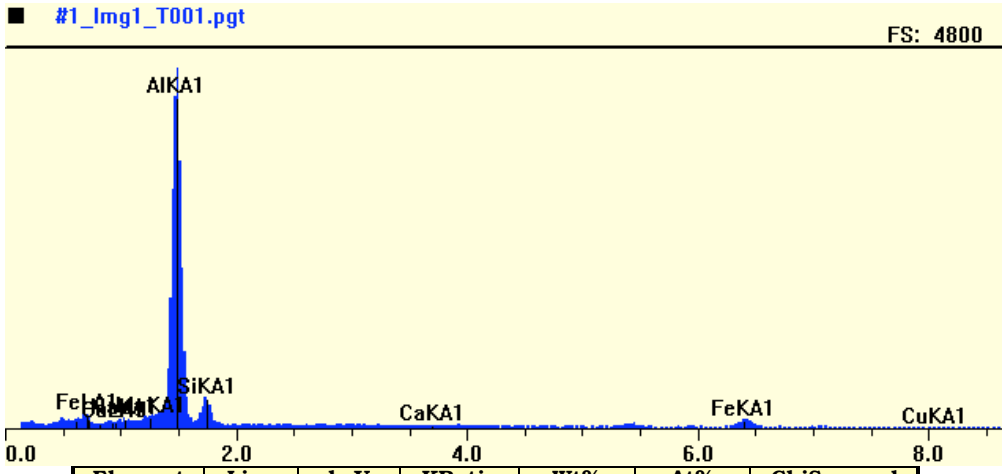

Element	Line	keV	KRatio	Wt%	At%	ChiSquared
Na	KA1	1.041	0.0075	0.96	1.23	26.80
Si	KA1	1.740	0.0504	7.36	7.76	26.80
Ca	KA1	3.691	0.0000	0.00	0.00	0.00
Al	KA1	1.487	0.6573	72.48	79.58	26.80
Mg	KA1	1.254	0.0172	1.88	2.29	26.80
Fe	LA1	0.705	0.1259	16.61	8.81	26.80
Cu	LA1	0.930	0.0047	0.71	0.33	26.80
Total				**100.00**	**100.00**	**21.49**

Figure A8. EDS spectrum for the spot “1” designated in Figure 18 (a) suggesting Al, Fe, and Si mixture particle (acceleration voltage=10 kV).

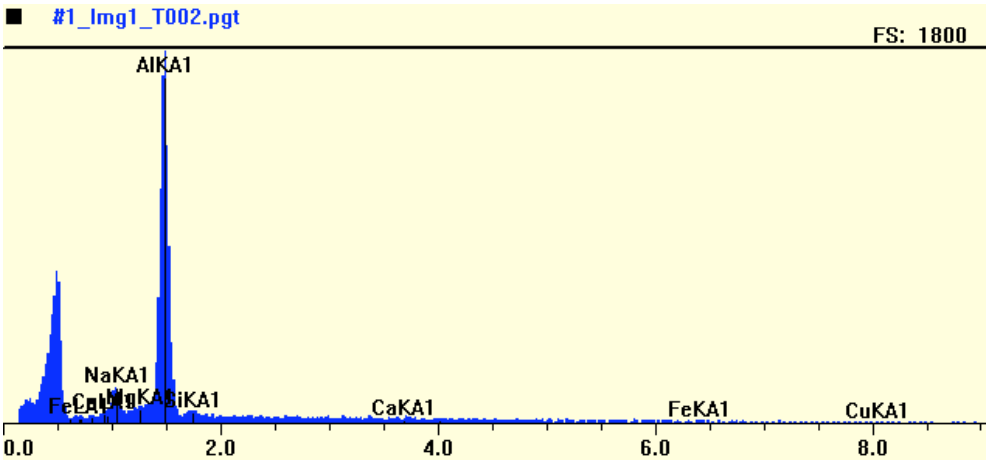

Element	Line	keV	KRatio	Wt%	At%	ChiSquared
Na	KA1	1.041	0.0679	7.61	9.10	58.22
Si	KA1	1.740	0.0146	2.25	2.20	58.22
Ca	KA1	3.691	0.0034	0.37	0.26	1.21
Al	KA1	1.487	0.7366	81.30	82.84	58.22
Mg	KA1	1.254	0.0247	2.64	2.98	58.22
Fe	LA1	0.705	0.0131	1.76	0.87	58.22
Cu	LA1	0.930	0.0336	4.06	1.75	58.22
Total				**100.00**	**100.00**	**106.27**

Figure A9. EDS spectrum for the spot “2” designated in Figure 18 (a) suggesting mainly Al hydroxide with some NaOH precipitate (acceleration voltage=10 kV).

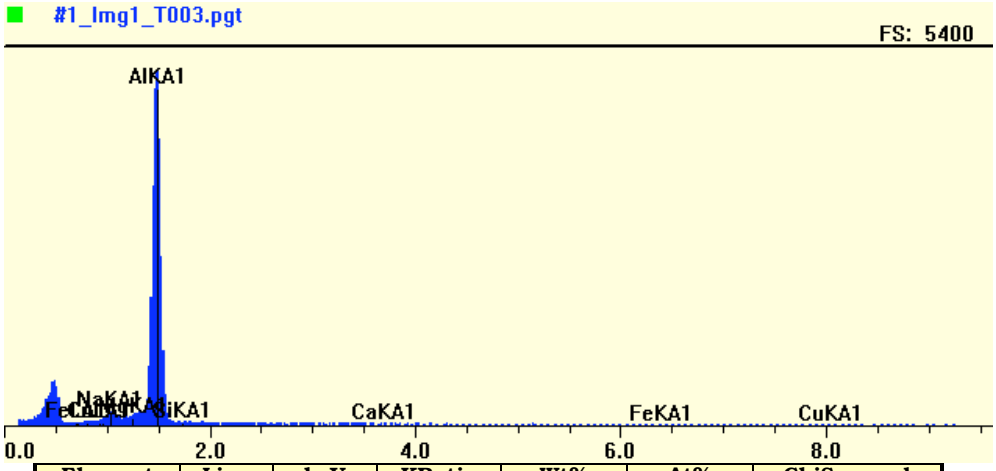

Element	Line	keV	KRatio	Wt%	At%	ChiSquared
Na	KA1	1.041	0.0317	3.37	3.97	57.32
Si	KA1	1.740	0.0005	0.09	0.08	57.32
Ca	KA1	3.691	0.0000	0.00	0.00	0.00
Al	KA1	1.487	0.8758	92.20	92.62	57.32
Mg	KA1	1.254	0.0218	2.13	2.37	57.32
Fe	LA1	0.705	0.0015	0.21	0.10	57.32
Cu	LA1	0.930	0.0171	2.02	0.86	57.32
Total				**100.00**	**100.00**	**77.35**

Figure A10. EDS spectrum for the spot “3” designated in Figure 18 (a) suggesting mainly Al hydroxide on the Al plate surface (acceleration voltage=10 kV).

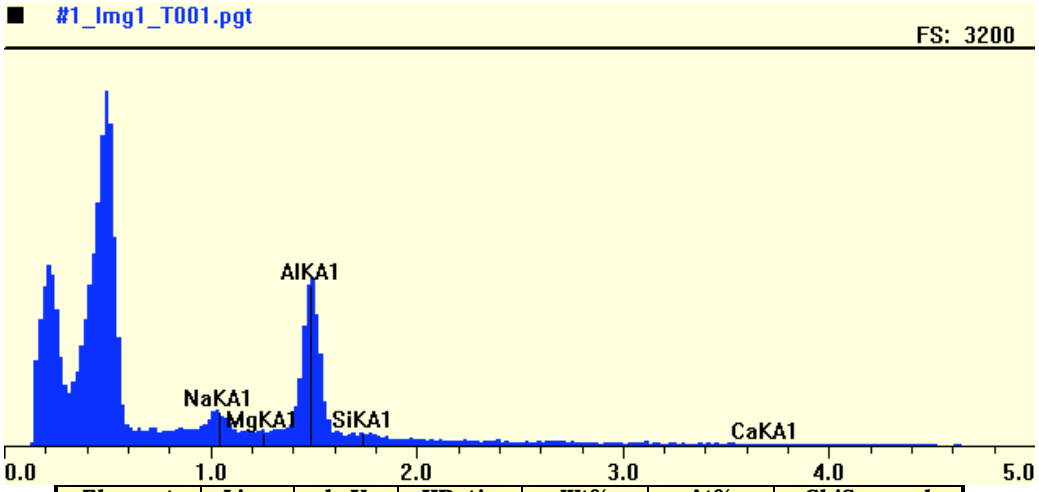

Element	Line	keV	KRatio	Wt%	At%	ChiSquared
Na	KA1	1.041	0.1189	11.68	13.47	8.57
Si	KA1	1.740	0.0187	2.15	2.03	8.57
Ca	KA1	3.691	0.0106	1.17	0.77	0.00
Al	KA1	1.487	0.8144	83.79	82.40	8.57
Mg	KA1	1.254	0.0127	1.22	1.33	8.57
Total				**100.00**	**100.00**	**968.66**

Figure A11. EDS spectrum for the spot “1” designated in Figure 19 (b): top region of the NUKON bed used in the 1100 Al test suggesting mainly Al hydroxide (acceleration voltage=5 kV).

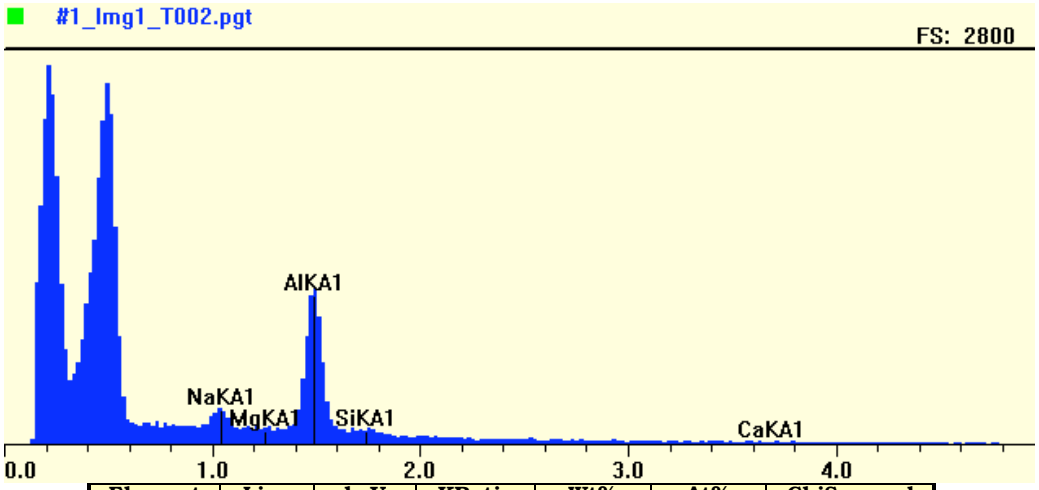

Element	Line	keV	KRatio	Wt%	At%	ChiSquared
Na	KA1	1.041	0.0978	9.58	11.10	5.70
Si	KA1	1.740	0.0320	3.66	3.47	5.70
Ca	KA1	3.691	0.0081	0.90	0.60	0.00
Al	KA1	1.487	0.8382	85.63	84.58	5.70
Mg	KA1	1.254	0.0024	0.23	0.25	5.70
Total				**100.00**	**100.00**	**1148.60**

Figure A12. EDS spectrum for the spot “2” designated in Figure 19 (b): top region of the NUKON bed used in the 1100 Al test suggesting mainly Al hydroxide (acceleration voltage=5 kV).

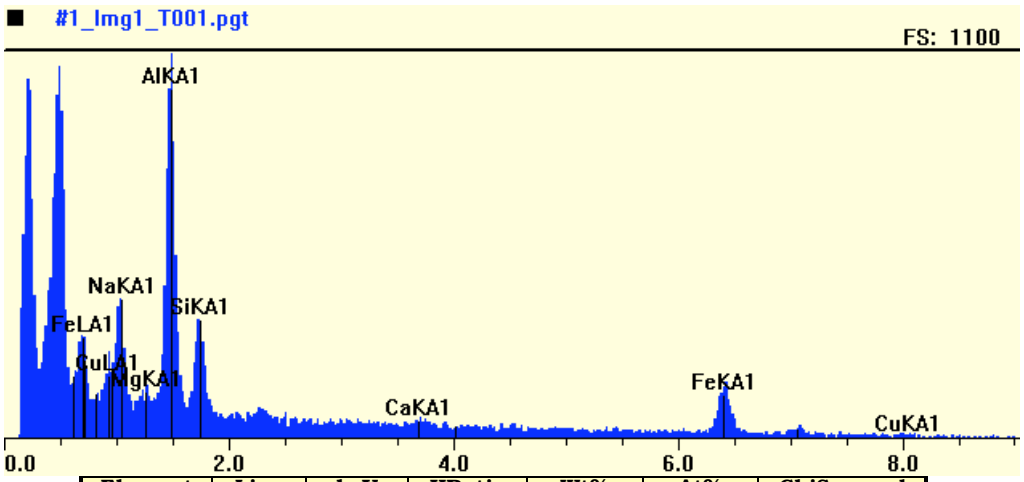

Element	Line	keV	KRatio	Wt%	At%	ChiSquared
Na	KA1	1.041	0.0713	12.48	20.07	56.96
Si	KA1	1.740	0.0537	6.97	9.18	56.96
Ca	KA1	3.691	0.0047	0.46	0.43	1.56
Al	KA1	1.487	0.1880	25.08	34.39	56.96
Mg	KA1	1.254	0.0046	0.69	1.05	56.96
Fe	LA1	0.705	0.3466	40.77	27.00	56.96
Cu	LA1	0.930	0.0724	13.54	7.88	56.96
Total				**100.00**	**100.00**	**178.25**

Figure A13. EDS spectrum for the spot “1” designated in Figure 21 (a): middle region of the NUKON bed used in the 1100 Al test suggesting Al-Fe-Cu intermetallics (acceleration voltage=10 kV).

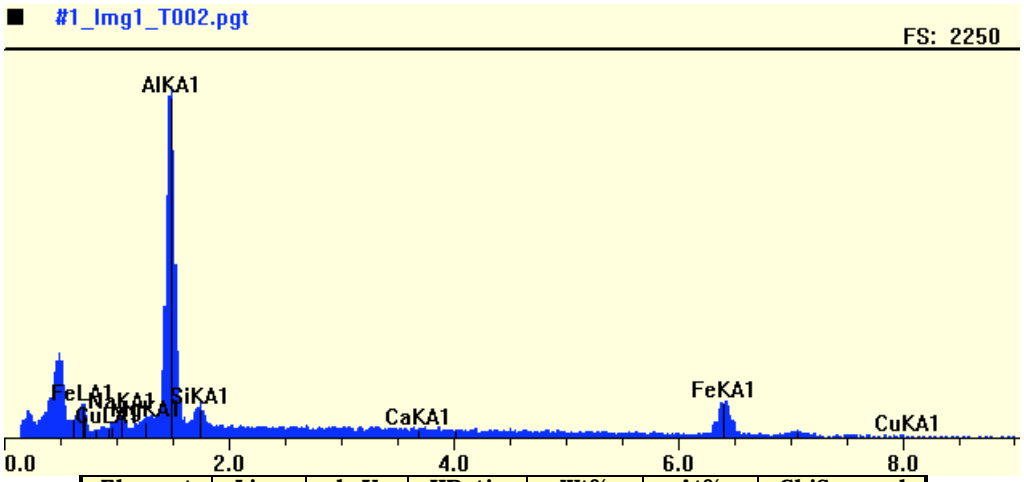

Element	Line	keV	KRatio	Wt%	At%	ChiSquared
Na	KA1	1.041	0.0218	2.96	4.01	20.78
Si	KA1	1.740	0.0333	4.80	5.32	20.78
Ca	KA1	3.691	0.0052	0.55	0.42	1.16
Al	KA1	1.487	0.5663	64.31	74.18	20.78
Mg	KA1	1.254	0.0098	1.14	1.45	20.78
Fe	LA1	0.705	0.2035	26.24	14.62	20.78
Cu	LA1	0.930	0.0000	0.00	0.00	0.00
Total				**100.00**	**100.00**	**27.53**

Figure A14. EDS spectrum for the spot “2” designated in Figure 21 (a): middle region of the NUKON bed used in the 1100 Al test suggesting mainly Al-Fe intermetallics (acceleration voltage=10 kV).

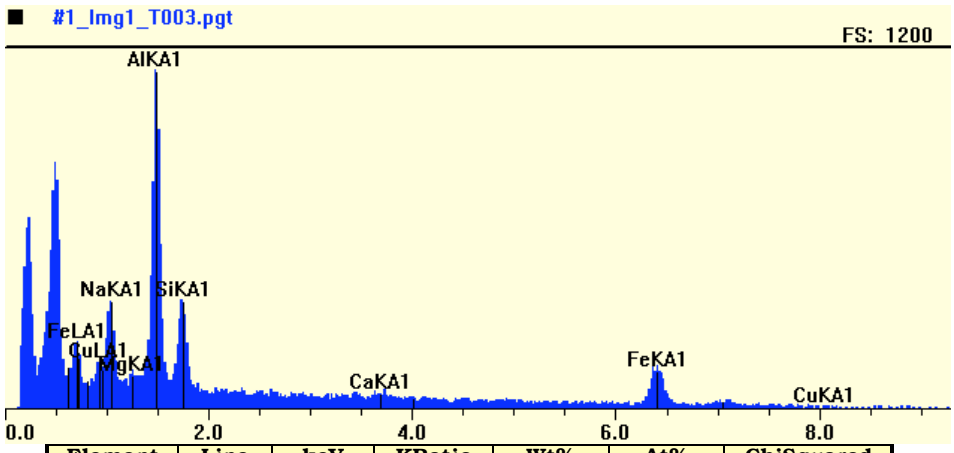

Element	Line	keV	KRatio	Wt%	At%	ChiSquared
Na	KA1	1.041	0.0908	14.23	20.58	41.28
Si	KA1	1.740	0.0821	10.92	12.92	41.28
Ca	KA1	3.691	0.0065	0.67	0.56	1.26
Al	KA1	1.487	0.2731	34.53	42.57	41.28
Mg	KA1	1.254	0.0036	0.50	0.69	41.28
Fe	LA1	0.705	0.2456	30.42	18.11	41.28
Cu	LA1	0.930	0.0493	8.73	4.57	41.28
Total				**100.00**	**100.00**	**93.98**

Figure A15. EDS spectrum for the spot “3” designated in Figure 21 (a): middle region of the NUKON bed used in the 1100 Al test suggesting mainly Al-Fe-Cu intermetallics (acceleration voltage=10 kV).

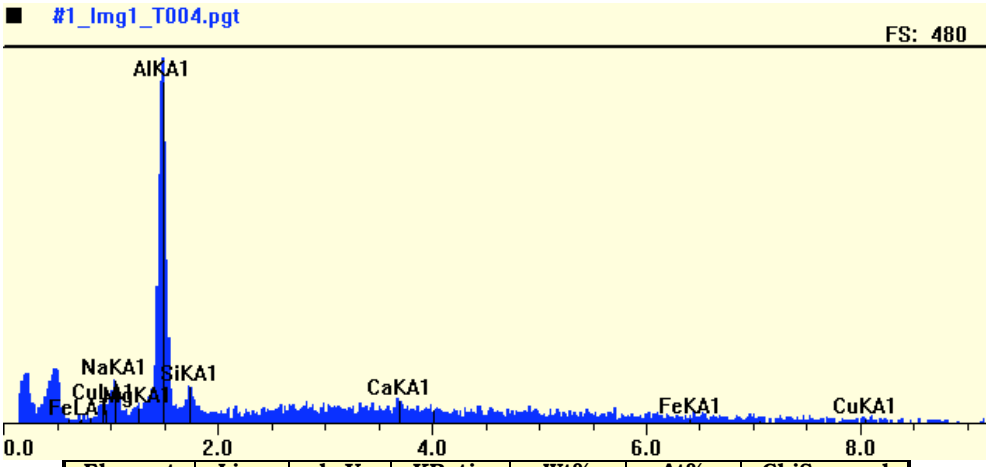

Element	Line	keV	KRatio	Wt%	At%	ChiSquared
Na	KA1	1.041	0.0725	8.37	10.16	3.84
Si	KA1	1.740	0.0385	5.80	5.76	3.84
Ca	KA1	3.691	0.0286	3.13	2.18	0.81
Al	KA1	1.487	0.6899	76.01	78.66	3.84
Mg	KA1	1.254	0.0039	0.43	0.49	3.84
Fe	LA1	0.705	0.0000	0.00	0.00	0.00
Cu	LA1	0.930	0.0520	6.26	2.75	3.84
Total				**100.00**	**100.00**	**5.82**

Figure A16. EDS spectrum for the spot “4” designated in Figure 21 (a): middle region of the NUKON bed used in the 1100 Al test suggesting mainly Al hydroxide (acceleration voltage=10 kV).

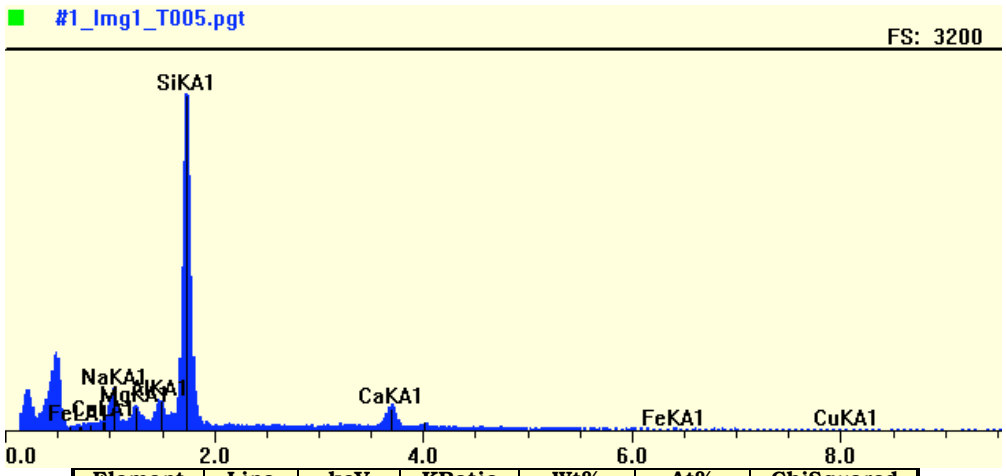

Element	Line	keV	KRatio	Wt%	At%	ChiSquared
Na	KA1	1.041	0.0743	9.04	11.25	48.73
Si	KA1	1.740	0.6437	70.56	71.89	48.73
Ca	KA1	3.691	0.0839	9.41	6.72	6.75
Al	KA1	1.487	0.0393	4.38	4.65	48.73
Mg	KA1	1.254	0.0300	3.47	4.08	48.73
Fe	LA1	0.705	0.0000	0.00	0.00	0.00
Cu	LA1	0.930	0.0231	3.13	1.41	48.73
Total				**100.00**	**100.00**	**77.59**

Figure A17. EDS spectrum for the spot “5” designated in Figure 21 (a): fiber surface in the middle region of the NUKON bed used in the 1100 Al test (acceleration voltage=10 kV).

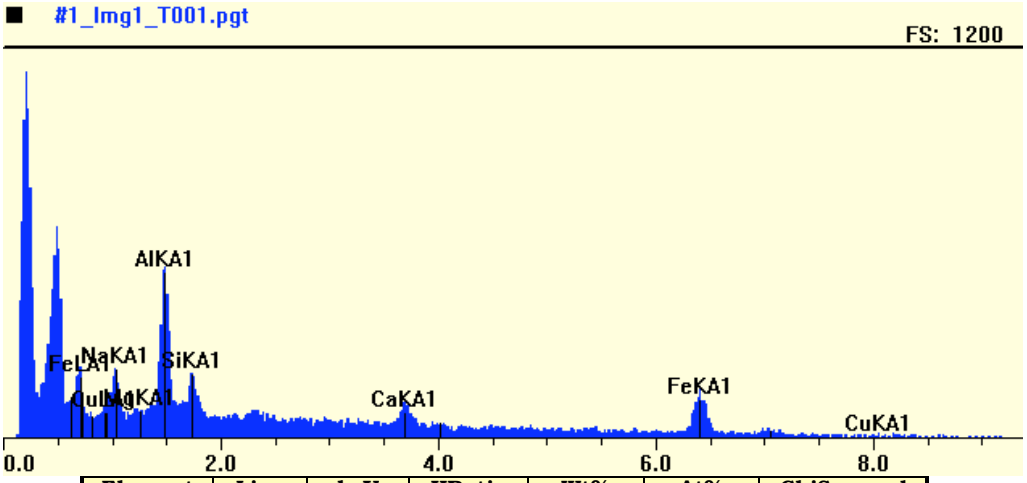

Element	Line	keV	KRatio	Wt%	At%	ChiSquared
Na	KA1	1.041	0.0648	11.17	17.85	34.67
Si	KA1	1.740	0.0565	7.18	9.39	34.67
Ca	KA1	3.691	0.0547	5.43	4.98	3.09
Al	KA1	1.487	0.1924	24.80	33.81	34.67
Mg	KA1	1.254	0.0042	0.61	0.93	34.67
Fe	LA1	0.705	0.3557	45.50	29.95	34.67
Cu	LA1	0.930	0.0257	5.33	3.08	34.67
Total				**100.00**	**100.00**	**184.94**

Figure A18. EDS spectrum for the spot “1” in Figure 23 (a): bottom region of the NUKON bed used in the 1100 Al test suggesting Al-Fe-Cu intermetallics (acceleration voltage=10 kV).

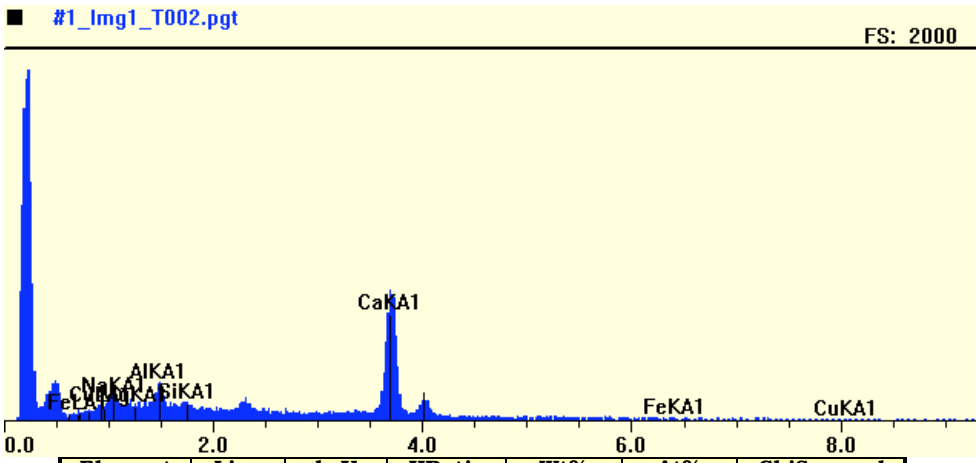

Element	Line	keV	KRatio	Wt%	At%	ChiSquared
Na	KA1	1.041	0.0514	8.18	13.12	8.29
Si	KA1	1.740	0.0135	1.53	2.01	8.29
Ca	KA1	3.691	0.7306	73.99	68.09	41.85
Al	KA1	1.487	0.0590	7.27	9.95	8.29
Mg	KA1	1.254	0.0125	1.69	2.56	8.29
Fe	LA1	0.705	0.0008	0.22	0.14	8.29
Cu	LA1	0.930	0.0383	7.13	4.14	8.29
Total				**100.00**	**100.00**	**484.12**

Figure A19. EDS spectrum for the spot “2” in Figure 23 (a): bottom region of the NUKON bed used in the 1100 Al test suggesting Ca oxide (acceleration voltage=10 kV).

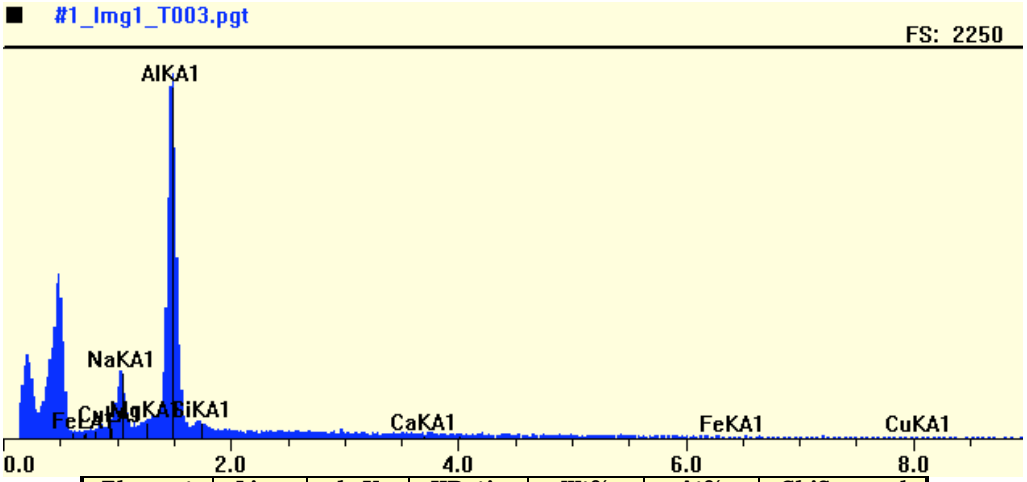

Element	Line	keV	KRatio	Wt%	At%	ChiSquared
Na	KA1	1.041	0.1186	12.92	15.09	66.02
Si	KA1	1.740	0.0135	2.08	1.99	66.02
Ca	KA1	3.691	0.0018	0.20	0.13	1.27
Al	KA1	1.487	0.7147	79.99	79.65	66.02
Mg	KA1	1.254	0.0147	1.62	1.79	66.02
Fe	LA1	0.705	0.0000	0.00	0.00	0.00
Cu	LA1	0.930	0.0272	3.19	1.35	66.02
Total				**100.00**	**100.00**	**145.41**

Figure A20. EDS spectrum for the spot “3” in Figure 23 (a): bottom region of the NUKON bed used in the 1100 Al test suggesting Al hydroxide and NaOH (acceleration voltage=10 kV).

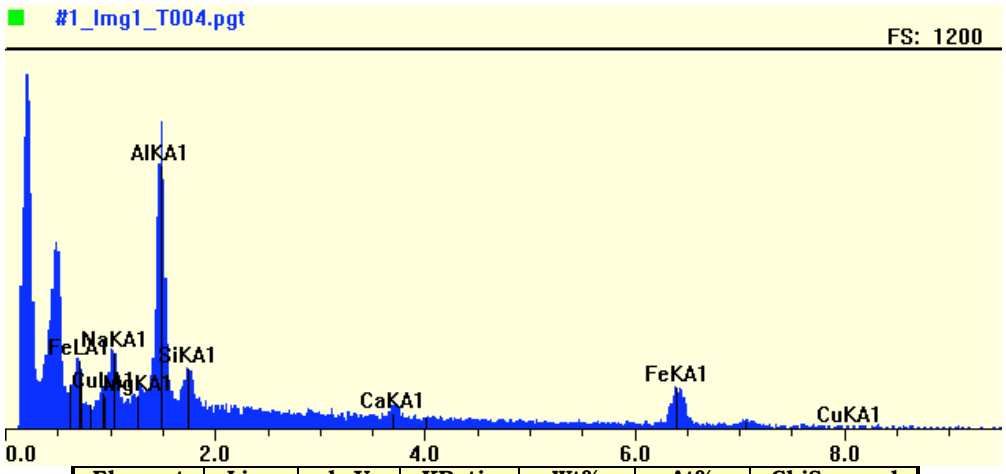

Element	Line	keV	KRatio	Wt%	At%	ChiSquared
Na	KA1	1.041	0.0728	11.58	17.10	25.71
Si	KA1	1.740	0.0428	5.74	6.94	25.71
Ca	KA1	3.691	0.0208	2.11	1.79	2.14
Al	KA1	1.487	0.3082	38.65	48.66	25.71
Mg	KA1	1.254	0.0043	0.60	0.83	25.71
Fe	LA1	0.705	0.2846	35.51	21.59	25.71
Cu	LA1	0.930	0.0311	5.80	3.10	25.71
Total				**100.00**	**100.00**	**161.41**

Figure A21. EDS spectrum for the spot “4” in Figure 23 (a): bottom region of the NUKON bed used in the 1100 Al test suggesting Al-Fe-Cu intermetallics (acceleration voltage=10 kV).

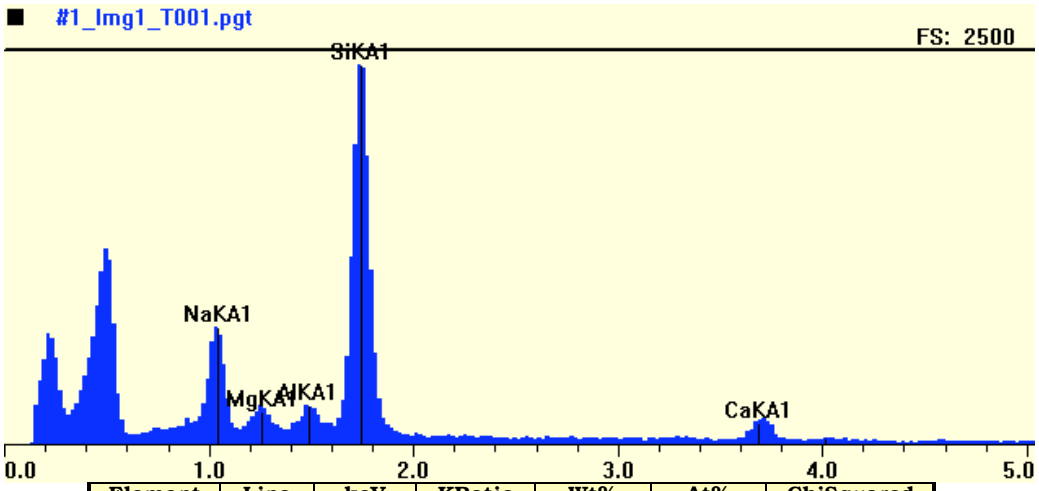

Element	Line	keV	KRatio	Wt%	At%	ChiSquared
Na	KA1	1.041	0.1851	21.19	25.01	24.71
Si	KA1	1.740	0.5427	61.97	59.87	24.71
Ca	KA1	3.691	0.0639	7.20	4.88	5.48
Al	KA1	1.487	0.0388	4.61	4.64	24.71
Mg	KA1	1.254	0.0407	5.02	5.60	24.71
Total				**100.00**	**100.00**	**200.10**

Figure A22. EDS spectrum for the spot “1” in Figure 24 (a): fiber surface of the unexposed NUKON (acceleration voltage=10 kV).

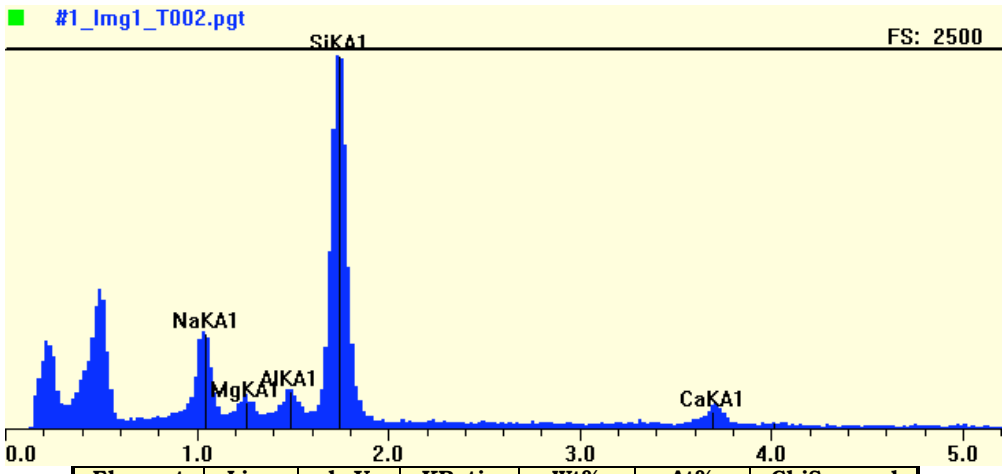

Element	Line	keV	KRatio	Wt%	At%	ChiSquared
Na	KA1	1.041	0.1661	19.03	22.55	23.70
Si	KA1	1.740	0.5714	64.69	62.77	23.70
Ca	KA1	3.691	0.0606	6.84	4.65	5.72
Al	KA1	1.487	0.0435	5.07	5.12	23.70
Mg	KA1	1.254	0.0361	4.37	4.90	23.70
Total				**100.00**	**100.00**	**127.53**

Figure A23. EDS spectrum for the spot “2” in Figure 24 (a): fiber surface of the unexposed NUKON (acceleration voltage=10 kV).

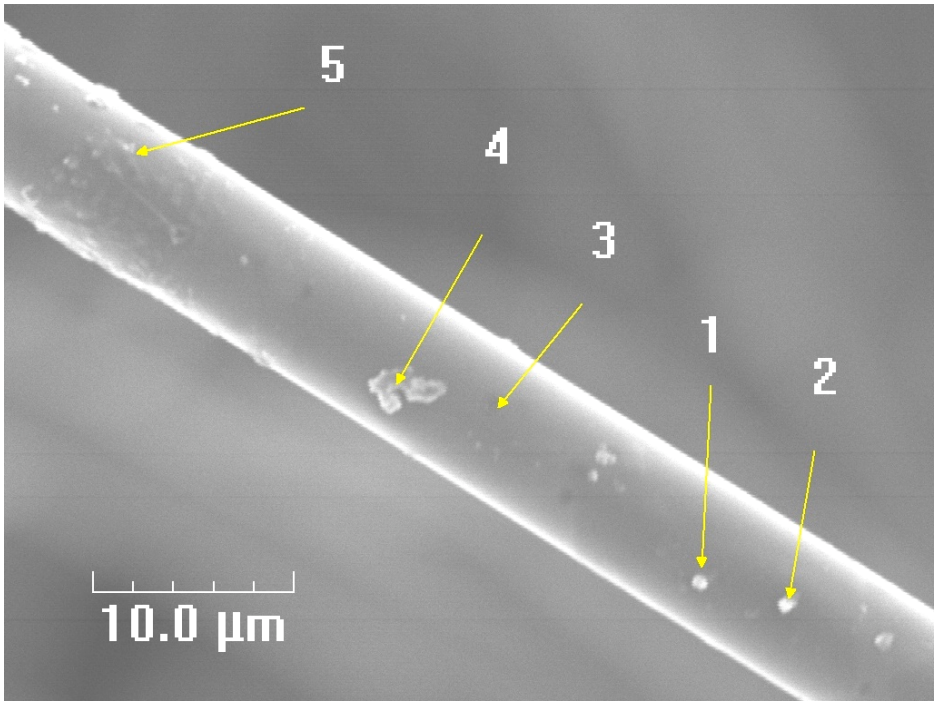

Figure A24. SEM micrograph for a fiber in the NUKON patch #2 showing precipitates formed on the fiber surface; “1” is NaOH, “2” is similar to fiber, “3” is similar to typical fiber composition, “4” is Al hydroxide, and “5” is Al hydroxide (2700X magnification).

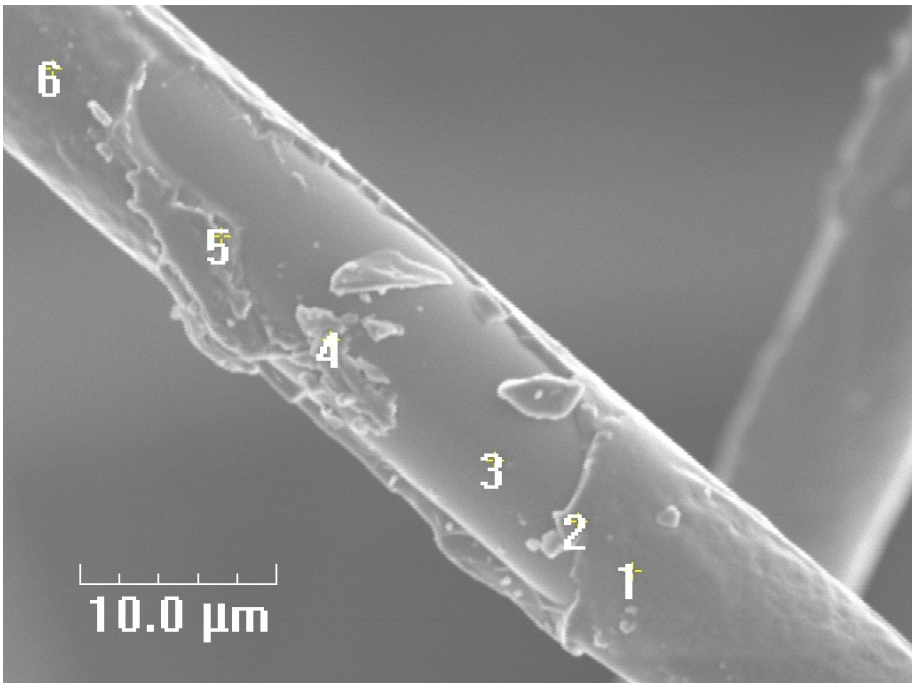

Figure A25. SEM micrograph for a fiber in the NUKON patch #3 showing precipitates formed on the fiber surface; “1” is Na-depleted zone, “2” is Na and Al-enriched region, “3” is similar to “1”, “4” is NaOH precipitate, “5” is NaOH precipitates, and “6” is similar to “1” (2700X magnification).

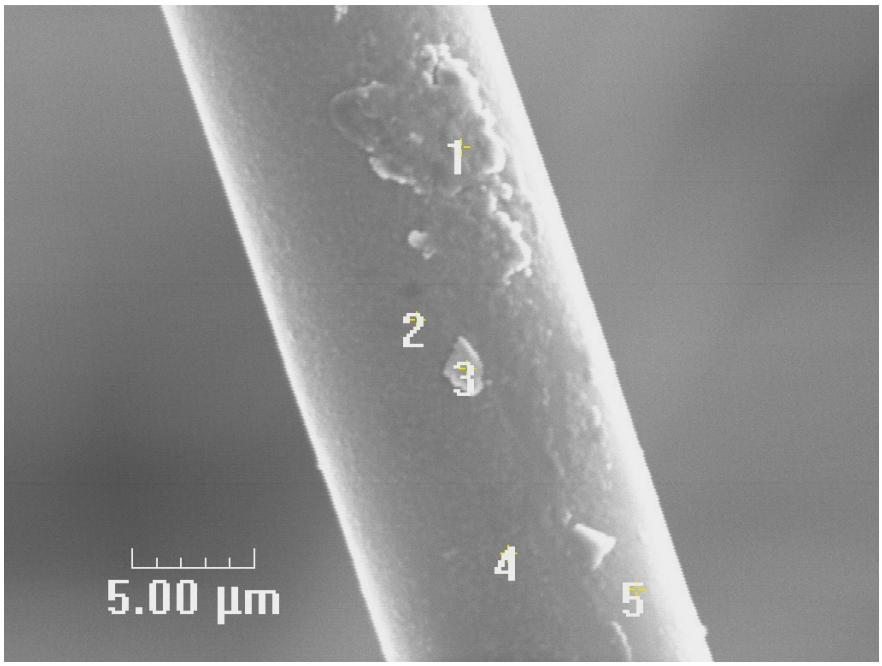

Figure A26. SEM micrograph for a fiber in the NUKON patch #4 showing precipitates formed on the fiber surface; “1” is Na and Al enriched oxides, “2” is similar to typical fiber composition, “3” is Cu-Fe enriched intermetallics, “4” is similar to “2”, and “5” is similar to “2” but Na concentration is less (3500X magnification).

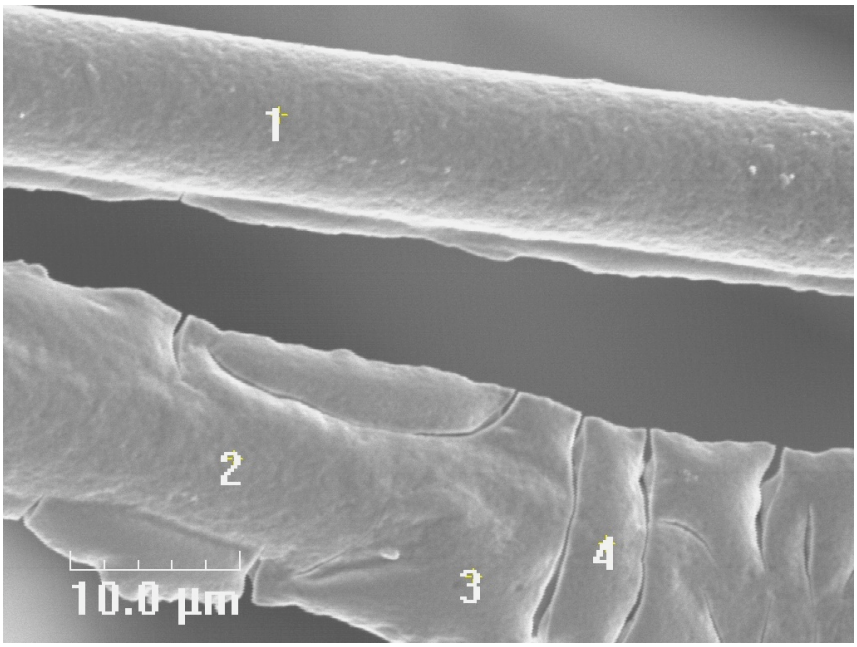

Figure A27. SEM micrograph for a fiber in the NUKON patch #5 showing precipitates formed on the fiber surface; “1” is similar to typical fiber composition but higher Al, “2” is similar to “1” but more Al, and “3” and “4” are Al hydroxide precipitates with some NaOH (2500X magnification).

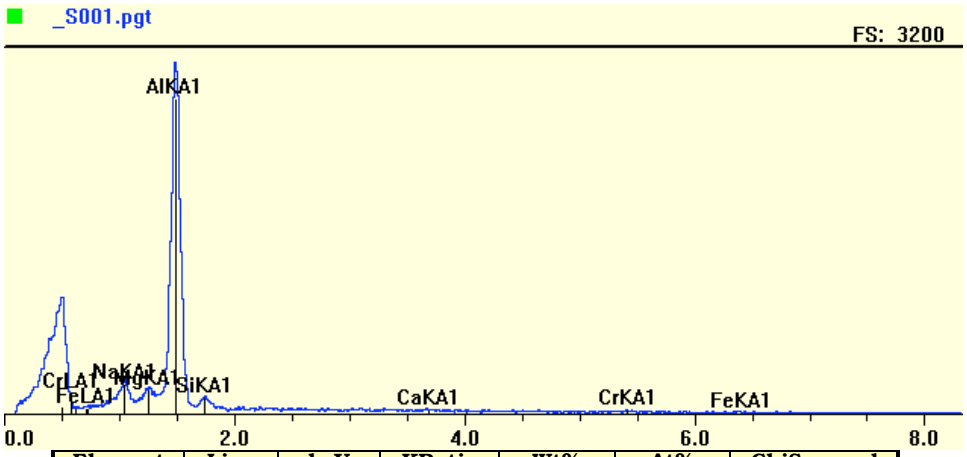

Element	Line	keV	KRatio	Wt%	At%	ChiSquared
Na	KA1	1.041	0.0635	6.93	8.18	26.77
Al	KA1	1.487	0.7326	80.54	81.03	26.77
Si	KA1	1.740	0.0230	3.51	3.39	26.77
Ca	KA1	3.691	0.0058	0.63	0.43	0.80
Cr	KA1	5.414	0.0123	1.47	0.77	1.03
Fe	KA1	6.403	0.0196	2.38	1.16	1.19
Mg	KA1	1.254	0.0436	4.53	5.05	26.77
Total				**100.00**	**100.00**	**139.66**

Figure A28. EDS spectrum for the particle-free region of 6061 Al coupon without other metal coupon tested at 140 F and pH=9.4 for one week suggesting mainly Al oxide.

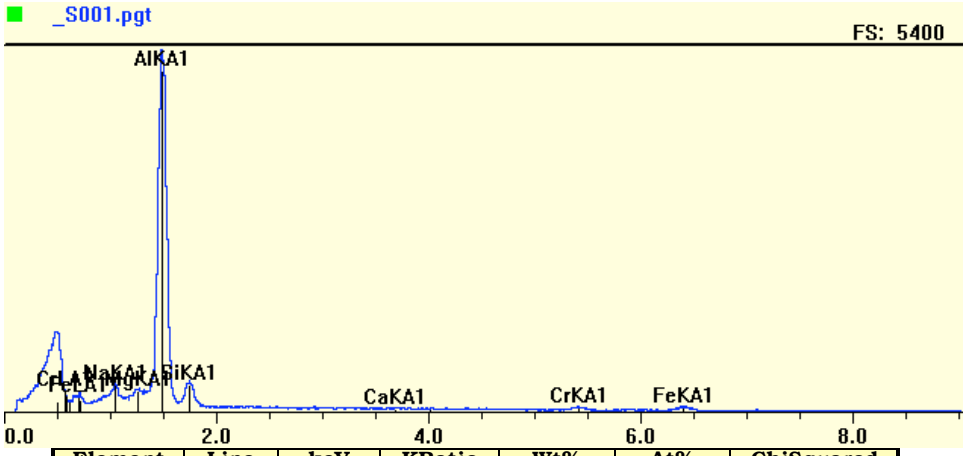

Element	Line	keV	KRatio	Wt%	At%	ChiSquared
Na	KA1	1.041	0.0339	4.23	5.37	36.23
Al	KA1	1.487	0.6321	70.70	76.49	36.23
Si	KA1	1.740	0.0404	5.90	6.13	36.23
Ca	KA1	3.691	0.0027	0.29	0.21	1.09
Cr	KA1	5.414	0.0344	3.94	2.21	1.30
Fe	KA1	6.403	0.1035	12.31	6.43	1.49
Mg	KA1	1.254	0.0236	2.62	3.14	36.23
Total				**100.00**	**100.00**	**114.56**

Figure A29. EDS spectrum for the particles formed on 6061 Al coupon without other metal coupon tested at 140 F and pH=9.4 for one week.

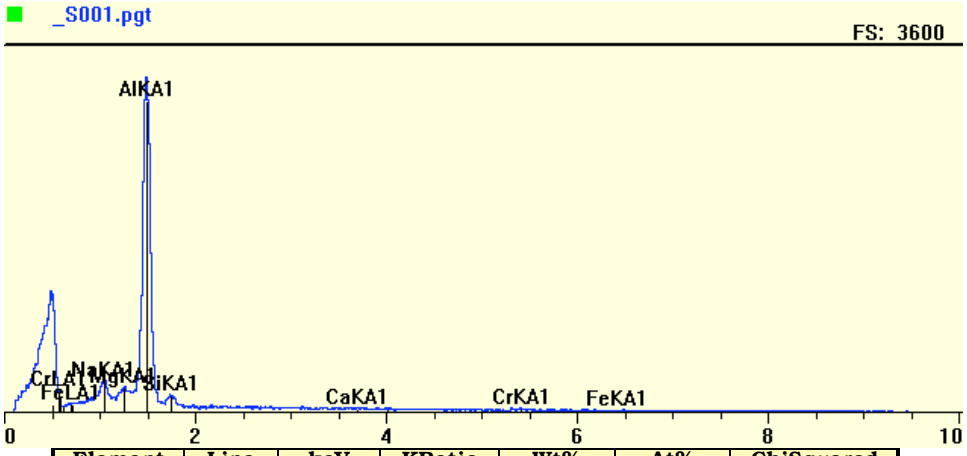

Element	Line	keV	KRatio	Wt%	At%	ChiSquared
Na	KA1	1.041	0.0640	6.87	8.05	28.60
Al	KA1	1.487	0.7477	81.82	81.71	28.60
Si	KA1	1.740	0.0245	3.77	3.61	28.60
Ca	KA1	3.691	0.0019	0.21	0.14	0.96
Cr	KA1	5.414	0.0102	1.22	0.63	1.37
Fe	KA1	6.403	0.0121	1.47	0.71	0.80
Mg	KA1	1.254	0.0452	4.64	5.14	28.60
Total				**100.00**	**100.00**	**163.63**

Figure A30. EDS spectrum for the particle-free region of 6061 Al coupon with SS coupon tested at 140 F and pH=9.4 for one week.

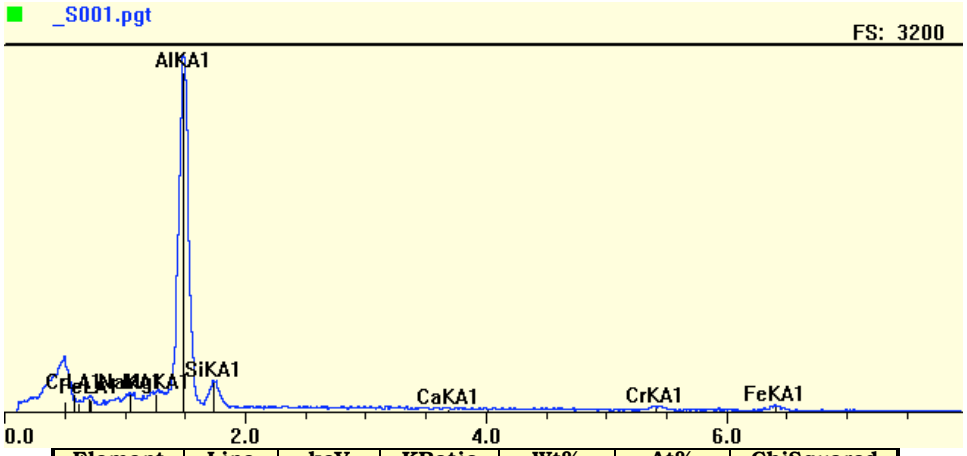

Element	Line	keV	KRatio	Wt%	At%	ChiSquared
Na	KA1	1.041	0.0169	2.16	2.79	22.09
Al	KA1	1.487	0.6305	70.11	77.28	22.09
Si	KA1	1.740	0.0445	6.45	6.82	22.09
Ca	KA1	3.691	0.0024	0.26	0.19	1.06
Cr	KA1	5.414	0.0433	4.92	2.81	1.16
Fe	KA1	6.403	0.1173	13.89	7.39	1.34
Mg	KA1	1.254	0.0201	2.23	2.72	22.09
Total				**100.00**	**100.00**	**35.37**

Figure A31. EDS spectrum for the particles formed on 6061 Al coupon with SS coupon tested at 140 F and pH=9.4 for one week.

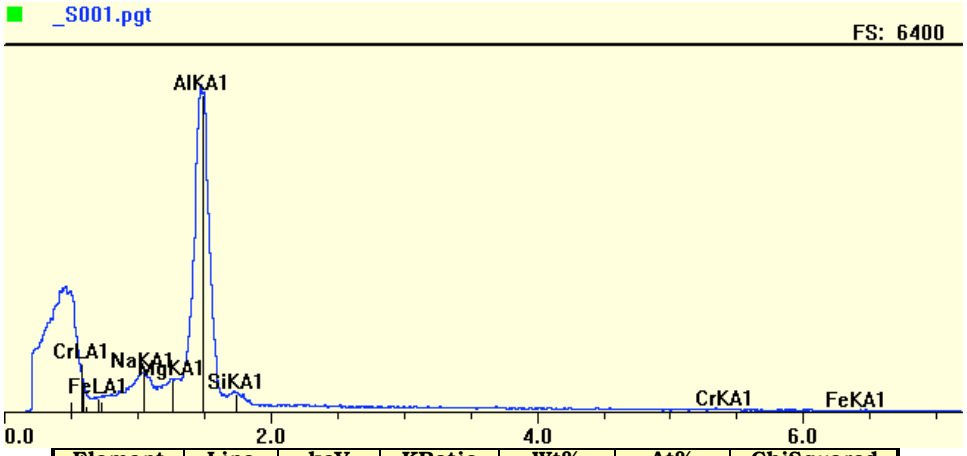

Element	Line	keV	KRatio	Wt%	At%	ChiSquared
Mg	KA1	1.254	0.0603	6.99	7.61	405.68
Al	KA1	1.487	0.6187	77.39	75.97	405.68
Si	KA1	1.740	0.0264	5.56	5.24	405.68
Na	KA1	1.041	0.0837	9.44	10.86	405.68
Cr	KA1	5.414	0.0040	0.48	0.24	1.23
Fe	KA1	6.403	0.0012	0.14	0.07	0.98
Total				**100.00**	**100.00**	**438.86**

Figure A32. EDS spectrum for the particle-free region of 6061 Al coupon with CS coupon tested at 140 F and pH=9.4 for one week.

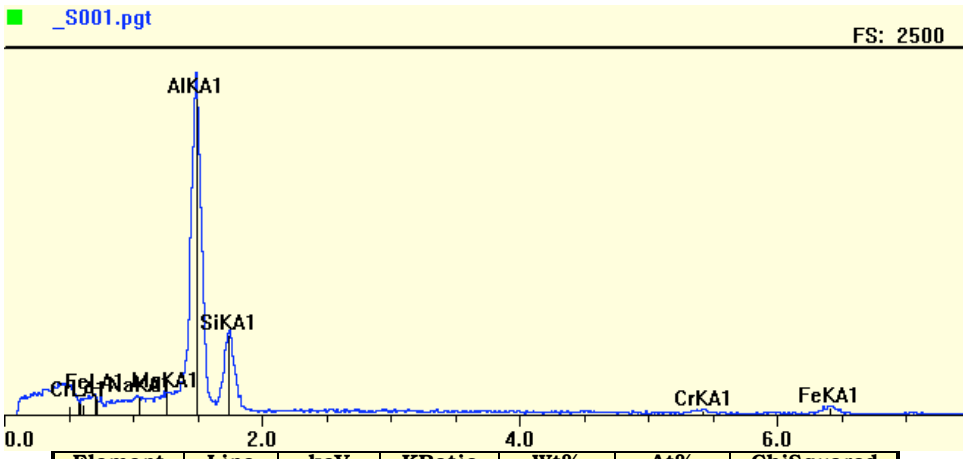

Element	Line	keV	KRatio	Wt%	At%	ChiSquared
Al	KA1	1.487	0.5321	59.22	66.98	13.81
Si	KA1	1.740	0.1206	16.65	18.09	13.81
Cr	KA1	5.414	0.0340	3.82	2.24	0.76
Fe	KA1	6.403	0.1539	18.14	9.91	1.30
Na	KA1	1.041	0.0055	0.73	0.97	13.81
Mg	KA1	1.254	0.0128	1.44	1.81	13.81
Total				**100.00**	**100.00**	**22.10**

Figure A33. EDS spectrum for the particles formed on 6061 Al coupon with CS coupon tested at 140 F and pH=9.4 for one week.

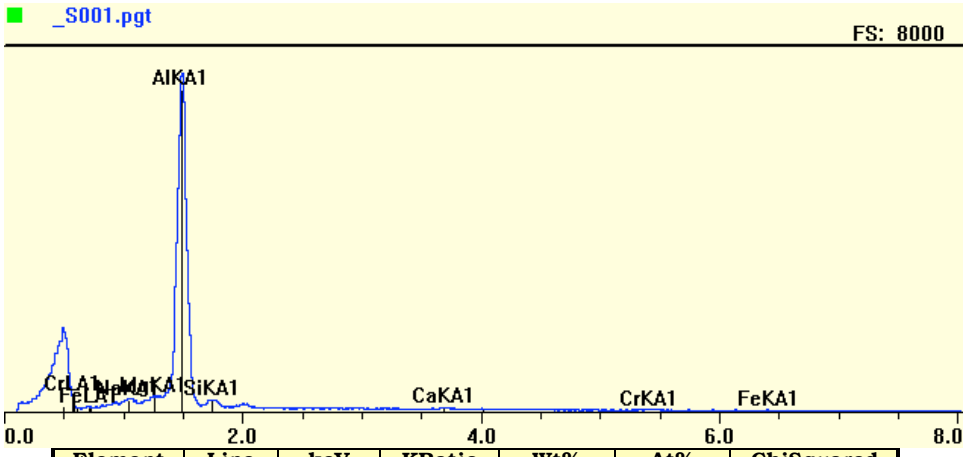

Element	Line	keV	KRatio	Wt%	At%	ChiSquared
Al	KA1	1.487	0.8402	88.32	89.63	58.14
Si	KA1	1.740	0.0163	2.51	2.45	58.14
Fe	KA1	6.403	0.0154	1.88	0.92	0.89
Na	KA1	1.041	0.0210	2.27	2.70	58.14
Mg	KA1	1.254	0.0254	2.48	2.79	58.14
Cr	KA1	5.414	0.0123	1.47	0.77	0.88
Ca	KA1	3.691	0.0098	1.07	0.73	0.85
Total				**100.00**	**100.00**	**212.33**

Figure A34. EDS spectrum for the particle-free region of 6061 Al coupon without other metal coupons tested at 140 F and pH=8.0 for one week suggesting mainly Al oxide.

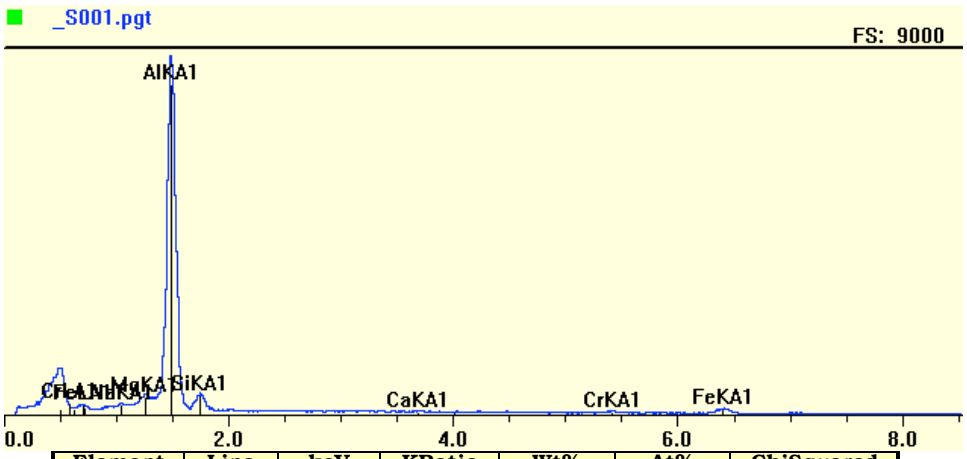

Element	Line	keV	KRatio	Wt%	At%	ChiSquared
Al	KA1	1.487	0.6489	72.33	80.00	62.26
Si	KA1	1.740	0.0293	4.29	4.55	62.26
Fe	KA1	6.403	0.1405	16.61	8.87	1.68
Na	KA1	1.041	0.0075	0.96	1.25	62.26
Mg	KA1	1.254	0.0266	2.93	3.59	62.26
Cr	KA1	5.414	0.0219	2.47	1.42	0.89
Ca	KA1	3.691	0.0039	0.42	0.31	1.03
Total				**100.00**	**100.00**	**99.37**

Figure A35. EDS spectrum for the particles formed on 6061 Al coupon without other metal coupons tested at 140 F and pH=8.0 for one week.

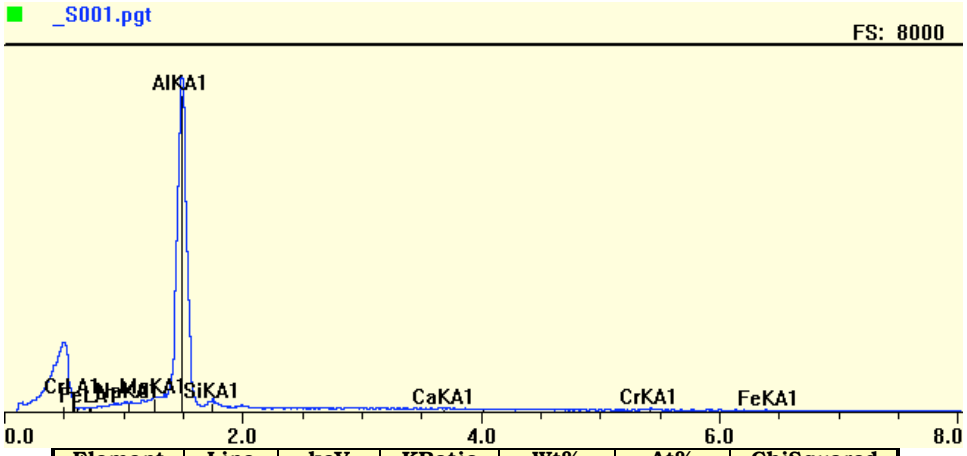

Element	Line	keV	KRatio	Wt%	At%	ChiSquared
Al	KA1	1.487	0.8704	90.44	92.37	55.95
Si	KA1	1.740	0.0113	1.74	1.71	55.95
Fe	KA1	6.403	0.0128	1.55	0.77	1.08
Na	KA1	1.041	0.0071	0.77	0.93	55.95
Mg	KA1	1.254	0.0204	1.96	2.22	55.95
Cr	KA1	5.414	0.0221	2.63	1.39	0.92
Ca	KA1	3.691	0.0082	0.90	0.62	1.21
Total				**100.00**	**100.00**	**170.81**

Figure A36. EDS spectrum for the particle-free region of 6061 Al coupon with CS coupon tested at 140 F and pH=8.0 for one week suggesting mainly Al oxide.

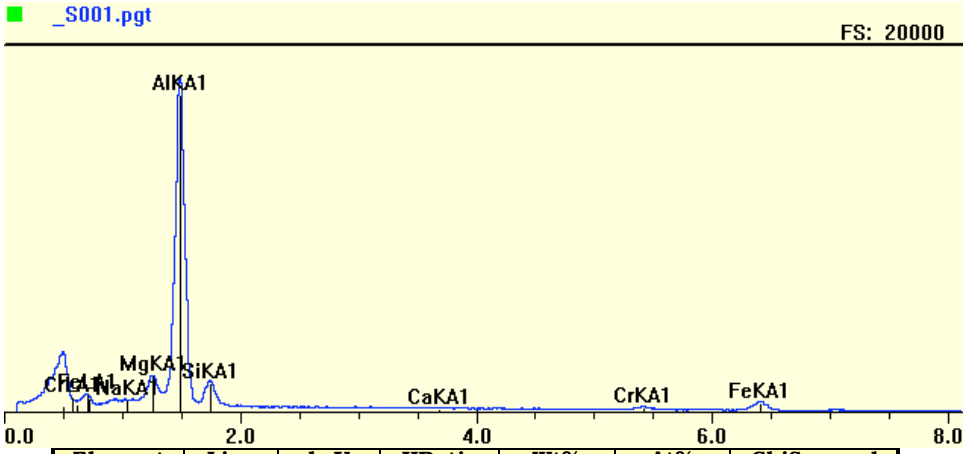

Element	Line	keV	KRatio	Wt%	At%	ChiSquared
Al	KA1	1.487	0.5158	60.27	69.95	105.65
Si	KA1	1.740	0.0406	5.76	6.42	105.65
Fe	KA1	6.403	0.2110	24.57	13.77	2.83
Na	KA1	1.041	0.0044	0.62	0.84	105.65
Mg	KA1	1.254	0.0462	5.40	6.95	105.65
Cr	KA1	5.414	0.0295	3.22	1.94	1.28
Ca	KA1	3.691	0.0015	0.16	0.12	0.92
Total				**100.00**	**100.00**	**255.13**

Figure A37. EDS spectrum for the particle formed on 6061 Al coupon with CS coupon tested at 140 F and pH=8.0 for one week.

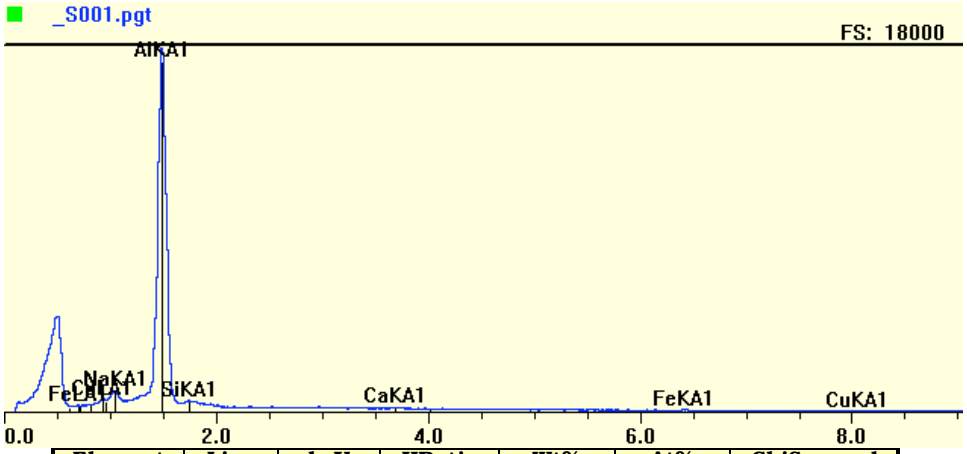

Element	Line	keV	KRatio	Wt%	At%	ChiSquared
Na	KA1	1.041	0.0272	3.04	3.69	586.88
Al	KA1	1.487	0.8467	89.09	92.09	84.84
Ca	KA1	3.691	0.0076	0.83	0.58	1.11
Fe	KA1	6.403	0.0198	2.39	1.19	1.39
Si	KA1	1.740	0.0048	0.74	0.74	84.84
Cu	LA1	0.930	0.0319	3.90	1.71	586.88
Total				**100.00**	**100.00**	**574.59**

Figure A38. EDS spectrum for the particle-free region of 1100 Al coupon without any other metal coupons tested at 140 F and pH=9.4 for one week suggesting Al oxide having some Fe and Cu.

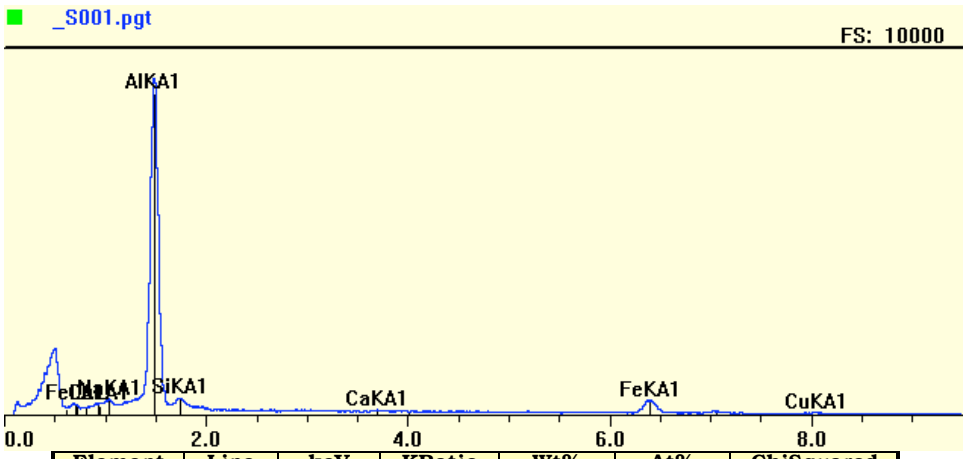

Element	Line	keV	KRatio	Wt%	At%	ChiSquared
Na	KA1	1.041	0.0081	1.24	1.80	175.71
Al	KA1	1.487	0.5003	58.76	73.09	28.55
Ca	KA1	3.691	0.0030	0.31	0.26	1.33
Fe	KA1	6.403	0.3082	35.02	21.04	1.63
Si	KA1	1.740	0.0143	2.00	2.39	28.55
Cu	LA1	0.930	0.0146	2.68	1.42	175.71
Total				**100.00**	**100.00**	**155.35**

Figure A39. EDS spectrum for the particle formed on 1100 Al coupon without any other metal coupons tested at 140 F and pH=9.4 for one week suggesting Al-Fe-Si intermetallics possibly with Cu-containing intermetallics.

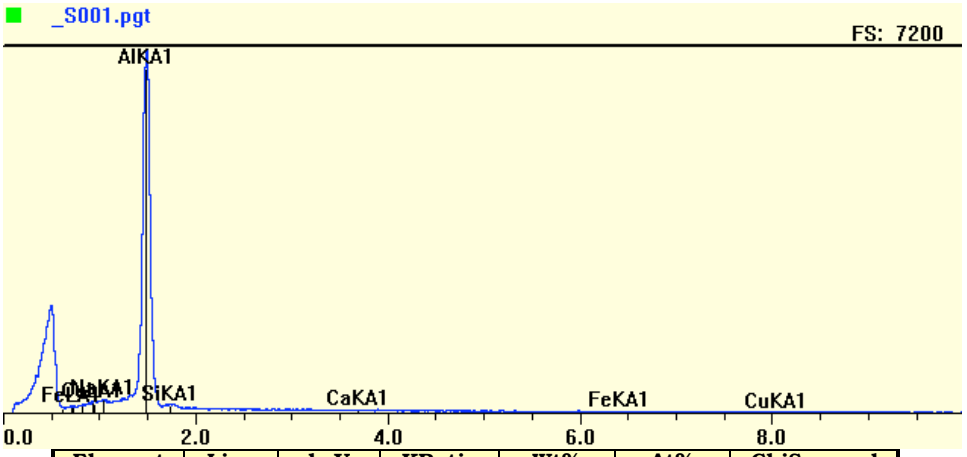

Element	Line	keV	KRatio	Wt%	At%	ChiSquared
Na	KA1	1.041	0.0118	1.33	1.61	314.80
Al	KA1	1.487	0.8707	90.91	94.45	49.70
Ca	KA1	3.691	0.0018	0.20	0.14	1.15
Fe	KA1	6.403	0.0214	2.58	1.30	0.91
Si	KA1	1.740	0.0035	0.55	0.55	49.70
Cu	LA1	0.930	0.0364	4.44	1.96	314.80
Total				**100.00**	**100.00**	**303.10**

Figure A40. EDS spectrum for the particle-free region of 1100 Al coupon with SS coupon tested at 140 F and pH=9.4 for one week suggesting Al oxide having some Fe and Cu.

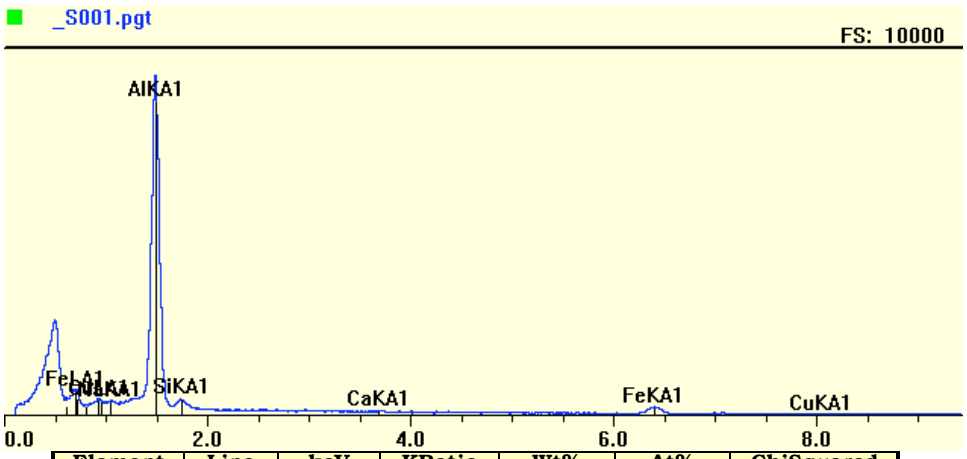

Element	Line	keV	KRatio	Wt%	At%	ChiSquared
Na	KA1	1.041	0.0049	0.69	0.95	278.09
Al	KA1	1.487	0.6001	68.05	80.38	53.33
Ca	KA1	3.691	0.0020	0.21	0.17	0.92
Fe	KA1	6.403	0.2000	23.16	13.21	1.29
Si	KA1	1.740	0.0146	2.11	2.39	53.33
Cu	LA1	0.930	0.0360	5.78	2.90	278.09
Total				**100.00**	**100.00**	**295.62**

Figure A41. EDS spectrum for the particle formed on 1100 Al coupon with SS coupon tested at 140 F and pH=9.4 for one week suggesting Al-Fe-Si intermetallics possibly with Cu-containing intermetallics covered by Al hydroxide.

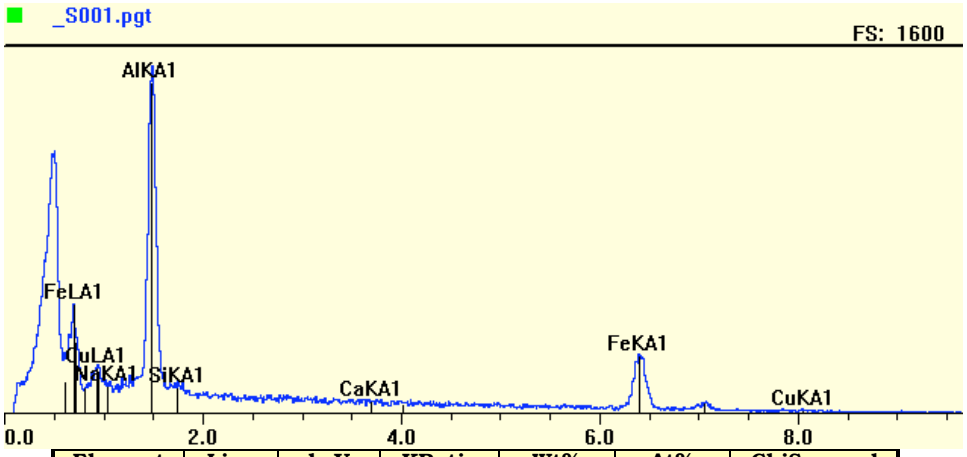

Element	Line	keV	KRatio	Wt%	At%	ChiSquared
Na	KA1	1.041	0.0017	0.33	0.62	117.47
Al	KA1	1.487	0.2082	27.10	43.55	8.94
Ca	KA1	3.691	0.0021	0.20	0.21	1.06
Fe	KA1	6.403	0.5682	59.94	46.52	2.37
Si	KA1	1.740	0.0056	0.70	1.09	8.94
Cu	LA1	0.930	0.0505	11.73	8.00	117.47
Total				**100.00**	**100.00**	**144.83**

Figure A42. EDS spectrum for the particle formed on 1100 Al coupon with SS coupon tested at 140 F and pH=9.4 for one week suggesting Al-Fe-Cu intermetallics covered by Al hydroxide.

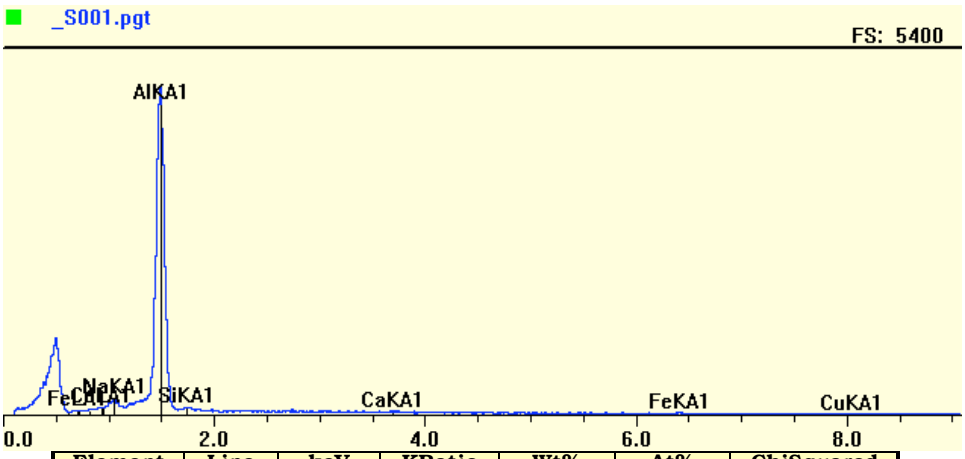

Element	Line	keV	KRatio	Wt%	At%	ChiSquared
Na	KA1	1.041	0.0231	2.54	3.05	148.07
Al	KA1	1.487	0.8795	91.64	93.79	33.98
Ca	KA1	3.691	0.0034	0.37	0.26	1.21
Fe	KA1	6.403	0.0273	3.30	1.63	0.82
Si	KA1	1.740	0.0041	0.64	0.62	33.98
Cu	LA1	0.930	0.0122	1.51	0.66	148.07
Total				**100.00**	**100.00**	**128.79**

Figure A43. EDS spectrum for the particle-free region of 1100 Al coupon with CS coupon tested at 140 F and pH=9.4 for one week suggesting Al oxide having some Fe and Cu.

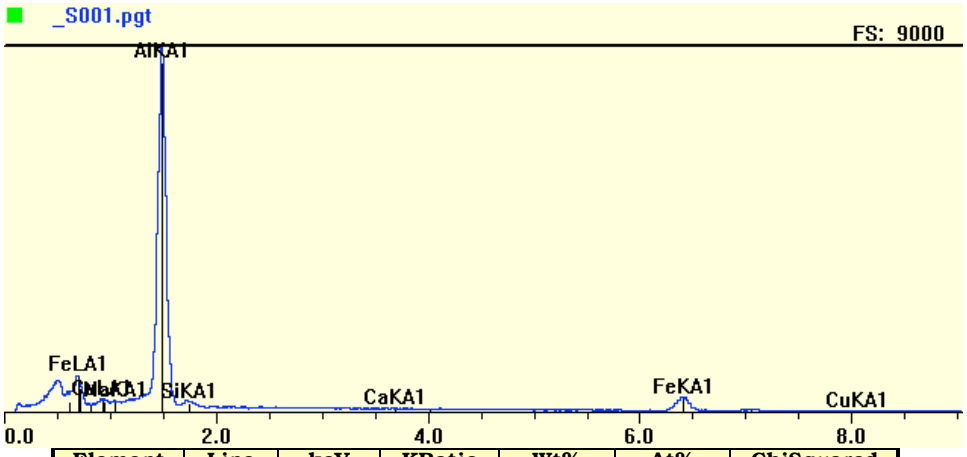

Element	Line	keV	KRatio	Wt%	At%	ChiSquared
Na	KA1	1.041	0.0011	0.17	0.25	54.18
Al	KA1	1.487	0.5196	60.78	75.94	49.30
Ca	KA1	3.691	0.0011	0.11	0.10	0.88
Fe	KA1	6.403	0.3065	34.79	20.99	2.44
Si	KA1	1.740	0.0056	0.79	0.94	49.30
Cu	LA1	0.930	0.0183	3.35	1.78	54.18
Total				**100.00**	**100.00**	**52.00**

Figure A44. EDS spectrum for the particle formed on 1100 Al coupon with CS coupon tested at 140 F and pH=9.4 for one week suggesting Al-Fe-Si intermetallics possibly with Cu-containing intermetallics.